Optimal Rigid-Body Rotational Maneuvers

by

Rajiv S. Chowdhry

Dissertation submitted to the Faculty of the

Virginia Polytechnic Institute and State University

in partial fulfillment of the requirements for the degree of

Doctor of Philosophy

in

Aerospace Engineering

APPROVED:

Dr. E. M. Cliff, Chairman

Dr. J. A. Burns

Dr. F. H. Lutze

Dr. K. H. Well

Dr. L. G. Kraige

October 26, 1989.

Blacksburg, Virginia

Optimal Rigid-Body Rotational Maneuvers

by

Rajiv S. Chowdhry

Dr. E. M. Cliff, Chairman

Aerospace Engineering

(ABSTRACT)

Optimal rigid-body angular maneuvers are investigated, using restricted control moments - a problem inspired in the context of rotational maneuvers for *super-maneuverable* aircraft. Most of the analysis is based on the formulation with no direct control over the roll component of angular velocity. The present research effort is conducted in two phases. In the first phase, optimal control of angular *rates* is closely examined. The second phase deals with the problem of optimal *attitude* control.

Optimal rigid-body angular *rate* control is first examined via an *approximate* dynamic model. The proposed model admits analytical solutions of the optimality conditions. The analysis reveals that over a large range of boundary conditions, there are, in general, *several* distinct extremal solutions. Second-order necessary conditions are investigated to establish local optimality of candidate minimizers. Global optimality of the extremal solutions is discussed.

Next, the optimal angular *rate* problem is studied using the *exact* dynamic model. Numerical solutions of optimality conditions are obtained which corroborate and

extend the findings of the *approximate* problem. The qualitative feature of *multiple extremal solutions* is retained. Several of these extremal solutions did not satisfy the Jacobi necessary condition. The choice of *minimizing* solution could be narrowed down to two sub-families of extremal solutions. A locus of Darboux Points is obtained which demarcates the domain over which these two sub-families are globally minimal.

The above studies look at *minimum control effort* families of extremal solutions. As a next step, we examine the *minimum time* control of angular rates, with prescribed hard bounds on available control. Existence of singular subarcs in time-optimal trajectories is explored. Qualitative features exhibited by the *exact* problem are preserved. In addition, the control space is deformed to allow roll control and its effect on extremal solutions is investigated.

In the next phase, we introduce the *kinematics* into the optimal control problem. Minimum time *attitude* control of a rigid-body is investigated with prescribed hard bounds on available control. The attitude of the rigid-body is defined using Euler parameters. Existence of singular subarcs in time-optimal trajectories is explored. A numerical survey of first-order necessary conditions reveals that there are *several* distinct extremal solutions. The character of extremal solutions depend whether *pitch* or *yaw* motion assumes the dominating role in controlling *roll* motion. Moreover, certain *spatial symmetries* are identified. Maneuvers such as a *Roll Around the Velocity Vector* and *Fuselage Pointing* are analyzed.

Acknowledgements

I am deeply indebted to Dr. Eugene M. Cliff for his invaluable contribution to this research, to my knowledge and to my professional growth. His constant encouragement and guidance made this a wonderful learning experience. I am grateful to Dr. F. H. Lutze for his enthusiasm and very valuable suggestions throughout the course of this study. I feel privileged and thankful to have the opportunity to associate with Dr. H. J. Kelley, Dr. J. A. Burns, Dr. K. H. Well, Dr. H. L. Stalford and Dr. L. G. Kraige.

I wish to express my sincere gratitude to the and families for their kindness and hospitality during the past four years and for providing a home away from home. Finally, I take this opportunity to thank all my friends and colleagues at ICAM and Department of Aerospace Engineering for their help and advice.

This research was supported in part by DARPA under contract [ACMP] F49620-87-C-0016, and in part by SDIO/IST under contract F49620-87-C0088 and is gratefully acknowledged.

To my family for their unfaltering love and encouragement

Table of Contents

List of Figures

Chapter 1: Introduction

1.1: An Overview

In this study we investigate the *optimal control* of *rotational* motions of a *rigid* body, using *thrust vectored* control moments. The preceding statement has several key words which require some explanation. The term *rigid* body implies an idealization of a *real* body which, in general, undergoes deformation when it is subject to forces. However, the assumption of rigidity is permissible if the changes in shape are negligible compared to the overall dimensions of the body or to the "overall" changes in the position of the body [1,2]. In this study, the rigid body of "interest" is a combat aircraft and the study of its "overall" motion is of concern.

Moreover, in the study of dynamics, the term rigid-body dynamics relates to six-degree-of-freedom motion as opposed to point mass dynamics which deal only

with translational motion. Chasle's Theorem [1] states that any general displacement of a rigid body can be represented as a translation plus a rotation. It is often possible to divide the problem of rigid body motion into two separate phases, one concerned solely with the translational motion of the body, the other, with its rotational motion. In the present study, we only deal with the rotational motion of the rigid body.

The term *optimal control* suggests that out of the many possible ways of performing a desired rotational maneuver using the available control, we pick the one which extremizes a given performance index. The available control, moments in our case, are obtained by *vectoring* the thrust force, which has some distinguishing features. The optimal choice of control is obtained using the Minimum Principle of variational calculus [3,4,5,6,7].

The above discussion loosely defines the class of problems investigated herein. There are several gaping questions yet not addressed. For example, what are the desired rotational maneuvers ? What is the *metric*, i.e., performance index of interest ? What are the distinguishing features of available control generated by thrust vectoring ? Naturally, the answer to these details lies in the engineering problem which provoked the present study.

The need for analysis of this class of problems arose in the context of a proposed new concept for the next generation of combat aircraft. These fighter aircraft, sometimes referred to as *super-maneuverable* aircraft or highly *agile* aircraft, are

being designed to perform controlled maneuvers, called *super-maneuvers*, beyond today's conventional flight boundaries. This enhancement of performance is achieved by incorporating new technologies. As one can imagine, there are a plethora of issues which need to be sorted out for a successful development of a new concept. In the next sub-section, we introduce the notion of the *super-maneuverable* aircraft.

1.2: Super-maneuverable Aircraft

A review of air combat scenario for the latter part of this century and early next century, carried out at *Messerschmitt-Bölokow-Blohm GmbH* (MBB) under the leadership of W. B. Herbst, revealed the need for a new fighter aircraft. These studies, started almost two decades ago, are based on results of extensive unmanned and manned computer simulations of air combat. The models used in these simulations included modern/projected air-to-air weapon technology [8], such as the all-aspect short range (SR) missiles, a more capable gun and coupled flight/fire control capability and a new generation of autonomous/ semi-autonomous radar guided medium range (MR) missiles. Simulation studies showed a significant change in "dynamics" of air combat [9], necessitating a departure from classical design requirements for a fighter aircraft.

The new requirements for air superiority called for a radical expansion of maneuvering flight envelope for the fighter aircraft. The all-aspect nature of SR

weapons, employed in low subsonic Within Visual Range combat situation, leads to an increase in importance of instantaneous maneuver capability over the classical sustained performance [9]. On the other hand, the MR missiles with autonomous terminal phase and semi-autonomous mid-course guidance, employed in Beyond Visual Range combat demand a maneuvering-type combat in the supersonic regime. A solution for the conflicting requirements demanded of this new fighter is presented by Herbst in [10]. This solution requires the combination of three key technologies : Digital Fly-by-wire control, the aerodynamic advancements of delta wings and *super-maneuverability*.

The term *super-maneuverability* introduced by Herbst [10], describes the

> " ... combined post-stall (PST) and direct force (DFM) capability, PST represents the aircraft to perform controlled tactical maneuvers beyond maximum lift angle of attack up to at least 70 deg; DFM represents the ability of the aircraft to yaw and pitch independently of flight path, or to maneuver at constant fuselage attitude. "

Fighter aircraft with conventional aerodynamic control surfaces cannot perform tactical maneuvers beyond the maximum lift angle of attack. This is due to the fact that flow separates causing the conventional aerodynamic control surfaces to lose their effectiveness. In addition, low dynamic pressure contributes to a further loss of control power. These factors result in instability/ trim problems for the aircraft and cause departures from controlled flight. To overcome this

problem additional reaction control systems are required. Studies at MBB showed that PST maneuvers of tactical value are characterized by high pitch and yaw rates in the post-stall maneuvering regime. A solution offered by Herbst [10] is to deflect the thrust vector, e.g. a vectored nozzle, to augment the pitch and yaw control power.

Computation of optimal trajectories for a high T/W ratio aircraft with PST capabilities was carried out by Well [11]. This study was carried out to investigate whether PST capability improves performance for turning maneuvers. Minimum time trajectories, aiming to return to the point of departure at the same airspeed and altitude but with opposite heading, could be achieved in less airspace and maneuver time for an aircraft with PST capabilities. The *slicing* maneuver was found to be a typical PST maneuver, offering time advantage over conventional aircraft. The *slicing* maneuvering technique developed by the MBB-study pilots consisted of a pull up to approximately 90 degree angle of attack, followed by a quick reaction controlled yaw (as viewed in body axes) which produced a roll about the flight path. The *slicing* maneuver is potentially a maneuver of significant tactical value.

In about the same time period, it was discovered in the course of F-14 flight testing that the aircraft could be pulled up to 55 degrees angle of attack in transient maneuvers and to 30 degrees in steady state, without pitch-up and wing-dropping tendencies, unlike other high-speed fighter designs. The aircraft's high level of effective dihedral hindered rolling in the post-stall regime, limiting

the extent to which the high-alpha maneuvering capability could be exploited. In a research program at David W. Taylor Naval Ship Research and Development Center, yaw vanes were installed on a Navy F-14A. These vanes, designed by David Lacey, offered a practical means of thrust vectoring. Flight test results indicated an increased roll response due primarily to the enhanced yaw control power. For a standard F-14A, it takes almost 30 sec to roll 90 degrees at a 40-degree angle of attack flying near 130 kt. The yaw-vane equipped F-14A can perform the same maneuver in 5 sec, as is reported in [12]. Moreover, the 90-degree roll maneuver could be performed in around the same 5 sec at varying high angles of attack and slow speeds.

A manned one-on-one simulation study [13] was carried out at NASA Langley Differential Maneuvering Simulator. A reaction control equipped aircraft engaged in a duel against an identical non-reaction controlled aircraft. The results of the study showed a 4 to 1 Time on advantage (TOA) ratio in favor of reaction control equipped aircraft starting in a neutral position. TOA ratios were 1.66 to 1 and 28 to 1 when the reaction controlled aircraft was placed at a disadvantage and advantage respectively.

The operational need and utility of *super-maneuverable* aircraft is well established, based on the results of combat simulation. The technological feasibility of achieving *super-maneuverability* has been demonstrated to a certain extent, e.g. thrust vectoring. Several research programs are currently underway, notably the Rockwell International/ MBB X-31A enhanced fighter

maneuverability demonstrator, Defense Advanced Research Projects Agency/ Navy enhanced fighter maneuverability program, USAF's Flight Dynamics Laboratory program on *super-maneuverability* [14] at Wright-Patterson AFB and the F/A-18 High Angle-of-Attack Research Vehicle program at NASA Langley Research Center. These programs have opened new vistas for research in many diverse fields. In particular, challenging research opportunities exist in the area of generation and analysis of optimal trajectories for this class of vehicles.

1.3: Trajectory Optimization for Super-Maneuverable Aircraft

The endeavor of trajectory optimization for *super-maneuverable* aircraft is to understand, analyze, and characterize the *super-maneuvers*, using a systematic, accurate yet a tractable procedure. Studies of this nature may be used for

i) obtaining new maneuvers.
ii) providing a baseline for systematic comparison to manned simulations.
iii) pilot training.
iv) synthesis of guidance and control laws.

The issue of mathematical models representing the aircraft's dynamics is central in optimal trajectory analysis. There is usually a trade-off between the fidelity of the model and the associated difficulty in analysis. Studies of optimal flight usually employ dynamic models based on point-mass equations of motion.

Inherent in such models is the singular perturbation idea which has its basis in the conventional flight mechanics wisdom that the aircraft's motion *about* the center of mass is fast compared to its translational motion (Short Period *vis-a-vis* Phugoid frequencies). Indeed, point mass models and lower-order models, e.g. *energy* models are adequate in ordinary circumstances. However, in the context of yet largely unexplored domain of *super-maneuvering*, maneuvers of interest such as the *slicing* maneuver first appeared in six degree-of-freedom (DOF) manned simulations. Fuselage pointing maneuvers are imbedded in the rotational degrees of freedom. Thus, to understand these maneuvers, there is a fundamental need to study optimal rigid-body rotational motions.

To encompass all the possibilities of *super-maneuvering* would require a most detailed description of aircraft dynamics, based on the six-DOF model. The generic six-DOF model consists of three force equations of motion describing the translational motion of the center of mass and the three moment equations describing the rotational dynamics about the center of mass. In addition, a set of three trajectory equations are required to track the position of the center of mass. If one ignores the variations in atmospheric properties with position, then these coordinates are "ignorable", as they do not appear on the right-hand side of the differential equations. To describe the angular orientation with respect a reference coordinate frame, three Euler angles may be used. However, in order to avoid the singularity that arises in the Euler angle rates when $\cos(\theta)$ vanishes, it would be judicious to use Euler parameters (four variables) to represent the angular orientation. The controls, variables which are chosen and are not

governed by differential equations, comprise of usual aerodynamic surface deflections, throttle setting, and a model of thrust vectoring (e.g. nozzle swivelling angles). Thus, the state in this generic model consists of ten coordinates, if Euler parameters are used and position coordinates are not retained in the model. The equations describing the evolution of the state are coupled and highly nonlinear.

It is well known that the application of Minimum Principle leads to a set of differential equations whose order is twice that of the state equations. Moreover, the boundary conditions are usually mixed and even in the simplest situations, generation of optimal trajectories requires a solution of a nonlinear two-point boundary-value problem. If there are constraints on the state and/or control variables, which is quite often the case, then one usually ends up with a multi-point boundary-value problem. The solutions of these problems are obtained numerically using iterative procedures. In general, the numerical solutions are difficult to obtain, especially so if one does not have *apriori* knowledge about the character of the optimal solution. Thus, these detailed models come along with the "curse of dimensionality".

It is the opinion of the author, that solutions of complex optimal control problems, such as the trajectory optimization problem for *super-maneuverable* aircraft, should be approached in a step-by-step fashion. An *inside-out* approach is adopted in the present study. This approach starts out with identifying a "simple" model which incorporates some distinguishing characteristic of "interest" in the original problem. This problem is analyzed and special features

of its solutions are noted. The model is then successively refined by adding more details, until solutions of the "larger" problem are obtained. This is underlying philosophy in which the present research effort may be perceived. In the next subsection, we elaborate on the above ideas.

1.4: Scope of Present Study

The objective of the present study is to understand the rotational maneuvers for a rigid aircraft, performed in some optimal sense, using only thrust vectored control moments. These moments may be thought as being generated by deflection of the thrust force, assumed to be applied at the aft end of the fuselage. Deflection of this force in the plane of symmetry is used for generating *pitching* moment and a *yawing* moment is obtained by deflection of the thrust force out of the plane of symmetry of the aircraft. However, *no rolling* moment can be generated using this simple scheme. If one considers a twin-engine configuration, engines being located on either side of the centerline at the aft end of the fuselage, then *differential* deflection of the thrust force may be used to generate rolling moment. However, even in this scheme, the available roll control is going to be *small* since the moment arm is small.

For the major portion of this study, we consider the case of *zero* roll control. Accordingly, the available control moment may be thought of as a point in the

M, N plane. This distinguishing feature of available control renders the problem of control of angular motion with some intriguing features, since the rolling motion is controlled only indirectly through pitch and yaw motions.

Optimal rigid-body rotational maneuvers were first studied in the context of spacecraft attitude control systems. The rotational dynamics about the center of mass of a rigid body are governed by the familiar Euler equations. These governing equations have quadratic non-linearities due to gyroscopic cross-coupling terms. In this and following paragraphs, we summarize some of the related optimal control studies existing in the literature. Athans and Falb [15] investigated the time-optimal and fuel-optimal angular velocity control of an axisymmetric rigid body. As a direct consequence of symmetry, the gyroscopic cross-coupling term along the axis of symmetry (spin axis) drops out, which decouples the angular velocity component about the spin axis (spin motion) from the other two components of angular velocity. Thus, the spinning motion may be controlled independently. For constant values of spin, the other two components of angular velocity are governed by a reduced second-order system, which is a harmonic oscillator. In Ref. [15], several different control schemes for the oscillator are compared. Furthermore, it has been shown in Refs. [15] and [6] that a time-optimal feedback law can be synthesized for regulating the angular momentum, for an asymmetric rigid body under special controller constraints.

Optimal linear feedback laws are obtained by Debs and Athans [16] and Dwyer [17] in closed-form for regulating the angular momentum of an arbitrarily

rotating asymmetric rigid body. The linear time-invariant feedback law is optimal with respect to a quadratic cost functional in angular momenta and control torques. Further in Ref. [16] nonlinear feedback laws are obtained which are optimal with respect to some non-quadratic cost functionals. Their method of solution is based on the " inverse problem " of optimal control. In a more recent study, Golubev and Demidov [18] have investigated minimum-time and minimum-control effort rotation stoppage for an asymmetric spacecraft. General solutions have been obtained in explicit form, using a family of first integrals of the unperturbed rigid-body Euler equations. The closed-form feedback law are applicable to a fairly general class of problems, with some restrictions on the actuator influence coefficients.

Optimal large-angle ***attitude*** maneuvers for a rigid asymmetric vehicle are investigated by Junkins and Turner [19]. A relaxation process is presented to obtain solutions of arbitrary boundary conditions starting with analytical solutions for single axis maneuvers. Carrington and Junkins [20] obtained a polynomial feedback law for large angle attitude maneuvers. Minimum time attitude slew maneuvers of a rigid spacecraft are obtained by Li and Bainum [21]. In all the above mentioned studies, the interesting possibility of controlling arbitrary angular motion, in the absence of direct control over one of the angular velocity component, is not explored. The underlying assumption in the previous studies is that the control torquers have direct influence over each of the three components of the angular velocity.

In the following study, the first part deals with the control of angular *rates* of the rigid body and the latter part investigates the problem of *attitude* control, using only pitch and yaw controllers. The problem of angular rate control is studied in three phases. In the first phase, the problem of rigid-body angular rate control is examined via an *approximate* dynamic model. The *approximate* dynamic model consists of two simple integrators, representing the pitch and yaw dynamics and a bilinear isoperimetric constraint, representing the roll dynamics. The *approximate problem* admits analytical solutions of the first-order necessary conditions for optimality and reveals an elaborate extremal solution structure. Second-order necessary conditions are examined to verify the local optimality of the extremal solutions. The formulation, analysis, and important results for this phase of study are contained in Chapter Two.

In the second phase, we investigate the problem of angular rate control based on the *exact* dynamic model, i.e., the Euler equations of motion. The solutions of the first-order necessary conditions for optimality, formulated with the *exact* dynamics are obtained numerically. These solutions corroborate and extend the findings of the *approximate problem.* Further, local optimality for the candidate minimizers is verified by examining the second-order necessary conditions. The analysis for this phase is presented in Chapter Three.

In the above two studies, we examined the *minimum control effort* families of extremal solutions, with no prescribed hard bounds on the available control moments. A reasonable *measure of merit*, in the context of *super-maneuverable*

aircraft, is the time required to execute a prescribed maneuver. Thus, in the third and final phase of angular *rate* control, we examine the *minimum time* problem with bounded control moments. Numerical solutions of the first-order necessary conditions are examined. Qualitative features, exhibited by the extremal solutions obtained in the above two phases of study, are retained. Chapter Four deals with the *minimum time* problem.

Next, the problem of *minimum time reorientation* of the aircraft is studied. In this problem, we control the *attitude* of the aircraft, in addition to its angular velocity. The attitude of the aircraft is defined using the Euler parameters. Hard bounds on the available control are prescribed. Several maneuvers of interest in the *super-maneuverability* application are examined. This problem of optimal control is rather intricate; however, the "road map" provided by the first part of this study makes the analysis tractable. In Chapter Five we investigate the *minimum time reorientation* problem.

The approach adopted, throughout the course of this study, is to keep the analysis and results fairly general. This is achieved by ample use of scaling. Whenever possible, the system parameters, such as the moments of inertia and the bounds on the control variables, are absorbed by transforming the state and control variables. The idea is to reduce the number of parameters appearing in the analysis of optimal control problem. While such an approach has several obvious merits, there are some pitfalls too. For instance, the transformation process is problem dependent. In other words, depending on the optimal control

problem, it may be meaningful to transform the variables in a given fashion. As has been indicated earlier, there are four major optimal control problems analyzed herein, in the following four chapters, each a little more complex than the one preceding it. In an effort to avoid confusion in nomenclature, variable names are to be interpreted in the context of each chapter. For instance, the variable p, has different mathematical meaning in each of the following four chapters; however, its physical meaning is the same, i.e., transformed roll component of the angular velocity. Thus, each chapter may be treated independently, complete in itself. Naturally, the price one pays for clarity is a certain amount of repetition.

Chapter 2: Approximate Problem

2.1: Introduction

Preliminary investigation of the *minimum time* and *minimum control effort* problems for a rigid body with pitch and yaw controllers showed some rather intriguing phenomena. In an effort to enhance our general understanding and also address some apparently inexplicable features of the these problems, we suggest an alternate *approximate problem.* The *approximate problem* seems to retain the important characteristics of the original problem, yet it admits analytical solutions and is thus more amenable to analysis. In the following sections, we define the *approximate problem* and present an analysis of the first and second-order necessary conditions for optimality.

2.2: Motivation

Consider the rotational dynamics of a rigid body in a body-fixed coordinate system. The coordinate system is centered at the center of mass of the body and aligned along its principal axes. Let p, q, and r denote the components of angular velocity, namely the roll, pitch, and the yaw rates. Assume the body is free of all external moments except the applied control moments. Then, the so-called Euler equations of motion are:

$$\dot{p} = J_x q r + \frac{L}{I_x} \qquad [2.2.1]$$

$$\dot{q} = J_y p r + \frac{M}{I_y} \qquad [2.2.2]$$

$$\dot{r} = J_z p q + \frac{N}{I_z} \qquad [2.2.3]$$

where $J_x = \frac{I_y - I_z}{I_x}$, $J_y = \frac{I_z - I_x}{I_y}$, $J_z = \frac{I_x - I_y}{I_z}$, and

I_x, I_y, I_z are the principal moments of inertia.

L, M, and N are the rolling, pitching, and yawing moment, respectively. We shall consider the case when $L(t)$ is identically zero.

The problem is to find the controls $M(t)$ and $N(t)$ to perform an arbitrary point-to-point maneuver (from a given fixed value to another in the state space) in a prescribed time t_f, while minimizing the *control effort*. That is, the performance index is

$$\mathcal{J} = \frac{1}{2}\int_0^{t_f}[M^2 + N^2]dt. \qquad [2.2.4]$$

The above problem we shall label as the *exact problem.* The class of minimum *control effort* problems for linear systems is formulated and discussed by Neustadt in Reference [22].

Note that the roll motion is controlled indirectly through the pitch and yaw motions. This particular characteristic endows the problem of control with some intriguing features. Further, for some initial and final conditions for p, q, and r, the cross-coupling terms $J_y pr$ in the $\dot{q}$ equation and the $J_z pq$ in the $\dot{r}$ equation may be ignored compared to the control moments, M and N, respectively. The resulting *approximate* equations are

$$\dot{p} = J_x q r \qquad [2.2.5]$$

$$\dot{q} = \frac{M}{I_y} \qquad [2.2.6]$$

$$\dot{r} = \frac{N}{I_z} \qquad [2.2.7]$$

Since p is now an ignorable variable, equation [2.2.5] can be identified with an isoperimetric constraint. Further, in this *approximate* model the q and r dynamics are governed by two first-order integrators, equations [2.2.6] and [2.2.7]. The problem of control remains the same, i.e., we seek to perform a

point-to-point maneuver in a given time t_f, while minimizing the *control effort.* This problem we will label as the *approximate problem.*

Suppressing, for the moment, some details, the Maximum Principle was applied to the exact and the approximate problems, and the resulting two-point boundary-value problem solved numerically using a multiple-shooting algorithm. The following numerical data was used : $I_x = 0.16174$, $I_y = 0.86524$ and $I_z = 1.0$, the initial states are prescribed to be $p(0) = 0$, $q(0) = 1$ and $r(0) = 1$, the final states to be $p(t_f) = q(t_f) = r(t_f) = 0$ and the maneuver time, $t_f = 2.0$. The resulting extremal trajectory and control histories are shown in Figure [1]. It is evident from these plots, that there is a good qualitative agreement between the exact and the approximate problems. We wish to emphasize that the suggested *approximate problem* captures in a qualitative sense, some of the interesting features of the *exact problem* of controlling rigid-body angular velocity with two controllers.

2.3: Problem Statement

In this section, we have a general formulation of the *approximate problem.* The state equations consist of two first-order integrators:

$$\dot{\hat{y}} = \alpha_y \hat{u} \qquad [2.3.1]$$

$$\dot{\hat{z}} = \alpha_z \hat{v} \qquad [2.3.2]$$

with $(\hat{u}, \hat{v}) \in U = \mathcal{R}^2$. We seek to perform a point-to-point maneuver, i.e.

$$\hat{y}(0) = \hat{y}_0 \qquad \hat{y}(t_f) = \hat{y}_f \qquad [2.3.3]$$

$$\hat{z}(0) = \hat{z}_0 \qquad \hat{z}(t_f) = \hat{z}_f \qquad [2.3.4]$$

while minimizing the performance index $\mathcal{J}$

$$\mathcal{J} = \frac{1}{2} \int_0^{t_f} [(\alpha_u \hat{u})^2 + (\alpha_v \hat{v})^2] dt \qquad [2.3.5]$$

subject to an isoperimetric constraint:

$$\int_0^{t_f} \alpha_l \hat{y}\, \hat{z}\, dt = \hat{\ell} \qquad [2.3.6]$$

where α_y, α_z, and α_l are non-zero constants characterizing the rigid body,

α_u and α_v are non-zero constants defining a generalized *control effort*, and

$\hat{\ell}$ is the prescribed value to the isoperimetric constraint.

Note that the nonlinear isoperimetric constraint on the states $\hat{y}$ and $\hat{z}$ renders this problem more interesting than an otherwise well-understood LQR problem.

2.4: Derivation of the First-Order Necessary Conditions

The problem stated in above section, may be formulated and analyzed for first-order necessary conditions for optimality, in several different ways. We choose, for convenience, the Mayer formulation. In this formulation the constraint and the cost appear as additional states x and c, respectively. First, we would like to point out that some of the constants which appear in the above problem may be absorbed using the following transformation. Let,

$$y = \frac{\alpha_u}{\alpha_y}\hat{y} \qquad z = \frac{\alpha_v}{\alpha_z}\hat{z} \qquad u = \alpha_u\hat{u} \qquad v = \alpha_v\hat{v} \qquad \ell = \frac{\alpha_u\alpha_v}{\alpha_y\alpha_z\alpha_l}\hat{\ell}. \quad [2.4.1]$$

Now, the problem stated in the above section simplifies to,

$$\dot{x} = y\,z \quad [2.4.2]$$

$$\dot{y} = u \quad [2.4.3]$$

$$\dot{z} = v \quad [2.4.4]$$

$$\dot{c} = \frac{1}{2}(u^2 + v^2) \quad [2.4.5]$$

where the controls $u(.)$ and $v(.)$ are real-valued functions. We seek to minimize $c(t_f)$ for prescribed values of t_f, subject to following boundary conditions:

$$x(t_f) - x(0) = \ell \quad [2.4.6]$$

$$y(0) = y_0 \quad \text{and} \quad y(t_f) = y_f \qquad [2.4.7]$$

$$z(0) = z_0 \quad \text{and} \quad z(t_f) = z_f \qquad [2.4.8]$$

$$c(0) = 0 \qquad [2.4.9]$$

Note a solution of the scaled problem has a one-to-one correspondence to the solution of the general problem, equations [2.3.1] - [2.3.6]. In all subsequent analysis, we shall deal with the scaled problem. We can identify y with $I_y q$ and z with $I_z r$ in equations [2.2.6] and [2.2.7]. The isoperimetric constraint, with appropriate scaling is analogous to equation [2.2.5].

Following the usual practice, we define the variational-Hamiltonian $\mathscr{H}$ as,

$$\mathscr{H} = \frac{\lambda_0}{2}(u^2 + v^2) + \lambda_y u + \lambda_z v + \mu (y z) \qquad [2.4.10]$$

where λ_0 is the adjoint variable associated with the cost

λ_y, λ_z are the adjoint variables associated with the states y, z respectively, and

μ is the Lagrange variable associated with the isoperimetric constraint.

If we assume normality, we can scale λ_0 such that $\lambda_0(t) \equiv 1$.

The first-order necessary conditions for optimality states that an optimal control (u^*, v^*) , is one which minimizes the Hamiltonian $\mathscr{H}$ over all possible controls (u, v). We obtain, quite simply, the extremal control u^*, v^* as,

$$u^*(t) = -\lambda_y^*(t) \qquad v^*(t) = -\lambda_z^*(t) \qquad [2.4.11]$$

where the adjoint variables λ_y and λ_z satisfy

$$\dot{\lambda}_y = -\mu z \qquad \dot{\lambda}_z = -\mu y \qquad [2.4.12]$$

Note the problem is *regular*, since the matrix of the second partial derivatives of $\mathscr{H}$ with respect to controls u, v is the identity matrix. Thus, the Legendre-Clebsch condition is strictly satisfied.

Analytical Solutions

The equations [2.4.3] and [2.4.4] along with algebraic conditions [2.4.11] and the adjoint equations [2.4.12], form a set of four first-order linear homogenous equations, which can be readily integrated. Further, these equations may be represented by a single fourth-order homogenous equation of the form :

$$\ddddot{\phi} - \mu^2 \phi = 0 \qquad [2.4.13]$$

where ϕ is any one of $\{y, z, \lambda_y, \lambda_z\}$. For $\mu \neq 0$ solutions of equation [2.4.13] are, in general, linear combinations of circular and hyperbolic functions. It can be verified that for positive μ, we have

$$y(t) = -\frac{A}{\sqrt{\mu}} \sin\sqrt{\mu}\, t + \frac{B}{\mu} \cos\sqrt{\mu}\, t - \frac{C}{\sqrt{\mu}} \sinh\sqrt{\mu}\, t - \frac{D}{\mu} \cosh\sqrt{\mu}\, t \qquad [2.4.14]$$

$$z(t) = \frac{A}{\sqrt{\mu}} \sin\sqrt{\mu}\, t - \frac{B}{\mu} \cos\sqrt{\mu}\, t - \frac{C}{\sqrt{\mu}} \sinh\sqrt{\mu}\, t - \frac{D}{\mu} \cosh\sqrt{\mu}\, t \qquad [2.4.15]$$

where the constants A, B, C, and D are given in terms of known initial conditions and unknown initial costates as follows :

$$A = \frac{\lambda_y(0) - \lambda_z(0)}{2} \qquad B = \frac{-\mu\,(z(0) - y(0))}{2}$$
$$C = \frac{\lambda_y(0) + \lambda_z(0)}{2} \qquad D = \frac{-\mu\,(z(0) + y(0))}{2}. \qquad [2.4.16]$$

The isoperimetric constraint [2.4.6] may then be evaluated as

$$\ell = -(A^2 + \frac{B^2}{\mu} + C^2 - \frac{D^2}{\mu})\,\frac{t_f}{2\mu} + (A^2 - \frac{B^2}{\mu})\,\frac{\sin 2\sqrt{\mu}\, t_f}{4\mu^{\frac{3}{2}}} + (C^2 + \frac{D^2}{\mu})\,\frac{\sinh 2\sqrt{\mu}\, t_f}{4\mu^{\frac{3}{2}}} - \frac{AB}{2\mu^2}\,[\cos 2\sqrt{\mu}\, t_f - 1] + \frac{CD}{2\mu^2}\,[\cosh 2\sqrt{\mu}\, t_f - 1] \qquad [2.4.17]$$

and the corresponding cost $c(t_f)$ of the extremal can be evaluated as

$$c(t_f) = (A^2 + \frac{B^2}{\mu} + C^2 - \frac{D^2}{\mu})\ \frac{t_f}{2} + (A^2 - \frac{B^2}{\mu})\ \frac{\sin 2\sqrt{\mu}\ t_f}{4\sqrt{\mu}} +$$

$$(C^2 + \frac{D^2}{\mu})\ \frac{\sinh 2\sqrt{\mu}\ t_f}{4\sqrt{\mu}} - \frac{A\,B}{2\mu}\ [\cos 2\sqrt{\mu}\ t_f - 1] + \qquad [2.4.18]$$

$$\frac{C\,D}{2\mu}\ [\cosh 2\sqrt{\mu}\ t_f - 1]$$

Similar equations can be obtained for the case when $\mu < 0$. These will be referred to as equations [2.4.14′] - [2.4.18′].

It is entirely conceivable that for some boundary conditions, y_0, z_0, y_f, z_f , and ℓ, the isoperimetric constraint is "naturally" satisfied. This is the degenerate case which corresponds to $\mu = 0$. Some discussion of this special case is presented in the next section.

In principle, extremal solutions may be obtained for some given data y_0, z_0, y_f, z_f, t_f , and ℓ by "solving" for μ, $\lambda_y(0)$ and , $\lambda_z(0)$ making use of equations [2.4.14] - [2.4.17]. Recall that these equations have been derived for positive μ, while some boundary conditions may require negative values of μ , in which case equations [2.4.14′] - [2.4.17′] will yield meaningful "solutions" (real values for $\lambda_y(0)$, $\lambda_z(0)$ and μ). In any case, these are *nonlinear* transcendental algebraic equations, and as one may suspect, we may have more than one solution. In the next section we will show how these multiple solutions yield extremals belonging to different extremal sub-families.

2.5: Extremal Families

The extremal solutions of the *approximate problem* are in general, a six parameter family of solutions. Recall that extremals are paths that satisfy the usual first-order necessary conditions. In the present case these take the form [2.4.14]-[2.4.18]. Of the many choices for these parameters, one may choose for instance, t_f, y_0, z_0, ℓ, y_f , and z_f as these six parameters. As it turns out, the above parameter list is not adequate to describe all aspects of the problem. It is convenient, at times to choose t_f, y_0, z_0, μ, A , and C as a parameter list to provide a "better" insight. In this section we will show that for a given set of initial and final conditions, there are, in general, several distinct extremal solutions. The ***number*** of distinct extremal solutions, each of which has been classified to belong to a distinct sub-family, depends on the boundary conditions. By the way of numerical examples we shall characterize each sub-family of solutions. For the sake of clarity and ease of algebra, we shall confine our attention to the following case of the general problem:

i) We consider only those extremals which originate at the origin, i.e., $y_0 = 0, z_0 = 0$. By virtue of this assumption, the constants B ′ and ′ D are zero.

ii) We shall analyze completely the case when $\ell = 0$. In terms of analogy to rigid-body angular motion (section 2.2) this implies a maneuver where the

initial and final values of roll rate are the same, for example, when $p(t_0) = p(t_f) = 0$.

Making use of the above and evaluating [2.4.14] and [2.4.15] at t_f, along with the isoperimetric constraint [2.4.17], we obtain the following algebraic conditions:

$$y_f\sqrt{\mu} + A \sin\sqrt{\mu}\, t_f + C \sinh\sqrt{\mu}\, t_f = 0 \qquad [2.5.1a]$$

$$z_f\sqrt{\mu} - A \sin\sqrt{\mu}\, t_f + C \sinh\sqrt{\mu}\, t_f = 0 \qquad [2.5.1b]$$

$$(A^2 + C^2)\, 2\sqrt{\mu}\, t_f - A^2 \sin 2\sqrt{\mu}\, t_f - C^2 \sinh 2\sqrt{\mu}\, t_f = 0 \qquad [2.5.1c]$$

By restricting our attention to the class of solutions satisfying (i) and (ii), we have narrowed the parameter list down to three. For particular values of t_f, y_f, and z_f, we can in principle, obtain an extremal by finding constants A, C and μ which satisfy equation set [2.5.1]. Further, one can construct simple analytical arguments showing that if the product $y_f z_f > 0$ (i.e., the point (y_f, z_f) is in first or third quadrant of the $y_f - z_f$ plane) then μ must be strictly positive for real solutions of $\lambda_y(0)$ and $\lambda_z(0)$. Similarly, we can establish that if the product $y_f z_f < 0$ then μ must be strictly negative for real solutions of the initial costates. Next, we will proceed to obtain the domain of reachable points (y_f, z_f) in a given time t_f, along extremal paths. We shall distinguish three distinct categories of final conditions y_f and z_f, and analyze each separately.

Case 1 $y_f = 0$, arbitrary z_f

This is a degenerate case of a single integrator. It is evident that $y(t) \equiv 0$, by virtue of (i) and (ii). In this case $\mu = 0$, since the isoperimetric constraint is satisfied trivially. The problem reduces to driving z to its final state z_f, in the prescribed t_f. Since v is unbounded, all points z_f are reachable (by extremals) in given t_f. Similar arguments hold true for the case when $z_f = 0$, and y_f is arbitrary.

Case 2 $y_f = z_f = k$

This is a case of considerable interest. By virtue of (i) and (ii), the roles of y and z are completely interchangeable without affecting the control problem. Furthermore, $y(t)$ and $z(t)$ cannot be identical since we must maintain $\int_0^{t_f} y\, z dt = 0$. With this intuitive background in mind, we will analyze this case in detail. Rewrite [2.5.1] as,

$$y_f\sqrt{\mu} = -A \sin\frac{\omega}{2} - C \sinh\frac{\omega}{2} \qquad [2.5.2a]$$

$$z_f\sqrt{\mu} = A \sin\frac{\omega}{2} - C \sinh\frac{\omega}{2} \qquad [2.5.2b]$$

$$\frac{A}{C} = \pm\sqrt{f(\omega)} \qquad [2.5.2c]$$

where $f(\omega) \equiv \dfrac{\sinh\omega - \omega}{\omega - \sin\omega}$ and $\omega \equiv 2\sqrt{\mu}\, t_f$.

Note that $f(\omega) > 0 \;\forall\; \omega > 0$, so taking the square root in equation [2.5.2c] makes sense. The condition $y_f = z_f = k$, other than zero can be satisfied only if

$$\omega = 2\sqrt{\mu}\, t_f = 2n\pi \quad \text{where } n = 1, 2, \ldots \qquad [2.5.3]$$

and the constants A and C can be evaluated as

$$A = \pm\, C\sqrt{f(2n\pi)} \qquad C = -\,k\left(\frac{n\pi}{t_f}\right)\frac{1}{\sinh n\pi}. \qquad [2.5.4]$$

Note :

a) for each value of n, there exists two solutions for A corresponding to the $\pm$ signs, yielding two different extremals. In particular for each n, the two solutions corresponds to cases where the roles of $y(t)$ and $z(t)$ are identically interchanged.

b) Given k and t_f we can always find a A and C (in fact we can find countably many). So all points on the line $y_f = z_f$ are reachable (by extremals).

c) Corresponding to each n , the cost $c(t_f)$ is the same for the two solutions. Thus the line $y_f = z_f$ may be thought of as a locus of "*super*" Darboux points [23].

To facilitate notation, we attach labels to each extremal solution. We classify a particular extremal to belong to a sub-family of extremals based on the value of n and the associated sign in eqn.[2.5.4]. Thus for $n = 1$, positive and negative sign yield extremals belonging to the z - type and y - type sub-family of extremals, respectively. In short, these are referred to as the z - type or the y - type extremal. This nomenclature is based on the observation that the isoperimetric constraint

requires that the sign of the product yz change on the interval $[0, t_f]$. If one of the variables remains of a single sign then the other must be more "*dynamic*" or control-like. In the z (or y) - type sub-family, the state variable z (or y) assumes the role of control-like variable for the isoperimetric constraint. For $n = 2$, positive and negative sign yield extremals belonging to the zy - type and yz - type sub-family respectively. In zy - type sub-family, first z then y assumes the role of control-like variable. For $n = 3$, we get members of zyz - type and yzy - type sub-family corresponding to the positive and negative signs respectively, ... and so forth. We hope the ensuing numerical examples will help clarify the nomenclature.

Example 2.1

For $y_f = z_f = 1$, and $t_f = 2.0$ secs., the following extremals are presented.

i) $n = 1$ Using negative sign in [2.5.4], we get the solution labeled as y - type extremal which has cost $c(t_f) \simeq 1.5767$. Fig.[2] shows the relevant trajectories. For positive sign in [2.5.4], we get the z - type extremal, which may be envisioned by interchanging y and z state variables and u and v control variables in Fig.[2].

ii) $n = 2$ Using negative sign in [2.5.4], we get a yz - type extremal with cost $c(t_f) \simeq 3.1416$. Fig.[3] shows the relevant trajectories. For positive sign in [2.5.4], we get the zy - type extremal.

iii) $n = 3$ Using negative sign in [2.5.4], we get the $y\,z\,y$ - type extremal and cost $c(t_f) \simeq 4.7124$. Fig.[4] shows the relevant trajectories. For positive sign in [2.5.4], we get the $z\,y\,z$ - type extremal.

Case 3 y_f, z_f arbitrary

We shall now show, depending on the values y_f and z_f, we may have one extremal solution, two extremal solutions, ... and so forth. As we tend to the case $y_f = z_f$ the number of extremals increases and when $y_f = z_f$ there are countably many extremals. Using [2.5.2], we establish the following equations :

$$\frac{y_f}{z_f} = F(\omega) \quad \text{... + sign in [2.5.2c]} \qquad \frac{y_f}{z_f} = \frac{1}{F(\omega)} \quad \text{... - sign in [2.5.2c]} \quad [2.5.5]$$

where $$F(\omega) \equiv \frac{\sinh\frac{\omega}{2} + \sqrt{f(\omega)}\,\sin\frac{\omega}{2}}{\sinh\frac{\omega}{2} - \sqrt{f(\omega)}\,\sin\frac{\omega}{2}}$$

The curves $F(\omega)$ and $\frac{1}{F(\omega)}$ are plotted as a function ω in Figs. [5a] and [5b] respectively. These plots unfold the rich structure of this problem. The following information can be deduced from these plots.

a) If $\frac{y_f}{z_f} < F_b \simeq 0.36$ (see Fig. [5a]) there exists only one solution for ω, as is evident from Fig. [5b]

b) If $\frac{y_f}{z_f} > F_b'$ ($\equiv \frac{1}{F_b} \simeq 2.78$) (see Fig. [5b]) there exists only one extremal solution

c) If $F_b < \frac{y_f}{z_f} < F_b'$ there exists two or more extremal solutions

d) Given any y_f, z_f there is, in general, more than one solution to equation [2.5.5]. It turns out that the extremal solutions arising from the solution for ω along the arc $a\,b$ in Fig. [5a] are the z - type extremal; along the arc $b\,c$ the extremals are the $z\,y$ - type; along the arc $c\,d$ the extremals are the $z\,y\,z$ - type; ... and so forth. Similarly, extremal solutions arising along the arc $a'\,b'$ in Fig. [5b] turn out to be of y - type; along the arc $b'\,c'$ as the $y\,z$ - type extremals; ... and so forth.

e) Another key observation is that for $\frac{y_f}{z_f} > 1$ the z - type extremals are globally minimal and for $\frac{y_f}{z_f} < 1$ the y - type extremals are globally minimal. The cost of the z - type extremals is always less than the cost of the $z\,y$ - type extremals, $z\,y\,z$ - type extremals, and so forth. Similarly, the cost of the y - type extremals is always less than the cost of the $y\,z$ - type extremals, $y\,z\,y$ - type extremals, and so forth.

Example 2.2

Sample extremal trajectories are obtained for the case when $y_f = 0.8$ $z_f = 1.0$ $t_f = 2.0$ secs. The y - type extremal provides the global minimum and has a cost $c(t_f) \simeq 1.1254$. Fig.[6] shows the relevant time histories. The z - type extremal had a cost $c(t_f) \simeq 1.4392$. The $z\,y$ - type extremal had a cost $c(t_f) \simeq 2.3269$, while the $z\,y\,z$ - type extremal had a cost $c(t_f) \simeq 4.0927$.

Figure [7] shows schematically the domains of existence of some of these sub-families.

Some properties of extremal solutions

We now restrict our attention to those sub-classes of extremal solutions, which amount to scaling of the boundary conditions prescribed in any of the preceding three categories. Symbolically we may think of the left side of the system [2.5.1] as defining a vector-valued function G :

$$G(y_f, z_f, t_f, \mu, A, C) : \mathcal{R}_+ \times \mathcal{R}_+ \times \mathcal{R}_+ \times \mathcal{R}_+ \times \mathcal{R} \times \mathcal{R} \rightarrow \mathcal{R}^3$$

where, $\mathcal{R}_+ = \{ x \mid x \geq 0; x \in \mathcal{R} \}$. If $G(y_f, z_f, t_f, \mu, A, C) = \{0\}$ then we say that A, C, and μ are a local solution of [2.5.1] for prescribed values of y_f, z_f, and t_f.

Hypothesis

For a given y_{f_1}, z_{f_1}, and t_{f_1}, let A_1, C_1, and μ_1 be such that :

$$G(y_{f_1}, z_{f_1}, t_{f_1}, \mu_1, A_1, C_1) = \{0\}$$

Property 1. Scaling y_f and z_f

Let $y_{f_2} = \lambda y_{f_1}$, $z_{f_2} = \lambda z_{f_1}$ *and* $t_{f_2} = t_{f_1}$, *where* λ *is a real number, not zero, then:*

$G(y_{f_2}, z_{f_2}, t_{f_2}, \mu_1, \lambda A_1, \lambda C_1) = \{0\}$, *i.e.,* $A_2 = \lambda A_1$, $C_2 = \lambda C_1$ *and* $\mu_2 = \mu_1$.

It is evident then, if we scale the boundary conditions such that the ratio $(\frac{y_f}{z_f})$ remains fixed, the extremal solutions for this entire sub-class of boundary conditions may be obtained by merely scaling one of its members.

Property 2. Scaling of final time t_f

Let $y_{f_2} = y_{f_1}$, $z_{f_2} = z_{f_1}$ *and* $t_{f_2} = \lambda t_{f_1}$, *where* λ *is a positive real number, then it can be shown:*

$$G(y_{f_2}, z_{f_2}, t_{f_2}, \frac{\mu_1}{\lambda^2}, \frac{A_1}{\lambda}, \frac{C_1}{\lambda}) = \{0\} \text{ , i.e., } A_2 = \frac{A_1}{\lambda}, \; C_2 = \frac{C_1}{\lambda} \text{ and } \mu_2 = \frac{\mu_1}{\lambda^2} .$$

It follows then the extremal solutions for this sub-class of boundary conditions may be obtained by scaling one of its members.

Property 3. Monotoncity of cost with t_f

As a direct consequence of Property 2, we can show the following important property of extremal solutions. Holding the boundary conditions y_f and z_f fixed, if we scale the final time t_f as $t'_f = \lambda\, t_f$,then it can be shown that:

$$c(t'_f) = \frac{c(t_f)}{\lambda} .$$

In particular, if we increase (decrease) the final time, holding the boundary conditions y_f and z_f fixed, then cost decreases (increases). This seemingly obvious result is not necessarily true for all nonlinear systems. Using reciprocity

arguments, we can obtain ***minimum time*** solutions for a given maximum value of ***control effort***, by picking the smallest time t_f such that $c(t_f)$ does not exceed the prescribed maximum effort.

Here we digress to mention that the analysis for the case when the value of the isoperimetric constraint, ℓ, is other than zero, has been omitted for reasons of brevity. However, we would like to point out that multiple extremal solutions exist, which are similar in character to those found above. In addition, there is an emergence of a new type of extremal, one in which $y(t) \equiv z(t)$. Also, the envelopes containing the various extremal sub-families in the space of boundary conditions, y_f, z_f, ℓ, and t_f, are quite intricate. Moreover, for large values of ℓ, the *approximate problem* departs significantly from the *exact-problem*, since the cross-coupling terms which were ignored, become significant.

We have seen from the two examples presented in this section, that we may perhaps have a host of candidate minimizers. It is, therefore, imperative that we test the second-order necessary conditions to establish local optimality for these candidates. In the following section, the Jacobi test is developed to test candidate extremals.

2.6: Second-Order Necessary Conditions - Jacobi Test

Investigation of the first-order necessary conditions have shown that, there are, in general, several distinct candidate minimizers. Now it remains to establish, whether or not, each of these extremals also furnishes a relative minimum. The task of establishing local optimality for these extremals leads to the examination of second variation. In the classical Calculus of Variations, the Jacobi condition provides a check for non-negativity of second variation. A test extremal without *corners*, satisfying the strengthened Legendre-Clebsch condition is assured of local optimality if it passes the Jacobi-test successfully. These ideas have been extended to the more general problem of normal nonsingular optimal control by several investigators, notably Breakwell and Ho [24], Moyer [25], Kelley and Moyer [26], and Jacobson [27].

It has been well established that for extremals with end points sufficiently close together, the strengthened Legendre-Clebsch condition ensures the non-negativity of the second variation, thus for such extremals, if the Legendre-Clebsch condition is strictly satisfied, it yields a weak relative minimum [26]. For extremals of finite length, however, the examination of second variation for all admissible neighboring paths leads to an analysis analogous to the accessory-minimum problem of the Calculus of Variations. The crux of the accessory-minimum problem, described best by Kelley and Moyer, " ... amounts

to a search for a system of admissible variations, not identically zero, which offers the most severe competition in the sense of minimizing the second variation. If a system of (nonzero) variations can be found which gives to the second variation the value zero, then it clear that a neighboring path is competitive and that the test extremal furnishes at best an improper minimum of J and at worst merely a stationary value. The first value of $t = t^* > t_0$ for which such a nontrivial system can be found defines a ***conjugate point.***"

Recall that the *approximate problem* is ***regular***, i.e., all its extremals satisfy the *convexity* condition. Thus it *suffices* to show that if a test extremal satisfies the second-order test, it provides a relative minimum. Following the procedure outlined in Reference [26], the accessory-minimum problem for the *approximate problem,* equations [2.4.2]-[2.4.9], is stated as follows. The equations of variation, obtained by linearizing the equations [2.4.2]-[2.4.5] about a test-extremal are :

$$\dot{\delta x} = y\delta z + z\delta y \qquad [2.6.1]$$

$$\dot{\delta y} = \delta u \qquad [2.6.2]$$

$$\dot{\delta z} = \delta v \qquad [2.6.3]$$

$$\dot{\delta c} = u\delta u + v\delta v \qquad [2.6.4]$$

We seek to minimize the second variation,

$$\delta^2 \mathcal{J} = \frac{1}{2}\int_0^{t_f} [2\mu\delta y\delta z + \lambda_0(\delta u^2 + \delta v^2)]dt \qquad [2.6.5]$$

over all possible admissible variations. The Euler-Lagrange equations for the accessory-minimum problem are obtained to be,

$$\dot{\delta\mu} = 0 \qquad [2.6.6]$$

$$\dot{\delta\lambda}_y = -(\mu\delta z + z\delta\mu) \qquad [2.6.7]$$

$$\dot{\delta\lambda}_z = -(\mu\delta y + y\delta\mu) \qquad [2.6.8]$$

$$\dot{\delta\lambda}_0 = 0 \qquad [2.6.9]$$

while the minimum principle for the accessory-minimum problem gives

$$\delta u = -\frac{1}{\lambda_0}(\delta\lambda_y + u\delta\lambda_0) \qquad [2.6.10]$$

$$\delta v = -\frac{1}{\lambda_0}(\delta\lambda_z + v\delta\lambda_0) \qquad [2.6.11]$$

Since, we are seeking competitors of the test-extremal, the variation, if admissible, must satisfy the boundary conditions of the test-extremal, i.e.,

$$\begin{aligned} \delta x(0) &= 0 \qquad & \delta y(0) &= 0 \\ \delta z(0) &= 0 \qquad & \delta c(0) &= 0 \end{aligned} \qquad [2.6.12a]$$

and,

$$\begin{aligned} \delta x(t_f) &= 0 \qquad & \delta y(t_f) &= 0 \\ \delta z(t_f) &= 0 \qquad & \delta\lambda_0(t_f) &= 0 \end{aligned} \qquad [2.6.12b]$$

Here we digress to mention that there exists a first integral

$$\frac{d}{dt}(\mu\delta x + \lambda_y\delta y + \lambda_z\delta z + \lambda_0\delta c) = 0$$

or,

$$\mu\delta x + \lambda_y\delta y + \lambda_z\delta z + \lambda_0\delta c = \text{ constant} \qquad [2.6.13]$$

which may be verified by differentiation and using the relevant equations. Making use of the boundary condition [2.6.12a], we can evaluate the constant to be zero. Further, if we evaluate [2.6.13] at t_f, we get,

$$\lambda_0(t_f)\,\delta c(t_f) = 0 \qquad [2.6.14]$$

Since $\lambda_0(t_f)$ was prescribed to be unity (using the normality assumption), $\delta c(t_f)$ must be zero.

The equation [2.6.13] has an interesting geometric interpretation. If we think about the locus of end-points obtained by extremals, originating from a fixed point in the state-space (the origin in our case), stopped at fixed final time, the three-dimensional manifold defines the isochronal hypersurface or the wavefront [25]. The variations $\delta X^T = (\delta x\ \delta y\ \delta z\ \delta c)$ lie in the tangent manifold of the wavefront. Thus, the adjoint vector must be normal to the wavefront.

The equations [2.6.1] - [2.6.4] and [2.6.6] - [2.6.9] is a set of linear, although time-varying, differential equations, which along with the optimality conditions

[2.6.10] - [2.6.11], and the boundary conditions defined by [2.6.12a], and [2.6.12b] constitutes a two-point boundary-value problem. Note that the trivial solution satisfies all the necessary conditions and provides the minimum value for $\delta^2\mathscr{J}$ equal to zero. Furthermore, zero is the global minimum of $\delta^2\mathscr{J}$, as can be verified by straightforward integration of equation [2.6.5], using the Euler-Lagrange equations for the accessory minimum problem. Therefore, our search for competition, reduces to finding a non-trivial solution of the above-mentioned linear two-point boundary-value problem. However, we must specifically exclude those solutions which amount to a mere scaling of the adjoint vector of the test extremal.

Owing to the linearity and homogeneity of the state and adjoint variations, we may express the state variation in terms of the unspecified initial values of the adjoint variations, as follows,

$$\begin{bmatrix} \delta x(t) \\ \delta y(t) \\ \delta z(t) \\ \delta\lambda_0(t) \end{bmatrix} = \begin{bmatrix} \dfrac{\partial x(t)}{\partial \mu} & \dfrac{\partial x(t)}{\partial \lambda_{y_0}} & \dfrac{\partial x(t)}{\partial \lambda_{z_0}} & \dfrac{\partial x(t)}{\partial \lambda_{0_0}} \\ \dfrac{\partial y(t)}{\partial \mu} & \dfrac{\partial y(t)}{\partial \lambda_{y_0}} & \dfrac{\partial y(t)}{\partial \lambda_{z_0}} & \dfrac{\partial y(t)}{\partial \lambda_{0_0}} \\ \dfrac{\partial z(t)}{\partial \mu} & \dfrac{\partial z(t)}{\partial \lambda_{y_0}} & \dfrac{\partial z(t)}{\partial \lambda_{z_0}} & \dfrac{\partial z(t)}{\partial \lambda_{0_0}} \\ \dfrac{\partial \lambda_0(t)}{\partial \mu} & \dfrac{\partial \lambda_0(t)}{\partial \lambda_{y_0}} & \dfrac{\partial \lambda_0(t)}{\partial \lambda_{z_0}} & \dfrac{\partial \lambda_0(t)}{\partial \lambda_{0_0}} \end{bmatrix} \begin{bmatrix} \delta\mu(0) \\ \delta\lambda_y(0) \\ \delta\lambda_z(0) \\ \delta\lambda_0(0) \end{bmatrix} \qquad [2.6.15]$$

If for any $t_c \in (0, t_f]$, we can find a non-zero set of initial adjoint variations such that the column vector on the left is zero, then a non-trivial solution of the

accessory minimum problem is possible. The time t_c is then the conjugate time. For the purposes of locating the conjugate time, we may use the vanishing of the determinant of the test matrix as the criteria. Further, the last equation amounts to scaling of the multiplier $\lambda_0 + \delta\lambda_0$, therefore we may delete the last row and column of the above matrix without affecting its rank. The question of whether or not a particular extremal is locally optimal, now reduces to studying whether the following sub-matrix has a drop in rank on the interval $(0, t_f]$.

$$\Phi(t) = \begin{bmatrix} \frac{\partial x}{\partial \mu} & \frac{\partial x}{\partial \lambda_{y_0}} & \frac{\partial x}{\partial \lambda_{z_0}} \\ \frac{\partial y}{\partial \mu} & \frac{\partial y}{\partial \lambda_{y_0}} & \frac{\partial y}{\partial \lambda_{z_0}} \\ \frac{\partial z}{\partial \mu} & \frac{\partial z}{\partial \lambda_{y_0}} & \frac{\partial z}{\partial \lambda_{z_0}} \end{bmatrix}(t) \qquad [2.6.16]$$

If $\Phi(t)$ has full rank, or alternatively if $|\Phi(t)| \neq 0 \ \forall t \in (0, t_f]$, then the extremal passes the second-order test successfully, and the test extremal does indeed furnish a relative minimum. If $|\Phi(t_c)| = 0$ for some $t_c \in (0, t_f]$, then neighboring competition exists and the local optimality of the test extremal is in question. The elements of the test matrix $\Phi(t)$, or the sensitivity of the states with respect to the initial adjoints can be obtained analytically and are easily shown to be the following :

$$\frac{\partial x}{\partial \mu} = -\frac{3}{8\,\mu^{\frac{5}{2}}}(A^2 \sin 2\sqrt{\mu}\, t + C^2 \sinh 2\sqrt{\mu}\, t) + \frac{A^2 t}{4\mu^2}(\cos 2\sqrt{\mu}\, t + 2) \qquad [2.6.17a]$$
$$+ \frac{C^2 t}{4\mu^2}(\cosh 2\sqrt{\mu}\, t + 2)$$

$$\frac{\partial x}{\partial \lambda_{y_0}} = -(A + C)\frac{t}{2\mu} + \frac{1}{4\mu^{\frac{3}{2}}}(A \sin 2\sqrt{\mu}\, t + C \sinh 2\sqrt{\mu}\, t) \qquad [2.6.17b]$$

$$\frac{\partial x}{\partial \lambda_{z_0}} = (A - C)\frac{t}{2\mu} - \frac{1}{4\mu^{\frac{3}{2}}}(A \sin 2\sqrt{\mu}\, t - C \sinh 2\sqrt{\mu}\, t) \qquad [2.6.17c]$$

$$\frac{\partial y}{\partial \mu} = \frac{1}{2\mu^{\frac{3}{2}}}(A \sin \sqrt{\mu}\, t + C \sinh \sqrt{\mu}\, t) - \frac{t}{2\mu}(A \cos \sqrt{\mu}\, t + C \cosh \sqrt{\mu}\, t) \qquad [2.6.17d]$$

$$\frac{\partial y}{\partial \lambda_{y_0}} = -\frac{1}{2\sqrt{\mu}}(\sin \sqrt{\mu}\, t + \sinh \sqrt{\mu}\, t) \qquad [2.6.17e]$$

$$\frac{\partial y}{\partial \lambda_{z_0}} = \frac{1}{2\sqrt{\mu}}(\sin \sqrt{\mu}\, t - \sinh \sqrt{\mu}\, t) \qquad [2.6.17f]$$

$$\frac{\partial z}{\partial \mu} = -\frac{1}{2\mu^{\frac{3}{2}}}(A \sin \sqrt{\mu}\, t - C \sinh \sqrt{\mu}\, t) + \frac{t}{2\mu}(A \cos \sqrt{\mu}\, t - C \cosh \sqrt{\mu}\, t) \qquad [2.6.17g]$$

$$\frac{\partial z}{\partial \lambda_{y_0}} = \frac{1}{2\sqrt{\mu}}(\sin \sqrt{\mu}\, t - \sinh \sqrt{\mu}\, t) \qquad [2.6.17h]$$

$$\frac{\partial z}{\partial \lambda_{z_0}} = -\frac{1}{2\sqrt{\mu}}(\sin \sqrt{\mu}\, t + \sinh \sqrt{\mu}\, t) \qquad [2.6.17i]$$

The determinant can then be evaluated as

$$-8\,|\Phi(t)|\,\mu^{\frac{7}{2}} = A^2 \sinh\sqrt{\mu}\,t\,[\sin\sqrt{\mu}\,t\,(2\sqrt{\mu}\,t + \sin 2\sqrt{\mu}\,t) - (2\sqrt{\mu}\,t)^2\cos\sqrt{\mu}\,t\,] + C^2 \sin\sqrt{\mu}\,t\,[\sinh\sqrt{\mu}\,t\,(2\sqrt{\mu}\,t + \sinh 2\sqrt{\mu}\,t) - (2\sqrt{\mu}\,t)^2\cosh\sqrt{\mu}\,t\,] \qquad [2.6.18]$$

Now we can state the following criteria,

Conjugate point criteria

If for a given test extremal, characterized uniquely by the constants A, C, and μ, *there exists a time* $t_c \in (0, t_f]$, *such that* $|\Phi(t_c)| = 0$, *then* t_c *is labeled to be the conjugate time and the point* $(t_c, x(t_c), y(t_c), z(t_c))$ *is said to be conjugate to* (0,0,0,0) .

The major result of the investigation of the second-order necessary conditions for the *approximate problem* is that all the extremals which were labelled to be zy - type, yz - type, zyz - type extremals, and so forth, were found to satisfy the above mentioned conjugate point criteria. All these extremal types, although satisfying the stationarity conditions fail the second-order necessary condition, and are thus not minimizing solutions. Further, it was ascertained computationally that all the extremals of the zy - type or yz - type (extremal solutions along the arc *bc* in Fig.[5a], or arc $b'c'$ in Fig.[5b]) had one conjugate point, extremals of zyz - type or yzy - type had two conjugate points, and so forth.

A less general result than above may be deduced analytically using equation [2.6.18]. For strictly positive values of the argument $\sqrt{\mu}\,t$, we may rewrite equation [2.6.18] in the following form :

$$-8\,|\Phi(t)|\,\mu^{\frac{7}{2}} = g_2(\sqrt{\mu}\,t)\sinh\sqrt{\mu}\,t\,[A^2\,\frac{g_1(\sqrt{\mu}\,t)}{g_2(\sqrt{\mu}\,t)} + C^2\sin\sqrt{\mu}\,t\,] \quad [2.6.19]$$

where,

$$g_1(\sqrt{\mu}\,t) = \sin\sqrt{\mu}\,t\,(2\sqrt{\mu}\,t + \sin 2\sqrt{\mu}\,t) - (2\sqrt{\mu}\,t)^2\cos\sqrt{\mu}\,t$$

$$g_2(\sqrt{\mu}\,t) = (2\sqrt{\mu}\,t + \sinh 2\sqrt{\mu}\,t) - (2\sqrt{\mu}\,t)^2 coth\sqrt{\mu}\,t$$

Note,

i) $\sinh\sqrt{\mu}\,t > 0 \quad \forall\ \sqrt{\mu}\,t > 0$

ii) $g_2(\sqrt{\mu}\,t) > 0 \quad \forall\ \sqrt{\mu}\,t > 0$

Thus the term outside the bracket in [2.6.19] is positive for positive arguments. The sign of the right hand side (RHS) of the [2.6.19] is governed by the signs of $g_1(\sqrt{\mu}\,t)$ and $\sin\sqrt{\mu}\,t$ and the relative magnitudes of their coefficients. The function $g_1(\sqrt{\mu}\,t)$ is positive for the range $0 < \sqrt{\mu}\,t < \omega_c/2.0$ (where $\omega_c \simeq 9.0$) and has a zero crossing at $2\sqrt{\mu}\,t = \omega_c$. It is evident that, irrespective of the values of A and C , the RHS can never be zero if $2\sqrt{\mu}\,t \in (0,\ 2\pi)$ and must have a zero crossing if $2\sqrt{\mu}\,t$ exceeds the value of ω_c. Therefore all extremals with $\omega < 2\pi$ (recall $\omega = 2\sqrt{\mu}\,t_f$) can never have a conjugate point and extremal solutions

with $\omega > \omega_c$ must have at least one conjugate point. For values of ω in the range $2\pi \leq \omega \leq \omega_c$, the relative magnitudes of A and C determine whether or not a particular extremal has a conjugate point. It is interesting to note that the above mentioned grey area starts when the extremal loses its global minimality, i.e., at the Darboux point† . It is also comforting to have the reassurance that over the entire positive range of y_f/z_f and t_f, we have at least one extremal solution which satisfies all the necessary conditions for local minimum.

Further, the above analytic development of the Jacobi necessary condition was corroborated with the computational procedure based on the difference-quotient scheme suggested in Ref. [26]. Also, the *second* wavefront normal was constructed as suggested by Moyer in Ref. [25], and the collinearity of the two wavefront normals was used as a benchmark to verify all aspects of the computer program. Further, it was verified the wavefront normals switch from parallel to anti-parallel at the so called envelope contact point, or the conjugate point. The conjugate point conditions of the Theorems [3.1], [4.1], [4.2], [4.3], and [4.4] of Ref. [25] were all found to be satisfied. This geometric approach provided exceptional insight of the second-order necessary conditions and proved to be an excellent procedure to test for them.

---

† Instances of Darboux Points in extremal trajectories are reported in Refs. [28] and [29].

It may also be noted that the test for sufficiency conditions for a local minimum, presented by Bryson and Ho (Ref. [3]), based on the backward sweep method or the Riccati type solution of the accessory minimum problem, did not prove to be successful due to the following reason. The state weighting matrix of the LQR problem, H_{xx} in eqn.(6.1.16) in Ref. [3], turns out to be an indefinite matrix for the *approximate problem*, irrespective of the test extremal. It is well known that in such cases, the boundedness of the solution of the Riccati equation is not guaranteed. In fact, the less stringent sufficiency conditions for the boundedness of the solution of the Riccati equation given by Jacobson in Ref. [27] were not satisfied for the *approximate problem.* It was found that, with the exception of few special cases, the Riccati equation had a finite escape time, usually well before the conjugate time, if there was one. It was pointed out in Ref. [3], unboundedness of the solution of the Riccati equation did not necessarily violate the conjugate point criteria, and the *approximate problem* serves yet another testimony to that fact.

For purposes of illustration a typical example is presented. For the case when $y_f = 0.8$, $z_f = 1.0$, and $t_f = 2.0$ (Example 2.2), the z - type extremal and the y - type extremal did not have any conjugate points. The $z\,y$ - type extremal had a conjugate point at $t_c = 1.5305$ sec. The $z\,y\,z$ - type extremal had conjugate points at $t_{c1} = 0.9417$ sec and $t_{c2} = 1.5937$ sec.

2.7: Concluding Remarks

In this Chapter we analyzed the *approximate problem.* This problem retains the qualitative features of optimal control of rigid-body angular motion with two controllers aligned along its two principal axes of inertia. Any motion about the third axis must be controlled only indirectly. A survey of the first-order necessary conditions for optimality for the *approximate problem* showed an elaborate extremal structure. A classification in terms of sub-families of extremal solutions is presented. It is shown that over a large range of boundary conditions, there are in general, several distinct candidate minimizers. This rich extremal structure is inherent of the state equations, since qualitatively speaking, the roles of state variables y and z in influencing the indirectly controlled state x, may be interchanged. Some interesting properties of the extremal solutions are also deduced.

Analysis of the second-order conditions showed that we could narrow our choices for the minimizing solution down to two sub-families of extremals. The domains of reachability for these two sub-families is also established. Analytic arguments based on the conjugate point criteria showed that there exists at least one extremal solution over the entire range of final conditions, which passes the Jacobi test. Moreover, the locus of Darboux points are obtained, which are found to demarcate the domains over which the two sub-families were globally minimal.

The overall understanding of the *approximate problem* serves to provide guidelines in sorting out extremal sub-family structure of controlling the rigid-body angular velocity with two controllers.

Chapter 3: Exact Problem

3.1: Introduction

In this chapter we investigate the problem of optimal angular rate control, using the *exact* dynamic model. In the following sections, we define the considered optimal control problem and present an analysis of first and second-order necessary conditions for optimality.

3.2: Problem Statement

The *exact-problem*, introduced in the previous chapter, is restated in this section. Consider the rotational dynamics of a rigid body in a body-fixed coordinate system. The origin of the coordinate system is located at the center of mass of the body and the axes are aligned along the principal axes. Let ω_x, ω_y, and ω_z be

the components of angular velocity, denoting the roll, pitch, and the yaw rates respectively. Assume the body is free of all external moments except the applied control moments. Then the Euler equations of motion describing the rotational dynamics of the rigid body are :

$$\dot{\omega}_x = J_x \omega_y \omega_z + \frac{u_x}{I_x} \qquad [3.2.1]$$

$$\dot{\omega}_y = J_y \omega_x \omega_z + \frac{u_y}{I_y} \qquad [3.2.2]$$

$$\dot{\omega}_z = J_z \omega_x \omega_y + \frac{u_z}{I_z} \qquad [3.2.3]$$

where $J_x = \frac{I_y - I_z}{I_x}$, $J_y = \frac{I_z - I_x}{I_y}$, $J_z = \frac{I_x - I_y}{I_z}$, and

I_x, I_y, I_z are the principal moments of inertia, and

u_x, u_y, and u_z are the rolling, pitching, and yawing moment, respectively. We shall consider the case when $u_x(t) \equiv 0$.

We seek to perform an arbitrary point-to-point maneuver (from a given fixed point in state space to another) in a given time t_f, while minimizing a weighted integral norm on control, defined to be the *control effort*, as follows

$$\mathcal{J} = \frac{1}{2} \int_0^{t_f} [(\alpha_y u_y)^2 + (\alpha_z u_z)^2] dt \qquad [3.2.4]$$

where α_y and α_z are non-zero control weighting parameters.

Note the parameters of the above stated optimal control problem are :

i) boundary conditions, namely : $\omega_x(0), \omega_y(0), \omega_z(0), \omega_x(t_f), \omega_y(t_f), \omega_z(t_f)$, and t_f

ii) inertia characteristics : I_x, I_y, and I_z

iii) ratio of control weighting parameters : $\frac{\alpha_y}{\alpha_z}$

In an effort to consolidate the ensuing results for a wide spectrum of applications, we consider the following scaled version of the above stated problem. Assuming that $I_z > I_y > I_x$, which is typically true for combat aircraft configurations, we define the following transformation :

$$p = c_p \omega_x \qquad q = c_q \omega_y \qquad r = c_r \omega_z$$
$$M = \frac{c_q}{I_y} u_y \qquad N = \frac{c_r}{I_z} u_z \qquad [3.2.5]$$

where $c_p = \sqrt{J_y' J_z'}$, $c_q = \sqrt{J_x' J_z'}$, $c_r = \sqrt{J_x' J_y'}$, and

$J_x' = -J_x$, $J_y' = J_y$ and $J_z' = -J_z$.

The equations of motion, equations [3.2.1]-[3.2.3], are transformed to

$$\dot{p} = -qr \qquad [3.2.6]$$

$$\dot{q} = pr + M \qquad [3.2.7]$$

$$\dot{r} = -pq + N \qquad [3.2.8]$$

For a particular choice of the ratio of control weighting parameters,

$$\frac{\alpha_y}{\alpha_z} = \frac{c_q I_z}{c_r I_y},$$

whereby we weight equally the control *influence* in $\dot{q}$ and $\dot{r}$ equations, the *control effort*, equation [3.2.4], transforms to,

$$\mathcal{J} = \frac{1}{2}\int_0^{t_f} [M^2 + N^2]dt. \qquad [3.2.9]$$

The problem of control remains the same, i.e., we seek to perform a point-to-point maneuver in a given time t_f, subject to dynamics given by equations [3.2.6]-[3.2.8], while minimizing the *control effort*, given by [3.2.9]. The parameters for this problem are the initial and final conditions of the states p, q, and r, and the final time t_f. We wish to emphasize that the scaled problem retains the important ingredients of the unscaled problem, while reducing the number of parameters to be considered in analysis. All subsequent analysis pertains to the scaled problem.

3.3: Derivation of the First-Order Necessary Conditions

For convenience, we analyze the above stated problem for first-order necessary conditions for optimality, in the Mayer formulation. In this formulation the cost

appears as an additional state, c . We seek to minimize $c(t_f)$ for a given point-to-point maneuver in a prescribed time t_f. The state equations are :

$$\dot{p} = -qr \qquad [3.3.1]$$

$$\dot{q} = pr + M \qquad [3.3.2]$$

$$\dot{r} = -pq + N \qquad [3.3.3]$$

$$\dot{c} = \frac{1}{2}(M^2 + N^2) \qquad [3.3.4]$$

where the controls $M(.)$ and $N(.)$ are real-valued functions, with no prescribed bounds. The boundary conditions are prescribed to be :

$$p(0) = p_0 \text{ and } p(t_f) = p_f \qquad [3.3.5]$$

$$q(0) = q_0 \text{ and } q(t_f) = q_f \qquad [3.3.6]$$

$$r(0) = r_0 \text{ and } r(t_f) = r_f \qquad [3.3.7]$$

$$c(0) = 0 \qquad [3.3.8]$$

Following the conventional practice, we define the variational-Hamiltonian $\mathscr{H}$ as,

$$\mathscr{H} = \frac{\lambda_0}{2}(M^2 + N^2) + \lambda_p(-qr) + \lambda_q(pr + M) + \lambda_r(-pq + N). \qquad [3.3.9]$$

where λ_0 is the adjoint variable associated with the cost, and

λ_p, λ_q, and λ_r are the adjoint variables associated with the states p, q, and r, respectively.

Using a version of Pontryagin's Minimum Principle, which states that an optimal control (M^*, N^*) is one which minimizes the Hamiltonian $\mathscr{H}$ over all possible controls (M, N), we derive, quite simply the extremal control M^*, N^* as,

$$M^*(t) = -\lambda_q^*(t)/\lambda_0^*(t) \qquad [3.3.10]$$

$$N^*(t) = -\lambda_r^*(t)/\lambda_0^*(t) \qquad [3.3.11]$$

where the adjoint variables λ_0, λ_p, λ_q, and λ_r satisfy

$$\dot{\lambda}_0 = 0 \qquad [3.3.12]$$

$$\dot{\lambda}_p = -\lambda_q r + \lambda_r q \qquad [3.3.13]$$

$$\dot{\lambda}_q = \lambda_p r + \lambda_r p \qquad [3.3.14]$$

$$\dot{\lambda}_r = \lambda_p q - \lambda_q p \qquad [3.3.15]$$

If we assume normality, the transversality condition gives

$$\lambda_0(t_f) = 1, \qquad [3.3.16]$$

and we obtain $\lambda_0(t) \equiv 1$ by integrating equation [3.3.12]. Further, the problem is *regular*, since the matrix of the second partial derivatives of $\mathscr{H}$ with respect to controls M, N is the identity matrix. Thus, the Legendre-Clebsch condition is strictly satisfied.

The state equations, equations [3.3.1]-[3.3.4], the adjoint equations, equations [3.3.12]-[3.3.15] along with extremal control [3.3.10]-[3.3.11] and boundary conditions defined by [3.3.5]-[3.3.8] and [3.3.16], constitute a nonlinear two-point boundary-value problem (TPBVP). Numerical solutions of the TPBVP are obtained iteratively using a multiple-shooting algorithm [30]. The initial guess values of the state-adjoint trajectory, required by TPBVP solver, are obtained using the analytical solutions of the *approximate problem* presented in the previous chapter.

3.4: Extremal Families

Recall that extremals are paths that satisfy the usual first-order necessary conditions. In the present case, they are the solutions of the TPBVP defined in the preceding section. Observe that the extremal solutions of this TPBVP are in general, a seven parameter family of solutions. Of the many choices for these parameters, one may choose for instance, p_0, q_0, r_0, p_f, q_f, r_f, and t_f as these seven parameters. Since the problem is *non-linear* with split boundary conditions, *uniqueness* of the extremal solution is **not** guaranteed, for specified values of the above parameter list.

In this section we will show, via numerical examples, that for a given set of initial and final conditions, there are, in general, *several* distinct extremal solutions.

Each extremal solution is then classified to belong to a distinct sub-family, based on the nature of the extremal control. Further in a reduced parameter space, we shall establish domains of existence of some of the extremal sub-families and show that these domains overlap. In the regions of overlap, where more than one extremal solution exists, a locus of Darboux points will be obtained. It will be shown, via a numerical survey, that there is a loss of global minimality associated with the Darboux point. The foregoing discussion serves to provide an intuitive backdrop and now we shall examine, in some detail, the preceding notions.

Multiple Extremal Solutions

Examination of equation [3.3.1] shows that the roll dynamics is governed solely through the cross-coupling term $q\,r$. For some boundary conditions, it is conceivable that the pitch motion, q , is dominant in shaping the roll motion, while for other boundary conditions the yaw motion, r, assumes that responsibility. This *dichotomy* in the assumed dominant role in governing roll motion yields two basic sub-families of extremals. The one in which q is more *dynamic* is labeled to be the q - type extremal and similarly if r is more *dynamic* the extremal is called the r - type extremal. However, note that the roles of q and r are not identically interchangeable, as was the case in the *approximate problem.* In order to exhibit this phenomena and also to establish the nomenclature for the classification of different extremals, we present the following numerical example.

Example 3.1

For the following initial and final data :

$p_0 = 0 \quad q_0 = 0 \quad r_0 = 0$

$p_f = 0 \quad q_f = 0.3 \quad r_f = 0.3$.

$t_f = 2$,

we obtained the following extremal solutions.

i) **Extremal 1** : labeled as q - type extremal, corresponds to

$\lambda_p(0) \simeq -2.4548, \quad \lambda_q(0) \simeq 0.2240, \quad \lambda_r(0) \simeq -0.3055$ and has a cost $\simeq 0.1403$.

Fig. [8] shows the extremal trajectory and the control histories.

ii) **Extremal 2** : labeled as r - type extremal, corresponds to

$\lambda_p(0) \simeq -2.4799, \quad \lambda_q(0) \simeq -0.3026, \quad \lambda_r(0) \simeq 0.2209$ and has a cost $\simeq 0.1434$.

Fig. [9] shows the extremal trajectory and the control histories.

iii) **Extremal 3** : labeled as $q\,r$ - type extremal, corresponds to

$\lambda_p(0) \simeq -9.8880, \quad \lambda_q(0) \simeq 0.3721, \quad \lambda_r(0) \simeq -0.3790$ and has a cost $\simeq 0.2833$.

Fig. [10] shows the extremal trajectory and the control histories.

iv) **Extremal 4** : labeled as $r\,q$ - type extremal, corresponds to

$\lambda_p(0) \simeq -9.8512, \quad \lambda_q(0) \simeq -0.3800, \quad \lambda_r(0) \simeq 0.3728$ and has a cost $\simeq 0.2822$.

Fig. [11] shows the extremal trajectory and the control histories.

v) **Extremal 5** : labeled as $q\,r\,q$ - type extremal, corresponds to

$\lambda_p(0) \simeq -22.1909, \quad \lambda_q(0) \simeq 0.4606, \quad \lambda_r(0) \simeq -0.4609$ and has a cost $\simeq 0.4238$.

Fig. [12] shows the extremal trajectory and the control histories.

Observe that, since the initial and final values of the roll rate p , are zero, to achieve such a maneuver requires that the sign of the product $q\,r$ (equation [3.3.1]) change on the interval $[0, t_f]$. If one of the variables remains of a single sign then the other must be more dynamic or control-like, yielding the q - type and the r - type extremals. Furthermore, the maneuver may be achieved in two stages, although with an increase in cost, where first q (r) then r (q) assumes the role of a control-like variable, yielding extremals labeled to be $q\,r$ ($r\,q$) - type extremals. One may extend the same arguments for the more oscillatory solutions, like the $q\,r\,q$ - type extremal. For brevity, we do not show these more oscillatory solutions.

Here we digress to mention that angular *positions*, obtained by simply integrating the kinematic equations along a extremal trajectory, are *different* for the various extremals presented above. For instance, if we start out straight and level, $\psi_0 = \theta_0 = \phi_0 = 0^o$, we end up with the following angular orientations:

i) $\psi_f = 22.47^o, \theta_f = -2.10^o$ and $\phi_f = -0.58^o$ for the q - type extremal.

ii) $\psi_f = -1.85^o, \theta_f = 22.02^o$ and $\phi_f = 2.04^o$ for the r - type extremal.

iii) $\psi_f = 5.51^o, \theta_f = 5.45^o$ and $\phi_f = 0.74^o$ for the $q\,r$ - type extremal.

iv) $\psi_f = 5.48^o, \theta_f = 5.35^o$ and $\phi_f = 1.16^o$ for the $r\,q$ - type extremal.

v) $\psi_f = 6.04^o, \theta_f = 1.24^o$ and $\phi_f = 0.48^o$ for the $q\,r\,q$ - type extremal.

However, note that angular *position* coordinates are not included in the optimal control problem.

Envelopes of Extremal sub-families

With a possibility of a multitude of extremal solutions, some of which are shown in Example 3.1, we next investigate the domains of existence, in the parameter space, of the different types of extremal solution. To get a better grasp on this problem, we fix the values for five of the seven parameters. For $p_0 = q_0 = r_0 = p_f = 0$ and $t_f = 2.0$, we investigate the extremal solutions by varying the other two parameters, namely q_f and r_f. In this reduced parameter space, we pick an extremal solution and carefully deform the boundary conditions, q_f and r_f, solving a series of TPBVPs ensuring that we track the same extremal solution type. For example, we pick the q - type extremal of Example 3.1, fix $r_f = 0.3$, and traverse the boundary conditions along the arc $a\,c$ (see Fig.[13]). It was found that no members of the q - type sub-family could be found beyond the point b. The point b is referred to as the *envelope contact point.* We carry out the same procedure for different values of r_f and establish the locus of the envelope contact points for the q - type extremal sub-family, shown as arc Ob in Fig.[13]. Above the envelope we have members of the q - type sub-family of extremals, but none below.

Similarly, we pick the r - type extremal of Example 3.1, fix $q_f = 0.3$, and traverse the boundary conditions along the arc $a\,e$ (see Fig.[13]). It was found that no members of the r - type sub-family could be found above the point d. Following the same procedure as above, we establish the locus of the envelope contact points for the r - type extremal sub-family, shown as arc Od in Fig.[13]. The broken

lines shown in Fig.[13], almost coincident with arcs *Od* and *Ob* , are the envelopes of q and r - type sub-families as predicted by the *approximate-problem.*

Locus of Darboux Points

In order to investigate the comparative cost of the different extremal types, we scan the boundary condition q_f for $r_f = 0.3$, tracking the $q, r, q\,r$ etc. - type sub-families. The results are shown in Fig[14]. From this study it appears the more oscillatory solutions, i.e., the $q\,r$ - type, $r\,q$ - type, ... and so forth, extremals are more expensive than the q - type or the r - type extremals. However, between the q and the r - type extremals there is competition. For small values of q_f the q - type extremal is the minimizing solution, whereas for large values of q_f the r - type extremal is the minimizing solution. The two extremals yield the same cost at the Darboux point. In the reduced parameter space of end conditions q_f and r_f, the locus of Darboux points is obtained, as shown in Fig.[15]. The significance of the Darboux locus is that it demarcates this reduced parameter space into two regions, one in which the q - type extremals provide the globally minimal solution and the other where the r - type extremals are globally minimal. A summary of important results is shown in Fig.[15]. Arc *Ob* is the envelope of the r - type extremal sub-family, arc *Od* is the envelope of the q - type extremal sub-family, arc *Oc* is the locus of Darboux points. In the region *bOd* both q and r - type extremals exist, q - type extremals are globally minimal in the region *aOc* and r - type extremals are globally minimal in the region *cOe.*

Further, envelopes of the q and r - type sub-families of extremals and the Darboux locus is examined as we change the parameter p_f. For $p_f = 0.1$ and -0.1, the results are shown in Fig.[16] and Fig.[17] respectively.

Monotoncity of Cost with Maneuver time

Practical considerations require investigation of the trade-off between maximum available *control effort* and maneuver time, for given maneuvers. To achieve this, we study the cost, i.e. *control effort*, as a function of prescribed maneuver time t_f, while holding the initial and final states fixed. As a typical case, we present results obtained for Extremals 1 and 2 of Example 3.1 in Fig.[18]. For $t_f = 2$, the q - type extremal (Extremal 1) yields the globally minimal solution and the same trend is maintained for all values of t_f. For this extremal solution, we observe that the cost asymptotically approaches infinity as the maneuver time approaches zero and *vice versa*. The monotone behavior of cost with maneuver time is the key element of the *reciprocity* argument with which one may obtain *minimum time* solutions for a given maximum value of *control effort* by picking the smallest time t_f such that the cost does not exceed the prescribed maximum effort. It is interesting to note that the r - type extremal (Extremal 2), which is one of the non-minimal extremal solution ceases to exist at $t_f \simeq 19.355$ secs.. This is the envelope contact point and no members of the r - type extremal sub-family were found to exist for higher values of t_f.

It is evident that over large domains of boundary conditions, first-order necessary conditions provide several distinct candidate minimizers. It is imperative, therefore, to verify local optimality of these candidate extremals. In the following section, we develop the test for second-order necessary condition, which together with the Legendre-Clebsch condition, provide assurance of the minimizing character (at least locally) of candidate extremals.

3.5: Second-order necessary conditions - Jacobi test

Recall that the rigid-body rotation problem defined in section [3.3], is *regular*, i.e., all its extremals satisfy the *convexity* condition. Therefore, it *suffices* to show that if a test extremal satisfies the second-order necessary condition, it provides a local minimum. The *accessory minimum problem* for rigid-body rotation problem defined by equations [3.2.6]-[3.2.9], is obtained using the procedure outlined in section [2.6]. The equations of variation, obtained by linearizing the state and adjoint system (equations [3.3.1]-[3.3.4] and [3.3.12]-[3.3.15]) and the optimality conditions (equations [3.3.10]-[3.3.11]) about a test extremal are :

$$\dot{\delta p} = -r\delta q - q\delta r \qquad [3.5.1a]$$

$$\dot{\delta q} = r\delta p + p\delta r + \delta M \qquad [3.5.1b]$$

$$\dot{\delta r} = -q\delta p - p\delta q + \delta N \qquad [3.5.1c]$$

$$\delta\dot{c} = M\delta M + N\delta N \qquad [3.5.1d]$$

We seek to minimize the second variation,

$$\delta^2\mathcal{J} = \frac{1}{2}\int_0^{t_f}[2(-\lambda_p\delta q\delta r + \lambda_q\delta p\delta r - \lambda_r\delta p\delta q) + \lambda_0(\delta M^2 + \delta N^2)]dt \qquad [3.5.2]$$

over all possible admissible variations. The Euler-Lagrange equations for the *accessory minimum problem* are obtained to be,

$$\delta\dot{\lambda}_p = -\lambda_q\delta r + \lambda_r\delta q - r\delta\lambda_q + q\delta\lambda_r \qquad [3.5.3a]$$

$$\delta\dot{\lambda}_q = \lambda_p\delta r + \lambda_r\delta p + r\delta\lambda_p + p\delta\lambda_r \qquad [3.5.3b]$$

$$\delta\dot{\lambda}_r = \lambda_p\delta q - \lambda_q\delta p + q\delta\lambda_p - p\delta\lambda_q \qquad [3.5.3c]$$

$$\delta\dot{\lambda}_0 = 0 \qquad [3.5.3d]$$

while the minimum principle for the *accessory minimum problem* gives

$$\delta M = -\frac{1}{\lambda_0}(\delta\lambda_q + M\delta\lambda_0) \qquad [3.5.4a]$$

$$\delta N = -\frac{1}{\lambda_0}(\delta\lambda_r + N\delta\lambda_0) \qquad [3.5.4b]$$

Since, we are seeking competitors of the test-extremal, the variation, if admissible, must satisfy the boundary conditions of the test-extremal, i.e.,

$$\begin{array}{ll} \delta p(0) = 0 & \delta q(0) = 0 \\ \delta r(0) = 0 & \delta c(0) = 0 \end{array} \qquad [3.5.5a]$$

and,

$$\begin{array}{ll} \delta p(t_f) = 0 & \delta q(t_f) = 0 \\ \delta r(t_f) = 0 & \delta \lambda_0(t_f) = 0 \end{array} \qquad [3.5.5b]$$

A non-trivial solution of the above linear two-point boundary value problem indicates the existence of competetion.

Making use of the arguments presented in section [2.6], the question of whether or not a particular extremal is locally optimal, reduces to studying whether the following sub-matrix has a drop in rank on the interval $(0, t_f]$.

$$\Phi(t) = \begin{bmatrix} \dfrac{\partial p}{\partial \lambda_{p_0}} & \dfrac{\partial p}{\partial \lambda_{q_0}} & \dfrac{\partial p}{\partial \lambda_{r_0}} \\ \dfrac{\partial q}{\partial \lambda_{p_0}} & \dfrac{\partial q}{\partial \lambda_{q_0}} & \dfrac{\partial q}{\partial \lambda_{r_0}} \\ \dfrac{\partial r}{\partial \lambda_{p_0}} & \dfrac{\partial r}{\partial \lambda_{q_0}} & \dfrac{\partial r}{\partial \lambda_{r_0}} \end{bmatrix} \qquad [3.5.6]$$

The elements of the test matrix $\Phi(t)$, or the sensitivity of the states with respect to the initial adjoints can be obtained numerically using the following scheme. Four sets of initial conditions are assigned to the differential system, equations [3.5.1] and [3.5.3], with the algebraic conditions, equation [3.5.4], appropriately introduced. The initial state variations $\delta x(0)^T = (\delta p(0)\ \delta q(0)\ \delta r(0)\ \delta c(0))$ for each set is zero, while the initial adjoint variations $\delta \lambda(0)^T = (\delta \lambda_p(0)\ \delta \lambda_q(0)\ \delta \lambda_r(0)\ \delta \lambda_0(0))$ for the i^{th} set consists of all zero except the

i^{th} element of $\delta\lambda(0)^T$, which is taken to be unity. The state variations $\delta x_i(t)^T$ obtained by integrating this differential system along a test extremal provides the sensitivity of the states with respect to $\delta\lambda_{i0}$, and thus $\Phi(t)$ can be computed. If $\Phi(t)$ has full rank, or alternatively if $|\Phi(t)| \neq 0 \ \forall t \in (0, t_f]$, then the extremal passes the second-order test successfully, and the test extremal does indeed furnish a relative minimum. If $|\Phi(t_c)| = 0$ for some $t_c \in (0, t_f]$, then neighboring competition exists and the local optimality of the test extremal is in question.

The major result of the investigation of the second-order necessary conditions is that all extremals which belong to the q and r - type sub-families of extremals, in general, satisfied the second-order necessary conditions. If we deform the boundary conditions in a manner that members of these sub-families of extremals contact their envelopes (see Fig.[13] for example), then at envelope contact points the second-order necessary conditions are satisfied only in their *weakened* form, i.e., there is a conjugate point at t_f. This particular feature is reminiscent of the *catenary* type extremals of Surfaces of revolution of minimum area [31]. Furthermore, the q and r - type sub-families of extremals exhibit the popularly believed notion that the point at which an extremal ceases to be globally optimal does not as a rule coincide with envelope contact but rather precedes it. In other words global optimality is lost before local optimality, as is clearly evident from Fig.[15].

The extremal solutions which are oscillatory in character, labeled as $q\,r$ - type, $r\,q$ - type, $q\,r\,q$ - type extremals, and so forth, were found to fail the above

mentioned rank test. Thus all these extremal types, although satisfying the stationarity conditions, fail the second-order necessary conditions, which provides the guarantee of its minimizing character. Further, it was found that all extremals belonging to the $q\,r$ - type or $r\,q$ - type sub-families had one conjugate point, extremals belonging to $q\,r\,q$ - type or $r\,q\,r$ - type sub-families had two conjugate points, and so forth.

3.6: Concluding Remarks

The problem of optimal rigid-body angular rate control is studied in the absence of direct control over roll motion. While over a large range of boundary conditions several extremal sub-families satisfy the stationarity conditions, the more *oscillatory* type sub-families of extremal solutions may be discounted on the account they do not satisfy the second-order necessary condition. Thus, our choice for minimizing solution narrows down to two basic sub-families, classified as the q and r - type sub-families of extremals. These two basic sub-families arise due to a dichotomy in assumed dominant role of state variables q or r, in shaping the indirectly controlled state, p. Envelopes of these two sub-families are obtained in a reduced parameter space. A locus of Darboux points is obtained, which is found to demarcate the domains over which the two sub-families were globally minimal.

Chapter 4: Time Optimal Problem

4.1: Introduction

Optimal rigid-body rotational maneuvers with pitch and yaw controllers is investigated via an *approximate* dynamic model in Chapter Two. Further, the *exact* dynamic model is analyzed in Chapter Three. The above mentioned studies look at *minimum control effort* families of extremal solution with no prescribed *hard* bounds on control moments. A *measure of merit* of interest is the time required to execute a given maneuver, thus the present chapter deals with *minimum time* extremal solutions with bounded control moments. In the following sections, we define the considered optimal control problem and present an analysis of the first order necessary conditions for optimality. Numerical solutions are examined in the light of features exhibited by the *exact problem.*

4.2: Problem Statement

Again, we consider the rotational dynamics of a rigid body in a body-fixed coordinate system. The origin of the coordinate system is located at the center of mass and the axes are aligned along the principal axes of the rigid body. Let ω_x, ω_y, and ω_z be the components of angular velocity, denoting the roll, pitch, and the yaw rates, respectively. Assume the body is free of all external moments except the applied control moments. Then the Euler equations of motion describing the rotational dynamics of the rigid body are :

$$\dot{\omega}_x = J_x \omega_y \omega_z + \frac{u_x}{I_x} \qquad [4.2.1]$$

$$\dot{\omega}_y = J_y \omega_x \omega_z + \frac{u_y}{I_y} \qquad [4.2.2]$$

$$\dot{\omega}_z = J_z \omega_x \omega_y + \frac{u_z}{I_z} \qquad [4.2.3]$$

where $J_x = \frac{I_y - I_z}{I_x}$, $J_y = \frac{I_z - I_x}{I_y}$, $J_z = \frac{I_x - I_y}{I_z}$, and

I_x, I_y, I_z are the principal moments of inertia, and

u_x, u_y, and u_z are the rolling moment, pitching moment, and yawing moment, respectively.

We seek to perform an arbitrary point-to-point maneuver in *minimum time* t_f, where an admissible control vector function $u(t)^T = (u_x(t), u_y(t), u_z(t))$ is piecewise

continuous and its values are required to lie in one of the following control constraint sets:

i) $U_1(a_y, a_z) \equiv \{(u_x, u_y, u_z) \mid u_x = 0\,,\ (\frac{u_y}{a_y})^2 + (\frac{u_z}{a_z})^2 \leq 1\}$

ii) $U_2(a_x, a_y, a_z) \equiv \{(u_x, u_y, u_z) \mid (\frac{u_x}{a_x})^2 + (\frac{u_y}{a_y})^2 + (\frac{u_z}{a_z})^2 \leq 1\}$

iii) $U_3(a_y, a_z, \zeta) \equiv \{(u_x, u_y, u_z) \mid u_x = 0\,,\ |\frac{u_y}{a_y}|^{2\zeta} + |\frac{u_z}{a_z}|^{2\zeta} \leq 1\}$

iv) $U_4(a_y, a_z) \equiv \{(u_x, u_y, u_z) \mid u_x = 0\,,\ |u_y| \leq a_y\,,\ |u_z| \leq a_z\}$

where a_x, a_y, and a_z are prescribed positive real numbers, and

ζ is a real number, ≥ 1.0.

The above defined control constraint sets are closed, bounded, and convex. These represent models of net available control moments. We make use of U_1 as the nominal constraint set. This represents the case with **zero** available rolling moment, net available pitching and yawing moments are bounded in an ellipse characterized by a_y and a_z. The control constraint sets U_2, U_3, and U_4 are used to illustrate some special features.

Note the parameters of the above stated optimal control problem are :

a) boundary conditions, namely : $\omega_x(0)$, $\omega_y(0)$, $\omega_z(0)$, $\omega_x(t_f)$, $\omega_y(t_f)$, and $\omega_z(t_f)$

b) inertia characteristics : I_x, I_y and , I_z

c) parameters defining the control space : a_y, a_z, and possibly a_x or ζ (depending on U_l)

In an effort to consolidate the ensuing results for a wide spectrum of applications, we scale the above problem to eliminate some redundant parameters. Assuming that $I_z > I_y > I_x$, which is typically true for combat aircraft configurations, we define the following transformation :

$$p = Tc_x\,\omega_x \qquad q = Tc_y\,\omega_y \qquad r = Tc_z\,\omega_z$$

$$L = \frac{T^2 c_x}{I_x}\,u_x \qquad M = \frac{T^2 c_y}{I_y}\,u_y \qquad N = \frac{T^2 c_z}{I_z}\,u_z \qquad [4.2.4]$$

where $c_x = \sqrt{J_y'\,J_z'}$, $c_y = \sqrt{J_x'\,J_z'}$, $c_z = \sqrt{J_x'\,J_y'}$,

$J_x' = -J_x$, $J_y' = J_y$, $J_z' = -J_z$, and

T is a positive real number which is to be interpreted as a time scale.

Making use of the above transformation and changing the independent variable t to $\tau = \frac{t}{T}$, we may rewrite equations [4.2.1]-[4.2.3] as follows :

$$\dot{p} = -\,q\,r + L \qquad [4.2.5]$$

$$\dot{q} = \;\; p\,r + M \qquad [4.2.6]$$

$$\dot{r} = -\,p\,q + N \qquad [4.2.7]$$

Further, we define the constants a_l, a_m, and a_n which characterize the control constraint for the scaled problem as follows:

$$a_l = \frac{T^2 c_x}{I_x}\,a_x \qquad a_m = \frac{T^2 c_y}{I_y}\,a_y \qquad a_n = \frac{T^2 c_z}{I_z}\,a_z$$

Note we have an additional degree of freedom imbedded in the choice of the time scale T. We use this freedom to eliminate one of the three constants a_l, a_m, or a_n in the constraint set definition. We choose, arbitrarily, to normalize a_m to unity, which then defines T. The other two parameters a_l and a_n may be written as:

$$a_l = \frac{I_y c_x}{I_x c_y}\frac{a_x}{a_y} \qquad a_n = \frac{I_y c_z}{I_z c_y}\frac{a_z}{a_y}$$

The above choice of the time scale T leads us to identify the two important parameters which characterize the control constraint sets as:

a) maximum available yaw control (with maximum available pitch control normalized to unity)
b) maximum available roll control (with maximum available pitch control normalized to unity)

Then the control constraint sets U_l for the scaled problem can be identified as:

i) $\Omega_1(a_n) \equiv \{(L, M, N) \mid L = 0\,,\ (M)^2 + (\frac{N}{a_n})^2 \leq 1\}$

ii) $\Omega_2(a_l, a_n) \equiv \{(L, M, N) \mid (\frac{L}{a_l})^2 + (M)^2 + (\frac{N}{a_n})^2 \leq 1\}$

iii) $\Omega_3(a_n, \zeta) \equiv \{(L, M, N) \mid L = 0\,,\ |M|^{2\zeta} + |\frac{N}{a_n}|^{2\zeta} \leq 1\}$

iv) $\Omega_4(a_n) \equiv \{(L, M, N) \mid L = 0\,,\ |M| \leq 1\,,\ |N| \leq a_n\}$

The other parameters for the problem are the initial and final conditions of the states p, q, and r. We wish to emphasize that the scaled problem retains the important ingredients of the unscaled problem, while reducing the number of parameters to be considered in analysis. All subsequent analysis pertains to the scaled problem.

4.3: Optimality Conditions

In this section we derive the necessary conditions for optimality when the admissible control vector $u^T(t) = (L, M, N)$ is required to belong to the control constraint set Ω_1 . The analysis for this case is simple and illustrates the procedure. Relevant details for the cases when $u^T(t) \in \Omega_j$ ($j = 2$ or 3 or 4) are discussed in the subsequent section. Recall, the state equations describing the rigid-body rotational dynamics are given by [4.2.5]-[4.2.7]. Note the derivatives appearing in these equations are with respect to the scaled time variable τ. We seek to perform a maneuver to achieve a prescribed angular rate given an initial angular rate, i.e., the boundary conditions are prescribed to be :

$$\begin{array}{lll} p(0) = p_0 & q(0) = q_0 & r(0) = r_0 \\ p(\tau_f) = p_f & q(\tau_f) = q_f & r(\tau_f) = r_f \end{array} \qquad [4.3.1]$$

To arrive at optimal control to execute the prescribed maneuver in *minimum time*, we introduce the adjoint variables and define the variational-Hamiltonian $\mathscr{H}$ as,

$$\mathcal{H} = \lambda_p(-qr + L) + \lambda_q(pr + M) + \lambda_r(-pq + N) + 1. \qquad [4.3.2]$$

where λ_p, λ_q, and λ_r are the adjoint variables associated with the states p, q, and r respectively.

The adjoint variables λ_p, λ_q, and λ_r satisfy

$$\dot{\lambda}_p = -\lambda_q r + \lambda_r q \qquad [4.3.3]$$

$$\dot{\lambda}_q = \lambda_p r + \lambda_r p \qquad [4.3.4]$$

$$\dot{\lambda}_r = \lambda_p q - \lambda_q p \qquad [4.3.5]$$

Optimal choice of control can be obtained using the Pontryagins's Minimum Principle, which states that the optimal control (L^*, M^*, N^*) is one which minimizes $\mathcal{H}$ over all admissible control (L, M, N). The hodograph space (achievable state rates) and the adjoint vector projected on the $\dot{q} - \dot{r}$ plane is shown in Figure [19]. Since the domain of admissible control Ω_1, does not allow any direct control in the $\dot{p}$ equation (i.e. $L^* = 0$) it suffices to study the geometry in the $\dot{q} - \dot{r}$ plane. As time evolves the adjoint vector changes in direction and magnitude. However, at any given instant of time, the hodograph set is defined by an ellipse with the origin appropriately displaced by an amount equal to the gyroscopic terms. Thus, Figure [19] is representative of the geometry in a generic case. Note the control constraint set Ω_1 is compact and controls appear linearly in state equations. The optimal choice of controls (M^*, N^*) must lie on the

boundary of Ω_1 for almost all t , barring the possibility of singular *subarcs* where the Minimum Principle is vacuous. If one can rule out the possibility of singular *subarcs* in the optimal trajectory then the control *must almost always* lie on the boundary of Ω_1. In terms of the geometry, singular subarcs imply that the adjoint vector be orthogonal to the shown hodograph space for a finite duration of time. The following theorem takes care of this aspect.

Theorem 4.1 *Time-optimal trajectories cannot have subarcs where both control variables* M and N *are singular.*

Proof: Assume that there exists a subarc of optimal trajectory where both M and N are singular. It is evident from equation [4.3.2] that $\mathscr{H}_M = \lambda_q$ and $\mathscr{H}_N = \lambda_r$ are the switching functions associated with the control variables M and N, respectively. Then along a singular subarc:

$$(\frac{d}{d\tau})^{i_m}\mathscr{H}_M = 0 \qquad \text{and} \qquad (\frac{d}{d\tau})^{i_n}\mathscr{H}_N = 0 \qquad\qquad i_m, i_n = 0,1,2,...$$

The above conditions require

$$i_m, i_n = 0 \qquad \lambda_q = 0 \qquad \text{and} \qquad \lambda_r = 0$$

$$i_m, i_n = 1 \qquad \dot{\lambda}_q = \lambda_p r = 0 \quad \text{and} \quad \dot{\lambda}_r = \lambda_p q = 0$$

Further $\lambda_p \neq 0$ (trivial adjoint vector) which implies that $q = r = 0$.

$$i_m, i_n = 2 \qquad \ddot{\lambda}_q = \lambda_p \dot{r} = 0 \quad \text{and} \quad \ddot{\lambda}_r = \lambda_p \dot{q} = 0$$

or $\dot{q} = \dot{r} = 0$, which along with $q = r = 0$ implies that M and N are zero along the singular subarc. The only non-zero variables are p and λ_p which are constant along the singular subarc.

If the singular arc ($M(t) \equiv N(t) \equiv 0$) is *minimizing* then it must satisfy the *generalized* Legendre-Clebsch condition. We make use of the necessary conditions derived by Goh [32], for singular extremals involving multiple controls. The fundamental theorem of [32] states that for each component of a minimizing singular extremal, a certain matrix $Q_2 B_2$ be symmetric, and if this symmetry property is identically satisfied then another matrix R_4 must be positive semidefinite. For the problem in hand, we get

$$R_4 = \begin{bmatrix} 0 & -\lambda_p \\ -\lambda_p & 0 \end{bmatrix}$$

and $Q_2 B_2$ is a (2×2) null matrix, which is trivially symmetric. Clearly R_4 is positive semidefinite iff λ_p is identically zero. However, λ_p equal to zero implies a trivial adjoint vector, thus subarcs with *both* controls being simultaneously singular may not be a part of time-optimal trajectory.

Noting that since the optimal choice of control rides the control constraint, one can adequately describe the optimal control (M^*, N^*) using a single variable γ . Let,

$$M^* = \cos\gamma \qquad \text{and} \qquad N^* = a_n \sin\gamma \qquad 0 \le \gamma < 2\pi.$$

An application of Minimum Principle gives $\tan\gamma = \dfrac{a_n\lambda_r}{\lambda_q}$, or

$$M^* = -\frac{\lambda_q}{\sqrt{\lambda_q^2 + a_n^2\lambda_r^2}} \qquad N^* = -\frac{a_n^2\lambda_r}{\sqrt{\lambda_q^2 + a_n^2\lambda_r^2}}. \qquad [4.3.6]$$

The Legendre-Clebsch condition

$$\frac{\partial^2 \mathscr{H}}{\partial \gamma^2} = \sqrt{\lambda_q^2 + a_n^2\lambda_r^2} \ge 0$$

is satisfied along an extremal path.

The state equations [4.2.5]-[4.2.7], the adjoint equations [4.3.3]-[4.3.5], the optimality condition [4.3.6] and the boundary conditions [4.3.1] along with the transversality condition

$$\mathscr{H}\,|_{\tau=\tau_f} = 0 \qquad [4.3.7]$$

constitute a well defined two-point boundary-value problem (TPBVP). Solutions of the TPBVP (extremal paths) are then candidate minimizers. Since the two-point boundary value problem is nonlinear, there may be more than one extremal solution. In the following section, numerical solutions of the above mentioned TPBVP are investigated.

4.4: Extremal Solutions

In this section we will first show that for a given set of initial and final conditions, there are, in general, *several* distinct extremal solutions. Each extremal solution is then classified to belong to a distinct sub-family, based on the nature of the extremal control. Further, in a reduced parameter space, we shall establish domains of existence of some of the extremal sub-families and show that these domains overlap. In the regions of overlap, where more than one extremal solutions exists, a locus of Darboux points will be obtained. It will be shown, via a numerical survey, that there is a change in global minimality associated with the Darboux point. The above analysis parallels the investigation carried out for the *exact problem* and is based on the machinery developed in preceding section, i.e., domain of admissible control is Ω_1 .

Next we will introduce roll control by allowing the domain of admissible control to be Ω_2. We shall note the uniform dependence of extremal solution as we parametrically deform the control constraint to permit larger values of net available rolling moment. Further, we shall examine the extremal solutions as we deform the domain of admissible control from Ω_1 to Ω_4 via a series of intermediate problems using Ω_3. The foregoing discussion serves to provide an intuitive backdrop and now we shall examine, in some detail, the preceding notions.

Multiple Extremal Solutions

It is shown in Chapter Three, that there exist several extremal solutions for the *exact problem.* The *time-optimal problem* exhibits the same feature. The mechanism for controlling roll motion, in the absence of roll control, is through the gyroscopic cross-coupling term $q\,r$. Thus, one is led to the q - type extremal, adopting the terminology introduced in Chapter Three, if the pitch motion is dominant in controlling the roll motion, or a r - type extremal if the yaw motion assumes that responsibility. The following numerical example is presented to illustrate these ideas.

Example 4.1

For initial and final data :

$p_0 = 0 \quad q_0 = 0 \quad r_0 = 0$

$p_f = 0 \quad q_f = 0.3 \quad r_f = 0.3$

$a_n = 0.7$,

we obtained the following extremal solutions. Note the value of a_n is chosen arbitrarily.

i) **Extremal 1** : labeled as q - type extremal, corresponds to

$\lambda_p(0) \simeq -15.5659, \quad \lambda_q(0) \simeq 0.6292, \quad \lambda_r(0) \simeq -1.1103$ and minimum $\tau_f \simeq 0.92$.

Fig. [20] shows the extremal trajectory and the control histories.

ii) **Extremal 2** : labeled as r - type extremal, corresponds to

$\lambda_p(0) \simeq -14.4490$, $\lambda_q(0) \simeq -0.7342$, $\lambda_r(0) \simeq 0.9699$ and minimum $\tau_f \simeq 1.1479$.

Fig. [21] shows the extremal trajectory and the control histories.

iii) **Extremal 3** : labeled as $q\,r$ - type extremal, corresponds to

$\lambda_p(0) \simeq -24.5214$ $\lambda_q(0) \simeq 0.7072$, $\lambda_r(0) \simeq -1.0107$ and minimum $\tau_f \simeq 1.6606$.

Fig. [22] shows the extremal trajectory and the control histories.

iv) **Extremal 4** : labeled as $r\,q$ - type extremal, corresponds to

$\lambda_p(0) \simeq -25.9896$, $\lambda_q(0) \simeq -0.7083$, $\lambda_r(0) \simeq 1.0085$ and minimum $\tau_f \simeq 1.4147$.

Fig. [23] shows the extremal trajectory and the control histories.

Observe that, since the initial and final values of the roll rate p , are zero, to achieve such a maneuver requires that the sign of the product $q\,r$ (equation [4.2.5]) change on the interval $[0, t_f]$. If one of the variables remains of a single sign then the other must be more dynamic or control-like, yielding the q - type and the r - type extremals. Furthermore, the maneuver may be achieved in two stages, although with an increase in cost, where first q (r) then r (q) assumes the role of a control-like variable, yielding extremals labeled to be $q\,r$ ($r\,q$) - type extremals. One may extend the same arguments for the more oscillatory solutions, like the $q\,r\,q$ - type extremal. For brevity, we do not show these more oscillatory solutions.

The above numerical example corroborates the findings of the *exact problem.* The oscillatory solutions ($q\,r, r\,q, q\,r\,q$ - type extremals of *exact problem*) were found to have *conjugate points* thus violating the second order necessary conditions for optimality. In the present study the time required for these

oscillatory sub-families of extremals is considerably higher than the two basic q and r - type sub-families. Thus, we shall limit our discussion to the q and r - type extremal sub-families.

Envelopes of Extremal sub-families

With a possibility of a multitude of extremal solutions, some of which are shown in Example 4.1, we next investigate the domains of existence, in the parameter space, of the different types of extremal solution. To get a better grasp on this problem, we fix the values for five of the seven parameters. For $p_0 = q_0 = r_0 = p_f = 0$ and $a_n = 0.7$, we investigate the extremal solutions by varying the other two parameters, namely q_f and r_f. In this reduced parameter space, we pick an extremal solution and carefully deform the boundary conditions, q_f and r_f, solving a series of TPBVPs ensuring that we track the same extremal solution type. For example, we pick a q - type extremal, fix $r_f = 0.2$, and traverse the boundary conditions along the line $a\,c$ (see Figure [24]). It was found that no members of the q - type sub-family could be found beyond the point b. Consider the three-parameter family of extremals originating at the given initial point in state space and obtained by *small* variations of initial values of adjoint variables in the neighborhood of point b. The loci of end-points (p_f, q_f, r_f) are contained in a two-dimensional envelope. The point b, referred to as the *envelope contact point*, lies on this envelope. We carry out the same procedure for different values of r_f. Arc Ob shown in Figure [24], is the intersection of this envelope with

the $p_f = 0$ plane. Above the envelope we have members of the q - type sub-family of extremals, but none below.

Similarly, we pick a r - type extremal, say extremal 2 of Example 4.1, fix $q_f = 0.3$, and traverse the boundary conditions along the line $a\ e$ (see Figure [24]). It was found that no members of the r - type sub-family could be found above the point d. Following the same procedure as above, we establish the locus of the envelope contact points for the r - type extremal sub-family, shown as arc Od in Figure [24].

Locus of Darboux Points

A key result from the above discussion, is that the field of extremals originating from a fixed point in state space does not, in general, provide a *simple cover* in the space of end points (p_f, q_f, r_f). A particular incidence of such a phenomena is shown in Figure [24], where the field of extremals originating at the origin ($p_0 = q_0 = r_0 = 0$) has more than one extremal solution in some region of the subspace defined by $p_f = 0$. This naturally raises the following question. Of the two extremal sub-families which one provides the global minimal solution ? In order to investigate the comparative cost of the extremal solutions, we scan the boundary condition r_f for $q_f = 1.0$, tracking the q and r - type sub-families. The optimal cost as a function of r_f is shown in Figure [25]. As is evident there is competition between the q and the r - type extremals. For small values of r_f the r - type extremal is the minimizing solution, whereas for large values of r_f the q -

type extremal is the minimizing solution. The two extremals yield the same cost at the point referred to as the *Darboux point.* In the reduced parameter space of end conditions q_f and r_f, the locus of *Darboux points* is obtained, as shown in Figure [26]. The significance of this locus is that it demarcates this reduced parameter space into two regions, one in which the q - type extremals provide the globally minimal solution and the other where the r - type extremals are globally minimal. A summary of important results are shown in Figure [26], arc *Ob* is the envelope containing r - type extremal sub-family, arc *Od* is the envelope containing q - type extremal sub-family, arc *Oc* is the locus of Darboux points. In the region *bOd* both q and r - type extremals exist, q - type extremals are globally minimal in the region *aOc* and r - type extremals are globally minimal in the region *cOe.*

In principle, the locus of *Darboux points* may be obtained for other values of p_f. The two dimensional manifold of end points (p_f, q_f, r_f) where the q and the r - type extremals yield the same cost, may be thought of as a surface of Darboux points. Thus by definition, any extremal solution originating from the origin, which intersects the surface of Darboux points, i.e., contains a Darboux point, loses its global minimality.

Introduction of Roll Control

The above analysis is based on limiting the control vector to Ω_1 . It is of interest to study the extremal solution structure as we parametrically deform the control constraint set to permit nonzero values of roll control, L. The motivation is to investigate the behavior of the extremal solutions for *small* values of maximum available roll control and compare these to the case with no roll control. Further, as we increase the the roll control authority we expect the multiple solution structure to change as the roll dynamics are governed predominantly through rolling moment and to a lesser degree through the gyroscopic cross-coupling term. With these objectives in mind we analyze the optimal control problem stated in the preceding section but allow the domain of admissible control to be Ω_2. For small values of the parameter a_l, the geometry of the hodograph space is a "thin" ellipsoid. It is clear from arguments presented earlier that optimal choice of control *must almost always* lie on the surface of this ellipsoid. Minimization of $\mathscr{H}$ over Ω_2 gives the following algebraic conditions:

$$
\begin{aligned}
L^* &= -\frac{a_l^2 \lambda_p}{\sqrt{a_l^2 \lambda_p^2 + \lambda_q^2 + a_n^2 \lambda_r^2}} \\
M^* &= -\frac{\lambda_q}{\sqrt{a_l^2 \lambda_p^2 + \lambda_q^2 + a_n^2 \lambda_r^2}} \\
N^* &= -\frac{a_n^2 \lambda_r}{\sqrt{a_l^2 \lambda_p^2 + \lambda_q^2 + a_n^2 \lambda_r^2}} .
\end{aligned}
\qquad [4.4.1]
$$

The state equations [4.2.5]-[4.2.7], adjoint equations [4.3.3]-[4.3.5], boundary conditions [4.3.1] and [4.3.7] along with the optimality condition [4.4.1] defines the TPBVP, embodying the first-order necessary conditions for optimality.

As numerical evidence we present a one-parameter family of solutions, with a_l or maximum available roll control as the parameter. The maneuver considered in this study is the body-axis roll rate control, i.e., the boundary conditions are prescribed to be:

$$\begin{array}{lll} p_0 = 0 & q_0 = 0 & r_0 = 0 \\ p_f = 1 & q_f = 0 & r_f = 0 \end{array}$$

This maneuver is conceptually appealing as it provides a baseline for comparison. Since the prescribed initial and final pitch and yaw rates are zero, one can apply maximum available roll control to increase the roll rate to the desired value. This *single axis* roll rate control represents a possible minimum time extremal solution. However, if the roll control authority (characterized by the value of a_l) is small it may be advantageous to invoke pitch and yaw motions to assist the roll control moment via the gyroscopic cross-coupling term. This maneuver is labeled the *multi-axis* roll rate control. Figure [27] shows the comparison between the single and multi-axis roll rate control. For large values of a_l single-axis roll rate control is the only extremal solution. As we reduce the value of the parameter a_l a *bifurcation* of extremal solutions takes place ($a_l \simeq 0.4$). The multi-axis maneuver emerges and is achieved by either a q or r - type extremal. In the q - type extremal the pitch rate is negative and the yaw rate positive through out the

extremal trajectory, which then provides a positive contribution in the $\dot{p}$ equation. In the r - type extremal solution the signs of pitch and yaw rates are reversed. Owing to this symmetry the two distinct extremals yield the same minimum time, τ_f.

Further, the extremal solution can be made arbitrarily close to the extremal solution obtained with zero roll control by choosing a small enough value of a_l. In particular, as $a_l \to 0$, the extremal trajectories and controls "converge" to the corresponding $a_l = 0$ results. Thus, the *zero* roll control extremal solutions are representative of features to be expected with *small* values of available roll control.

Bang-Bang Control

In some applications of interest, the control moments may be generated by independent devices such as, pairs of throttleable steering jets. In the event these are mounted body fixed and aligned along the principal moments of inertia directions then the rigid-body dynamics are described by equations [4.2.5]-[4.2.7]. The domain of admissible control may then be modelled by control constraint set like Ω_4. In such cases, the time-optimal trajectories use *bang-bang* control, if one can rule out the possibility of singular subarcs. Using Theorem [4.1] one can eliminate the possibility of singular subarcs with both controls M and N singular. However, there is a possibility that one control is singular and the other bang-bang. In terms of geometry this implies that the adjoint vector is orthogonal

to one of the sides of the rectangle, describing the control constraint, for a finite duration of time. The following theorem takes care of this aspect.

Theorem 4.2 *Time-optimal trajectories cannot have subarcs where one control variable is singular and the other bang-bang, with the exception of degenerate case of single-axis rotation maneuvers.*

Proof: Assume that there exists a subarc of optimal trajectory where M is singular and N is non-singular (bang-bang). These conditions require:

$$\left(\frac{d}{d\tau}\right)^{i_m}\mathscr{H}_M = 0 \qquad \text{and} \qquad \mathscr{H}_N = \lambda_r \neq 0 \qquad i_m = 0,1,2,...$$

For

$i_m = 0 \qquad \lambda_q = 0$

$i_m = 1 \qquad \dot{\lambda}_q = \lambda_p r + \lambda_r p = 0$

$i_m = 2 \qquad \ddot{\lambda}_q = \lambda_p N = 0$

Since $N \neq 0$ by assumption, λ_p together with p must be zero.

$$i_m = 3 \qquad \dddot{\lambda}_q = \dot{\lambda}_p N = 0 \qquad \Rightarrow \qquad \dot{\lambda}_p = 0 \qquad \Rightarrow \qquad q = 0$$

$$i_m = 4 \qquad \ddddot{\lambda}_q = 0 \qquad \Rightarrow \qquad \dot{q} = 0 \qquad \Rightarrow \qquad M = 0$$

Thus along the singular subarc p, q, λ_p, λ_q and M are identically zero and by continuity must remain so throughout the entire trajectory. In other words the extremal solution consists of a single singular arc. The adjoint variable $\lambda_r \neq 0$ remains constant and r builds up or decreases depending on the sign of λ_r. Clearly if either or both r_0, r_f are nonzero, the remainder

of the boundary conditions being zero in [4.3.1], then the above described situation presents a possible extremal solution. This is the degenerate case of angular rate control about a single-axis. Similar arguments can be presented for the case with N singular and M bang-bang .

Thus, in general the minimization of $\mathscr{H}$ over Ω_4 gives

$$M^* = -\operatorname{sgn}(\lambda_q)1 \qquad N^* = -\operatorname{sgn}(\lambda_r)a_n \qquad [4.4.2]$$

as the optimality condition. Solutions of TPBVP with [4.4.2] as optimality conditions, in general pose numerical difficulties. As an alternate method, one may obtain extremal solutions by using the following numerical scheme. For a *pre*-determined switching structure, use the switching times as parameters and minimize the final time subject to the boundary conditions [4.3.1]. The optimality of the resulting trajectory is verified using the Minimum Principle [4.4.2]. In general, for nonlinear systems, such as the one considered here, *apriori* determination of switching structure poses a serious difficulty. To get a good guess of the switching structure we propose the following scheme, based on ideas presented in Refs. [33] and [34]. The control constraint set Ω_1 is deformed to approximate Ω_4 by using the control constraint set Ω_3. This is done by using the parameter ζ used in the definition of Ω_3. For $\zeta = 1.0$, $\Omega_3 = \Omega_1$ and for large values of ζ, $\Omega_3 \simeq \Omega_4$. Thus we solve a number of intermediate problems with allowable control out of Ω_3 with ζ as the continuation parameter. For ζ sufficiently large, the switching structure becomes readily apparent.

Minimization of $\mathscr{H}$ over Ω_3 gives

$$M^* = -\frac{\text{sgn}(\lambda_q)[\text{abs}(\lambda_q)]^{\frac{1}{2\zeta-1}}}{[(\lambda_q)^{\frac{2\zeta}{2\zeta-1}} + (a_n\lambda_r)^{\frac{2\zeta}{2\zeta-1}}]^{\frac{1}{2\zeta}}}$$

$$N^* = -\frac{\text{sgn}(\lambda_r)a_n[\text{abs}(a_n\lambda_q)]^{\frac{1}{2\zeta-1}}}{[(\lambda_q)^{\frac{2\zeta}{2\zeta-1}} + (a_n\lambda_r)^{\frac{2\zeta}{2\zeta-1}}]^{\frac{1}{2\zeta}}} \qquad [4.4.3]$$

as the optimality condition.

As numerical evidence to support the above mentioned ideas, we present the following study. Recall that the q - type extremal, Extremal 1 of Example 4.1, is the time-optimal solution with the control vector limited to $\Omega_1(0.7)$. The objective is to obtain the time-optimal solution for the same boundary conditions as above but now with the control vector limited to $\Omega_4(0.7)$. We know the time-optimal solution is *bang-bang*, however, the number of switching points and the structure is unknown. Thus, we introduce the control constraint set $\Omega_3(0.7, \zeta)$. The domain of admissible control is shown in Figure [28] for $\zeta = 1.0, 2.0$ and 3.0. A series of intermediate TPBVPs are solved for $\zeta \geq 1.0$. The resulting control time histories are shown in Figure [29a-b], for $\zeta = 1.0, 2.0$ and 3.0. As is evident from these plots that switching structure emerges with a value of $\zeta = 3.0$. Using this switching structure, the time-optimal bang-bang solution is obtained with relative ease.

No generalization could be made about the *number* of switching points and the switching structure for arbitrary values of the parameters of the problem. The prescribed boundary conditions seemed to critically determine the switching structure. These sensitivities, coupled with the fact that the structure is not *unique* (existence of q, r, $q\,r$ etc. - type sub-families of extremals), makes any such classification a difficult venture.

4.5: Concluding Remarks

In this chapter we studied the time-optimal control of the rigid body angular rates. A numerical survey of the optimality conditions with zero roll control showed that there are several distinct extremal solutions. The choice of *minimizing* extremal solution depends on the assigned values to the parameters of the problem, i.e., the boundary conditions. This feature of multiple extremal solutions is retained as the domain of admissible control is deformed to allow some roll control. If the gyroscopic cross-coupling terms influence the shaping of an optimal trajectory, arising in the present case due to a *deficiency* in control authority, then one can expect to find the features discussed in this chapter. Careful analysis is necessary to claim the *minimality* of extremal solutions in such cases. On this note we conclude the first phase of the present study, which dealt with the problem of optimal angular *rate* control.

Chapter 5: Minimum Time Attitude Control Problem

5.1: Introduction

The problem of optimal angular *rate* control has been examined extensively in the preceding three chapters. In this chapter, we investigate the problem of optimal *reorientation* of a rigid aircraft. That is, in addition to the angular velocity components, we include the angular position coordinates to describe the state of the system. We adopt the Euler parameters to define the relative orientation of the aircraft with respect to a given reference coordinate frame. The problem of *minimum time* prescribed changes in the state, using bounded control moments, is considered. In the following sections, we define the considered optimal control problem and present an analysis of the first-order necessary conditions for optimality.

5.2: Problem Statement

Rotational Dynamics and Kinematics

The rigid-body rotational dynamics are governed by familiar Euler equations [1]. Consider a body-fixed, cartesian coordinate system with the origin located at the center of mass and the axes aligned along the principal axes of the rigid body. Let ω_x, ω_y, and ω_z be the components of angular velocity, denoting the roll, pitch, and the yaw rates respectively. Assume the body is free of all external moments except the applied control moments. Then the evolution of angular motion is described by the following equation :

$$\dot{\omega} = f(\omega) + B\,u \qquad [5.2.1]$$

where $\omega^T = (\omega_x, \omega_y, \omega_z)$ $\quad u^T = (u_x, u_y, u_z)$

$$f^T(\omega) = (J_x\omega_y\omega_z\,,\; J_y\omega_x\omega_z\,,\; J_z\omega_x\omega_y)$$

$$B = \begin{bmatrix} I_x^{-1} & 0 & 0 \\ 0 & I_y^{-1} & 0 \\ 0 & 0 & I_z^{-1} \end{bmatrix}$$

$J_x = \dfrac{I_y - I_z}{I_x}$, $J_y = \dfrac{I_z - I_x}{I_y}$, $J_z = \dfrac{I_x - I_y}{I_z}$, and

I_x, I_y, I_z are the principal moments of inertia, and

u_x, u_y, and u_z are the rolling, pitching, and yawing moment, respectively.

Complete description of the relative orientation of a rigid aircraft with respect to a reference coordinate frame requires a minimum of three coordinates. It is well known that any three-angle description suffers from geometric singularities. In order to overcome this shortcoming, we adopt, as has been done in previous studies [35], the four coordinate once-redundant Euler parameter description to define the attitude of the rigid body. The Euler's Principal Rotation Theorem [1] guarantees that any arbitrary reorientation may be accomplished via a single rotation through a given angle (η) about a given axis ($\hat{\ell}$). The Euler parameters ($\beta_0, \beta_1, \beta_2, \beta_3$) are defined as follows :

$$\beta_0 = \cos\frac{\eta}{2} \qquad \text{and} \qquad \beta_i = \ell_i \sin\frac{\eta}{2} \quad (i = 1, 2, 3)$$

where ℓ_i are the direction cosines of the principal axis ($\hat{\ell}$) measured with respect to a reference cordinate frame.

The Euler parameters evolve in time according to the kinematic relationship :

$$\dot{\beta} = \Omega\,\beta \qquad [5.2.2]$$

where $\beta^T = (\beta_0, \beta_1, \beta_2, \beta_3)$ and

$$\Omega = \frac{1}{2}\begin{bmatrix} 0 & -\omega_x & -\omega_y & -\omega_z \\ \omega_x & 0 & \omega_z & -\omega_y \\ \omega_y & -\omega_z & 0 & \omega_x \\ \omega_z & \omega_y & -\omega_x & 0 \end{bmatrix}.$$

Note the above equations have quadratic nonlinearities, offering one more advantage over the conventional Euler angle description, whose kinematics involve transcendental nonlinearities.

The Control Problem

The state vector x consists of seven coordinates: three angular velocity components $(\omega_x, \omega_y, \omega_z)$ and four position coordinates $(\beta_0, \beta_1, \beta_2, \beta_3)$. The problem of control is to steer the rigid body from some given initial state to some prescribed final state. We seek to perform this point-to-point maneuver in *minimum time* t_f, using admissible values of control, where an admissible control vector function $u(t)^T = (u_x, u_y, u_z)$ is piecewise continuous and its values are required to lie in control constraint set U. For the purpose of this study we consider the following control constraint sets:

i) $U_1(a_y, a_z) \equiv \{(u_x, u_y, u_z) \mid u_x = 0\,,\ (\frac{u_y}{a_y})^2 + (\frac{u_z}{a_z})^2 \leq 1\}$

ii) $U_2(a_x, a_y, a_z) \equiv \{(u_x, u_y, u_z) \mid (\frac{u_x}{a_x})^2 + (\frac{u_y}{a_y})^2 + (\frac{u_z}{a_z})^2 \leq 1\}$

iii) $U_3(a_y, a_z, \zeta) \equiv \{(u_x, u_y, u_z) \mid u_x = 0\,,\ |\frac{u_y}{a_y}|^{2\zeta} + |\frac{u_z}{a_z}|^{2\zeta} \leq 1\}$

iv) $U_4(a_y, a_z) \equiv \{(u_x, u_y, u_z) \mid u_x = 0\,,\ |u_y| \leq a_y\,,\ |u_z| \leq a_z\}$

where a_x, a_y, and a_z are prescribed positive real numbers, and
ζ is a real number, ≥ 1.0.

The geometry of the feasible control set is an issue of great importance in generation of optimal trajectories. The above defined control constraint sets are

closed, bounded and convex, representing models of net available control moments. In any realistic application the domain of admissible control is usually closed and bounded, but not necessarily *convex*. The convexity of achievable moments is assumed to preclude *chattering* phenomena and possible nonexistence of optimal trajectories. If the domain is *strictly* convex (U_2 for instance) then some exotic singular behavior may be avoided. We make use of U_1 as the nominal constraint set. This represents the case with **zero** available rolling moment, net available pitching and yawing moments are bounded in an ellipse characterized by a_y and a_z. The control constraint sets U_2, U_3 and U_4 are used to illustrate some special features.

Some Transformation

For convenience, we introduce a time scale into the problem. Let

$$\tau = \frac{t}{T}$$

$$p = T\omega_x \qquad q = T\omega_y \qquad r = T\omega_z \qquad [5.2.3]$$

$$L = T^2 u_x \qquad M = T^2 u_y \qquad N = T^2 u_z$$

where T is a positive real number with units of time which may be interpreted as a time scale.

Making use of the above transformation and changing the independent variable t to τ, we may rewrite equations [5.2.1] and [5.2.2] as follows :

$$\dot{\bar{\omega}} = \bar{f}(\bar{\omega}) + B\,\bar{u} \qquad [5.2.4]$$

where $\bar{\omega}^T = (p, q, r) \qquad \bar{u}^T = (L, M, N)$

$$\bar{f}^T(\bar{\omega}) = (J_x qr,\ J_y pr,\ J_z pq)$$

and

$$\dot{\beta} = \bar{\Omega}\beta \qquad [5.2.5]$$

where

$$\bar{\Omega} = \frac{1}{2}\begin{bmatrix} 0 & -p & -q & -r \\ p & 0 & r & -q \\ q & -r & 0 & p \\ r & q & -p & 0 \end{bmatrix}$$

Note the derivatives in [5.2.4] and [5.2.5] are with respect to τ ; state variables $p, q,$ and r are nondimensional and control variables $L, M,$ and N have units of moments of inertia.

Further, we define the constants a_l, a_m, and a_n which are used to characterize the control constraint for the scaled problem as follows:

$$a_l = T^2 a_x \qquad a_m = T^2 a_y \qquad a_n = T^2 a_z$$

We make use of the additional degree of freedom imbedded in the choice of the time scale T, by choosing, arbitrarily, to normalize a_m to unity, which then defines T. Then the control constraint sets U_l for the scaled problem can be identified as:

i) $\Omega_1(a_n) \equiv \{(L, M, N) \mid L = 0\,,\ (M)^2 + (\frac{N}{a_n})^2 \leq 1\}$

ii) $\Omega_2(a_l, a_n) \equiv \{(L, M, N) \mid (\frac{L}{a_l})^2 + (M)^2 + (\frac{N}{a_n})^2 \leq 1\}$

iii) $\Omega_3(a_n, \zeta) \equiv \{(L, M, N) \mid L = 0\,,\ |M|^{2\zeta} + |\frac{N}{a_n}|^{2\zeta} \leq 1\}$

iv) $\Omega_4(a_n) \equiv \{(L, M, N) \mid L = 0\,,\ |M| \leq 1\,,\ |N| \leq a_n\}$

where $a_l = \frac{a_x}{a_y}$ and $a_n = \frac{a_z}{a_y}$.

The problem of optimal control remains the same, i.e., we seek to perform a point-to-point maneuver in minimum time τ_f, with admissible values of control. An admissible control is now constrained to belong to one of the above stated control constraint sets, Ω_l. The parameters of the stated optimal control problem may be identified as:

a) boundary conditions, i.e., initial and final states
b) ratio of principal moments of inertia eg. $\frac{I_x}{I_z}$ and $\frac{I_y}{I_z}$
c) parameters defining the control space : a_n and possibly a_l or ζ (depending on Ω_l)

As is evident there are many parameters which one may consider. Clearly we need to focus our attention to some problem of "interest". For the purpose of this study we fix an airframe (i.e., I_x, I_y and I_z are prescribed). From the geometry of engine location, its thrust characteristics, flow geometry and "vane" size/effectiveness, we make an educated estimate of available thrust-vectored moments. In most of the ensuing results we consider the case of zero available

rolling moment and a fixed geometry of available thrust in the M, N plane (control constraint set Ω_1). For initial and final conditions, we consider only rest-to-rest maneuvers, i.e., initial and final angular velocity are zero. The maneuvers considered are a subset of *minimum time* prescribed change in *attitude.* The attitude of the body axes $x^b y^b z^b$ are defined with respect to the local horizontal coordinate system $x^h y^h z^h$ (see Figure [30]). Although the kinematics are treated using Euler parameters, for purpose of discussion we make use of Euler angles to describe the body attitude. The transformation relating the Euler angles to the Euler parameters for the $\psi - \theta - \phi$ (local horizontal to body axes transformation) rotation sequence is available in [35].

5.3: Optimality Conditions

In this section we derive the necessary conditions for optimality for the general problem of rigid body reorientation in minimum time. We seek to steer the rigid body from a given initial state to a prescribed final target state, i.e., the boundary conditions are given to be :

$$\begin{array}{lll} p(0) = p_0 & q(0) = q_0 & r(0) = r_0 \\ p(\tau_f) = p_f & q(\tau_f) = q_f & r(\tau_f) = r_f \\ \beta_i(0) = \beta_{i0} & \beta_i(\tau_f) = \beta_{if} & i = 0,...,3 \end{array} \qquad [5.3.1]$$

To arrive at optimal control to execute the prescribed maneuver in *minimum time*, we introduce the adjoint variables and define the variational-Hamiltonian $\mathscr{H}$ as,

$$\begin{aligned}\mathscr{H} = {} & \lambda_p\left(J_x qr + \frac{L}{I_x}\right) + \lambda_q\left(J_y pr + \frac{M}{I_y}\right) + \lambda_r\left(J_z pq + \frac{N}{I_z}\right) + \\ & \frac{\gamma_0}{2}\left(-\beta_1 p - \beta_2 q - \beta_3 r\right) + \frac{\gamma_1}{2}\left(\beta_0 p - \beta_3 q + \beta_2 r\right) + \\ & \frac{\gamma_2}{2}\left(\beta_3 p + \beta_0 q - \beta_1 r\right) + \frac{\gamma_3}{2}\left(-\beta_2 p + \beta_1 q + \beta_0 r\right) + 1.\end{aligned} \qquad [5.3.2]$$

where λ_p, λ_q, and λ_r are the adjoint variables associated with the states p, q, and r respectively, and

γ_0, γ_1, γ_2, and γ_3 are the adjoint variables associated with the states β_0, β_1, β_2, and β_3, respectively.

The adjoint variables λ_p, λ_q, and λ_r satisfy

$$\begin{aligned}\dot{\lambda}_p &= -\left[J_y\lambda_q r + J_z\lambda_r q + \frac{1}{2}\left(-\gamma_0\beta_1 + \gamma_1\beta_0 + \gamma_2\beta_3 - \gamma_3\beta_2\right)\right] \\ \dot{\lambda}_q &= -\left[J_z\lambda_r p + J_x\lambda_p r + \frac{1}{2}\left(-\gamma_0\beta_2 - \gamma_1\beta_3 + \gamma_2\beta_0 + \gamma_3\beta_1\right)\right] \\ \dot{\lambda}_r &= -\left[J_x\lambda_p q + J_y\lambda_q p + \frac{1}{2}\left(-\gamma_0\beta_3 + \gamma_1\beta_2 - \gamma_2\beta_1 + \gamma_3\beta_0\right)\right]\end{aligned} \qquad [5.3.3]$$

and the adjoint variables γ_0, γ_1, γ_2, and γ_3 satisfy

$$
\begin{aligned}
\dot{\gamma}_0 &= -\frac{1}{2}(\gamma_1 p + \gamma_2 q + \gamma_3 r) \\
\dot{\gamma}_1 &= -\frac{1}{2}(-\gamma_0 p + \gamma_3 q - \gamma_2 r) \\
\dot{\gamma}_2 &= -\frac{1}{2}(-\gamma_3 p - \gamma_0 q + \gamma_1 r) \\
\dot{\gamma}_3 &= -\frac{1}{2}(\gamma_2 p - \gamma_1 q - \gamma_0 r)
\end{aligned}
\qquad [5.3.4]
$$

Optimal choice of control can be obtained using the Pontryagins's Minimum Principle, which states that the optimal control (L^*, M^*, N^*) is one which minimizes $\mathscr{H}$ over all admissible control (L, M, N). In the ensuing developments, we analyze the case when the control vector lives in Ω_1. Relevant details for the other cases are presented in the following sections.

The hodograph space (achievable state rates) and the adjoint vector projected on the $\dot{q} - \dot{r}$ plane is shown in Figure [19]. Since the inclusion of position coordinates in the optimal control problem does not affect the hodograph space, Figure [19] is still representative of the geometry in a generic case. Note the control constraint set Ω_1 is compact and controls appear linearly in state equations. The optimal choice of controls (M^*, N^*) must lie on the boundary of Ω_1 for *almost all* t, barring the possibility of singular *subarcs* where the Minimum Principle is vacuous. If one can rule out the possibility of singular *subarcs* in the optimal trajectory then the control *must almost always* lie on the boundary of Ω_1. In terms of the geometry, singular subarcs imply that the adjoint vector be orthogonal to the shown hodograph space for a finite duration of time. The following theorem takes care of this aspect.

Theorem 5.1 *Time-optimal trajectories cannot have subarcs where both control variables* M and N *are singular of finite order.*

Proof: Assume that there exists a subarc of optimal trajectory where both M and N are singular of finite order. It is evident from equation [5.3.2] that $\mathscr{H}_M = \lambda_q$ and $\mathscr{H}_N = \lambda_r$ are the switching functions associated with the control variables M and N respectively. Then along a singular subarc:

$$\left(\frac{d}{d\tau}\right)^{i_m}\mathscr{H}_M = 0 \quad \text{and} \quad \left(\frac{d}{d\tau}\right)^{i_n}\mathscr{H}_N = 0 \qquad i_m, i_n = 0,1,2,\ldots \quad [5.3.5]$$

Making use of condition [5.3.5], and state equations [5.2.4] and [5.2.5], the adjoint equations [5.3.3] and [5.3.4], we find that for $i_m = i_n = 2$, the control variables appear explicitly. Thus, there is possibly a first-order singular arc. For $\lambda_p \neq 0$, singular controls M_s and N_s may be evaluated using the following equation :

$$\begin{aligned} \frac{J_x \lambda_p M_s}{I_y} &= (J_y + 1)\mu_2 p + (J_x - 1)\mu_1 q \\ \frac{J_x \lambda_p N_s}{I_z} &= (J_x + 1)\mu_1 r + (J_z - 1)\mu_3 p \end{aligned} \qquad [5.3.6]$$

where $\mu_1 \equiv \frac{1}{2}(-\gamma_0\beta_1 + \gamma_1\beta_0 + \gamma_2\beta_3 - \gamma_3\beta_2)$

$$\mu_2 \equiv \frac{1}{2}(-\gamma_0\beta_2 - \gamma_1\beta_3 + \gamma_2\beta_0 + \gamma_3\beta_1)$$

$$\mu_3 \equiv \frac{1}{2}(-\gamma_0\beta_3 + \gamma_1\beta_2 - \gamma_2\beta_1 + \gamma_3\beta_0)$$

If the first-order singular arc suggested by [5.3.6] is *minimizing* then it must satisfy the *generalized* Legendre-Clebsch condition. We make use of the necessary conditions derived by Goh [32], for singular extremals involving multiple controls. The Fundamental Theorem of [32] states that for each component of a minimizing singular extremal, a certain matrix $Q_2 B_2$ be symmetric, and if this symmetry property is identically satisfied then another matrix R_4 must be positive semidefinite. For the problem in hand, we get

$$R_4 = \begin{bmatrix} 0 & \dfrac{J_x \lambda_p}{I_x I_z} \\ \dfrac{J_x \lambda_p}{I_x I_z} & 0 \end{bmatrix}$$

and $Q_2 B_2$ is a (2×2) null matrix, which is trivially symmetric. Clearly R_4 is positive semidefinite iff λ_p is identically zero. Thus, along a minimizing singular subarc in addition to λ_q and λ_r, λ_p must also be zero. Moreover, the first time derivatives of λ_p, λ_r and λ_r, which can now be expressed as

$$\dot{\lambda}_p = \mu_1 \qquad \dot{\lambda}_q = \mu_2 \qquad \dot{\lambda}_r = \mu_3$$

must also be identically zero. This implies that μ_1, μ_2 and μ_3 must identically vanish along the singular subarc. Since,

$$\begin{aligned} \dot{\mu}_1 &= \mu_2 r - \mu_3 q \\ \dot{\mu}_2 &= \mu_3 p - \mu_1 r \\ \dot{\mu}_3 &= \mu_1 q - \mu_3 p \end{aligned}$$

first and higher time derivatives of μ_1, μ_2 and μ_3 are automatically zero. Thus second and higher time derivatives of the switching functions λ_q and λ_r , which are homogenous in μ_i, are zero and control does not appear explicitly. Therefore, there exists no *minimizing* singular subarc of finite order.

Remarks :

a) If an *infinite* order singular subarc [36] exists, then any admissible control satisfies the necessary conditions !

b) If the kinematics are represented by Euler *angles* instead of Euler *parameters*, then infinite order singular arcs could be ruled out at all points in state space except at those points where the geometric singularity of Euler angles occured†.

---

† One can overcome this difficulty by locally eliminating the possibility of infinite order singular arcs using another Euler angle transformation (one which does not suffer geometric singularities at that point in state space).
Over parameterization may be a possible reason why the infinite order singular arc could not be eliminated for the case when the kinematics is represented by Euler parameters.
The above comments were suggested by Dr. A. J. Krener.

Noting that since the optimal choice of control rides the control constraint, one may adequately describe the optimal control (M^*, N^*) using a single variable σ . Let,

$$M^* = \cos\sigma \qquad \text{and} \qquad N^* = a_n \sin\sigma \qquad 0 \le \sigma < 2\pi.$$

An application of Minimum Principle gives $\tan\sigma = \dfrac{a_n I_y \lambda_r}{I_z \lambda_q}$, or

$$M^* = -\frac{\lambda_q/I_y}{\sqrt{(\lambda_q/I_y)^2 + (a_n\lambda_r/I_z)^2}} \qquad N^* = -\frac{a_n^2\lambda_r/I_z}{\sqrt{(\lambda_q/I_y)^2 + (a_n\lambda_r/I_z)^2}}. \qquad [5.3.7]$$

The Legendre-Clebsch condition

$$\frac{\partial^2 \mathcal{H}}{\partial \sigma^2} = \sqrt{(\lambda_q/I_y)^2 + (a_n\lambda_r/I_z)^2} \ge 0$$

is satisfied along an extremal path.

The state equations [5.2.4] and [5.2.5], the adjoint equations [5.3.3] and [5.3.4], the optimality condition [5.3.7] and the boundary conditions [5.3.1] along with the transversality condition

$$\mathcal{H}\,|_{\tau=\tau_f} = 0 \qquad [5.3.8]$$

constitute a two-point boundary value problem (TPBVP).

Note that equations [5.2.5] and [5.3.4] have *exact* integrals,

$$\sum_{i=0}^{3} \beta_i^2(t) = 1 \qquad \sum_{i=0}^{3} \gamma_i^2(t) = c$$

Clearly all admissible boundary conditions, β_{i0} and β_{f0} in [5.3.1] must satisfy the above equality constraint. It is apparent that the kinematic constraint is automatically enforced by the differential equations and need not be treated *per se*, as was observed by Vadali [37]. The associated adjoints γ_i are not unique, for definiteness we normalize γ_0 to unity at τ_f. With these modifications, the TPBVP is well-posed and its solutions are extremal paths or *candidate* minimizers. Numerical solutions of the TPBVP are obtained using a multiple shooting algorithm.

5.4: Extremal Solutions

In this section, we examine the numerical solutions of the TPBVP embodying the first-order necessary conditions for minimum time attitude control problem. In particular, we examine the extremal solutions yielding the following maneuvers:

a) Body Axes Bank

b) Roll Around Velocity Vector

c) Fuselage Pointing

The underlying rationale for the above classification is the prescribed boundary conditions. However, as the ensuing results indicate these maneuvers are intimately related.

A numerical survey of optimality conditions showed that, in general, there are *multiple extremal solutions* for a given set of parameters. By varying the parameters we examine the extremal solution structure, which is found to be fairly intricate. The domain of admissible control is deformed parametrically to allow roll control and its effect on extremal solutions is studied. Further, we present a systematic procedure to obtain-time optimal *bang-bang* solutions. The above discussion provides a general framework of the results and now we shall examine, in some detail, the preceding notions.

Multiple Extremal Solutions

With zero allowable roll control, i.e., the control vector lives in Ω_1 , the roll dynamics is governed solely through the gyroscopic cross-coupling term $J_x q r$. Thus, the pitch q and / or yaw r motion must dynamically shape the roll motion p. One may anticipate that for some maneuvers the pitch motion plays a dominating role (acts control-like) while the yaw motion plays a subservient role in controlling roll. Depending on boundary conditions, these roles can be interchangeable. This *dichotomy* in the assumed dominant role in governing roll motion yields multiple extremal solutions. Furthermore, certain spatial symmetries exist in performing a given maneuver, which also give rise to multiple

extremal solutions. In order to exhibit these features, we present the following numerical example.

Example 5.1

For the following prescribed values of the parameters:

$I_x = 0.162 \quad I_y = 0.865 \quad I_z = 1.0$

$\psi_0 = 0^o \quad \theta_0 = 0^o \quad \phi_0 = 0^o$

$\psi_f = 0^o \quad \theta_f = 0^o \quad \phi_f = 90^o$

$a_n = 0.7$,

we obtained the following six distinct extremal solutions, occurring as pairs.

i) **Extremal 1 and 2** : labeled as F1 and G1, both perform the maneuver with $\tau_f^* \simeq 5.42$. Figures [31a-d] show the F1 extremal trajectories and the control histories.

ii) **Extremal 3 and 4** : labeled as F2 and G2, both perform the maneuver with $\tau_f^* \simeq 5.71$. Figures [32a-d] show the F2 extremal trajectories and the control histories.

iii) **Extremal 5 and 6** : labeled as F3 and G3, both perform the maneuver with $\tau_f^* \simeq 5.98$. Figures [33a-d] show the F3 extremal trajectories and the control histories.

The extremal pairs (Fi , Gi i = 1, 2, 3) obey the following relationship.

$$p(\tau)^{(G)} = p(\tau)^{(F)} \qquad q(\tau)^{(G)} = -q(\tau)^{(F)} \qquad r(\tau)^{(G)} = -r(\tau)^{(F)}$$
$$\beta_0(\tau)^{(G)} = \beta_0(\tau)^{(F)} \qquad \beta_1(\tau)^{(G)} = \beta_1(\tau)^{(F)}$$
$$\beta_2(\tau)^{(G)} = -\beta_2(\tau)^{(F)} \qquad \beta_3(\tau)^{(G)} = -\beta_3(\tau)^{(F)}$$
$$M(\tau)^{(G)} = -M(\tau)^{(F)} \qquad N(\tau)^{(G)} = -N(\tau)^{(F)}$$

where $(.)^{(F)}$ refers to extremal Fi and $(.)^{(G)}$ refers to extremal Gi (same i).

Some insight about the character of these extremal solutions can be inferred. One can construct simple *admissible* (not optimal) trajectories to perform the *Body axes Bank of* 90^o using a composite of single axis rotations. For example, if we start out with wings level and pitch *up* 90^o followed by yaw *right* by 90^o followed by a pitch *down* of 90^o, it amounts to a body axis bank of 90^o. Similarly a *spatially symmetric* admissible trajectory is obtained by first pitching *down* followed by yawing *left* and followed by pitch *up* sequence of single axis rotations. With some reservations, we compare the character of the above described composite trajectory to that exhibited by the extremal pair (F1,G1). The "dominating" pitch up and pitch down sequence is observed in Figure [31a]. Analogous to the above composite, another pair of admissible trajectories can be synthesized by first yawing *right* (*left* for the spatially symmetric trajectory) followed by a pitch *down* (*up*) followed by a yaw *left* (*right*) to obtain the desired bank. The extremal pair (F2,G2) reflects the character suggested by the yaw-pitch-yaw composite. The "dominating" yaw right and yaw left sequence is observed in Figure [32a]. The extremal pair (F3,G3) is inherently a complex multi-axis maneuver and could not be associated with a simple composite.

In the above motivating example we considered a relatively simple maneuver. This maneuver highlights the reasons for multiple extremal solutions. Subsequently, we will analyze maneuvers of practical interest, but first we study the effect of allowing some roll control in minimum time attitude control problem.

Introduction of Roll Control

The above analysis is based on limiting the control vector to Ω_1 . It is of interest to study the extremal solution structure as we parametrically deform the control constraint set to permit nonzero values of roll control, L. The motivation is to investigate the behavior of the extremal solutions for *small* values of maximum available roll control and compare these to the case with no roll control. Further, as we increase the roll control authority we expect the multiple solution structure to change as the roll dynamics are governed predominantly through rolling moment and to a lesser degree through the gyroscopic cross-coupling term. With these objectives in mind we analyze the optimal control problem stated in the preceding section but allow the domain of admissible control to be Ω_2. For small values of the parameter a_l, the geometry of the hodograph space is a "thin" ellipsoid. It is clear from arguments presented earlier that optimal choice of control *must almost always* lie on the surface of this ellipsoid. Minimization of $\mathscr{H}$ over Ω_2 gives the following algebraic conditions:

$$L^* = -\frac{a_l^2 \lambda_p / I_x}{\sqrt{(a_l \lambda_p / I_x)^2 + (\lambda_q / I_y)^2 + (a_n \lambda_r / I_z)^2}}$$

$$M^* = -\frac{\lambda_q / I_y}{\sqrt{(a_l \lambda_p / I_x)^2 + (\lambda_q / I_y)^2 + (a_n \lambda_r / I_z)^2}} \qquad [5.4.1]$$

$$N^* = -\frac{a_n^2 \lambda_r / I_z}{\sqrt{(a_l \lambda_p / I_x)^2 + (\lambda_q / I_y)^2 + (a_n \lambda_r / I_z)^2}}$$

The state equations [5.2.4]-[5.2.5], adjoint equations [5.3.3]-[5.3.4], boundary conditions [5.3.1] and [5.3.8] along with the optimality condition [5.4.1] defines the TPBVP, embodying the first-order necessary conditions for optimality.

As numerical evidence we present a one parameter family of solutions, with a_l or maximum available roll control as the parameter. We consider the maneuver of *Body axes Bank of* 90^o presented in Example 5.1. Optimal cost τ_f^* for different extremal solutions is shown as a function of $\frac{a_l}{I_x}$ (maximum roll control influence) in Figure [34]. Points along the vertical axis represents the case with zero roll control and the cost of the six extremal solutions of Example 5.1 are shown. By introducing roll control we do not destroy the symmetry exhibited by the extremals Fi and Gi, thus the two distinct extremals yield the same cost. With some direct roll control available, the body axis bank can be achieved via a *single axis* roll maneuver, representing a possible extremal solution. Clearly, for "small" values of roll control influence ($\frac{a_l}{I_x} < 0.3$) it is advantageous to perform the maneuver using the *multi axis* extremal solutions. The trajectories for the F2

and G2 extremals asymptotically approach the single axis maneuver for values of $\frac{a_l}{I_x} > 0.3$.

Further, the extremal solution can be made arbitrarily close to the extremal solution obtained with zero roll control by choosing a small enough value of a_l. In particular, there is *pointwise* convergence of extremal trajectory and control. Thus, the *zero* roll control extremal solutions are representative of features to be expected with *small* values of available roll control.

The results of this study show the complexity of the extremal solution structure. At the point labeled A in Figure [34], the extremal families (F1,G1) cross (F2,G2) and four distinct extremal solutions exists yielding the same cost, indicating the existence of Darboux Points. The extremal families (F1,G1) coalesce with the extremal families (F3,G3) at the point B and these solutions could not be extended for higher values of $\frac{a_l}{I_x}$.

Roll Around the Velocity Vector

Since we are dealing with motion *about* the center of mass, for purpose of discussion, we may hypothesize the relative velocity V_{rel} of the center of mass is along the negative x^h direction (see Figure [30]). A "pure" or *constrained* Roll around the Velocity Vector (RVV) may be envisioned as a single axis rotation about the x^h axis with the initial pitch attitude being α . Geometrically, this implies that the nose of the aircraft traverses an arc of a circle and x^h lies on the

surface of cone with half angle α, pivoted at the center of mass. For definiteness, the following boundary conditions are specified:

$$\psi_0 = 0^o \quad \theta_0 = \alpha^o \quad \phi_0 = 0^o$$

$$\psi_f = \alpha^o \quad \theta_f = 0^o \quad \phi_f = 90^o$$

The *unconstrained* RVV maneuver is one which satisfies the above boundary conditions but the nose of the aircraft is not constrained to describe the arc of circle. Note the *Body axis Bank of* 90^o is a special member of the above class of maneuvers obtained by setting $\alpha = 0^o$. Also, note that the *constrained* maneuver cannot be performed without roll control, i.e., when the control vector lives in Ω_1 . However, the *unconstrained* maneuver may be performed as the following study indicates.

Extremal solutions to perform the *unconstrained* RVV are examined as a function of initial pitch attitude α. The optimal cost τ_f^* for the various extremal solutions as a function of α are shown in Figure [35]. On the vertical axis, corresponding to value of $\alpha = 0^o$, the cost of the extremal solutions of Example 5.1 are shown. For nonzero values of α, the "up"/"down" and the "right"/"left" symmetry breaks down as is indicated by splitting of (F1,G1) and (F3,G3) extremal pairs. The extremal pair (F2,G2) yield the same cost despite the apparent loss of symmetry.

Next, for a fixed value of α, we introduce the roll control and compare the extremal solutions for the *constrained* and *unconstrained* maneuvers as a function of a_t. For $\alpha = 45^o$ we have three extremal solutions F1, G1 and G3 (refer

Figure[35]). We introduce roll control by allowing the domain of admissible control to be Ω_2. The optimal cost τ_f^* of the extremal solutions F1, G1 and G3 are shown as a function of $\frac{a_l}{I_x}$ in Figure [36]. The dashed line represents the optimal cost τ_f^* for the *constrained* maneuver. The *unconstrained* maneuver outperforms the *constrained* maneuver for values of $\frac{a_l}{I_x} < 0.25$. For higher values of $\frac{a_l}{I_x}$, the optimal cost for the *unconstrained* and *constrained* maneuvers are close, although the extremal trajectories are quite different.

Fuselage Pointing Maneuver

Our fuselage pointing maneuver can be regarded as a *unconstrained* RVV with a "free" final value of bank angle ϕ_f. The necessary condition for optimality requires that the associated adjoint variable λ_ϕ be zero at final time τ_f^* . However, in the light of multiple extremal solutions, some caution needs to be exercised as the following study indicates.

For a fixed value of α, consider an *unconstrained* RVV obtained in the preceding subsection. For example, consider the F1 extremal for $\alpha = 45^o$ (refer Figure [35]). The final value of bank angle ϕ_f for this extremal is prescribed to be 90^o. We study the minimum time ϕ_f - family of extremal solutions, for fixed values of the remaining boundary conditions, i.e., $\psi_0 = 0^o$, $\theta_0 = 45^o$, $\phi_0 = 0^o$ and $\psi_f = 45^o$, $\theta_f = 0^o$. The optimal cost τ_f^* as a function of prescribed value of ϕ_f is shown in Figure [37]. The dashed line represents the final value of adjoint variable λ_ϕ . Clearly, there are four "natural" or "free" values of ϕ_f ,

corresponding to the four zero "crossing" of the final value of λ_ϕ. Two of these correspond to local maxima and two to local minima. The global minimum corresponds to a $\phi_f \simeq 35^o$ yielding an optimal cost $\tau_f^* \simeq 3.11$. This cost is substantially lower than the one corresponding to $\phi_f = 90^o$ ($\tau_f^* \simeq 4.36$).

Bang-Bang Control

In some applications of interest control moments may be generated by reaction control systems such as, pairs of throttleable steering jets. In the event these are mounted body fixed and aligned along the principle moments of inertia directions then the rigid body rotational dynamics are described by equations [5.2.4]. The domain of admissible control may then be modelled by control constraint set like Ω_4. It is well known that time-optimal trajectories use *bang-bang* control, if one can rule out the possibility of singular subarcs. Using Theorem [5.1] one can eliminate the possibility of singular subarcs with both controls M and N singular. However, there is a possibility that one control is singular and the other bang-bang. Barring this possibility, the optimality condition, obtained by the minimization of $\mathscr{H}$ over Ω_4 gives

$$M^* = -\operatorname{sgn}(\lambda_q)1 \qquad N^* = -\operatorname{sgn}(\lambda_r)a_n \ . \qquad [5.4.2]$$

Solutions of TPBVP with [5.4.2] as optimality conditions, in general pose numerical difficulties. As an alternate method, one may obtain extremal solutions by using the following numerical scheme. For a *pre*-determined switching structure, use the switching times as parameters and minimize the final

time subject to the boundary conditions [5.3.1]. The optimality of the resulting trajectory is verified using the Minimum Principle [5.4.2]. In general, for nonlinear systems, such as the one considered here, *apriori* determination of switching structure poses a serious difficulty.

To get a good guess of the switching structure we use the scheme proposed in Chapter Four. The control constraint set Ω_1 is deformed to approximate Ω_4 by using the control constraint set Ω_3. This is done by using the parameter ζ used in the definition of Ω_3. For $\zeta = 1.0$, $\Omega_3 = \Omega_1$ and for large values of ζ, $\Omega_3 \simeq \Omega_4$. Thus we solve a number of intermediate problems with allowable control out of Ω_3 with ζ as the continuation parameter. For ζ sufficiently large, the switching structure becomes readily apparent.

Minimization of $\mathscr{H}$ over Ω_3 gives

$$M^* = -\frac{\text{sgn}(\lambda_q)[\text{abs}(\lambda_q/I_z)]^{\frac{1}{2\zeta-1}}}{[(\lambda_q/I_y)^{\frac{2\zeta}{2\zeta-1}} + (a_n\lambda_r/I_z)^{\frac{2\zeta}{2\zeta-1}}]^{\frac{1}{2\zeta}}}$$

$$N^* = -\frac{\text{sgn}(\lambda_r)a_n[\text{abs}(a_n\lambda_q/I_z)]^{\frac{1}{2\zeta-1}}}{[(\lambda_q/I_y)^{\frac{2\zeta}{2\zeta-1}} + (a_n\lambda_r/I_z)^{\frac{2\zeta}{2\zeta-1}}]^{\frac{1}{2\zeta}}} \qquad [5.4.3]$$

as the optimality condition.

As numerical evidence to support the above mentioned ideas, we present the following study. Recall the extremal F1 for the *unconstrained* RVV for $\alpha = 45^o$

is a time-optimal solution obtained with the control vector limited to $\Omega_1(0.7)$. The objective is to obtain the time-optimal solution for the same boundary conditions as above but now with the control vector limited to $\Omega_4(0.7)$. To obtain a *guess* value for the switching structure, we introduce the control constraint set $\Omega_3(0.7, \zeta)$. A series of intermediate optimal control problems are solved for values of $\zeta > 1.0$. The resulting control time histories are shown in Figure [38a-b], for $\zeta = 1.0, 2.0$ and 3.0. It is evident from these plots that a clear switching structure emerges at a value of $\zeta = 3.0$. Using this switching structure, the time-optimal bang-bang solution is obtained with relative ease.

5.5: Concluding Remarks

In this chapter we examined the problem of *minimum time* attitude control of a rigid aircraft. A numerical survey of optimality conditions, with zero allowable roll control, revealed that there are *several distinct extremal* solutions. The nature of the extremal solution depends on whether *pitch* motion or *yaw* motion assumes the responsibility to dynamically shape the *roll* motion. Moreover, for some boundary conditions, for example the *Body Axis Bank of* 90^o, certain *spatial symmetries* exist in executing the given maneuver. Thus, in such cases the extremal solutions occur as *spatially symmetric* pairs. Furthermore, extremal solutions were examined as the control space is deformed to allow roll control. It was concluded that *small* amount of roll control does not significantly alter the

extremal solution structure. Thus, *zero* roll control extremal solutions are representative of the features to be expected with *small* values of roll control.

Maneuvers of practical interest like the *Roll Around the Velocity Vector* and *Fuselage Pointing* maneuvers are analyzed. The optimal time to execute the *unconstrained* RVV is significantly less than the *constrained* maneuver for *small* values of roll control. Analysis of *Fuselage Pointing* maneuver shows that there are four "natural" or "free" values of the bank attitude ϕ_f , two of these correspond to local minima and the other two to local maxima. In general, the extremal solution structure for the problem of attitude control using only two controllers is intricate and some care is required in analysis.

Chapter 6: Summary and Discussion

6.1: Introduction

In the present research effort, we investigate the problem of optimal rotational maneuvers for a rigid body. The distinguishing feature of this study, which sets it apart from existing literature, is that we examine the possibility of controlling *arbitrary* angular motion in the absence of direct control over one of the angular velocity components. This is achieved by gradually increasing the complexity of the optimal control problems investigated. The important results of each phase are summarized in the concluding remarks section of Chapters Two through Five. There is a unifying theme and the salient features are reiterated in the following sub-section.

6.2: Nature of Optimal Solutions

The common thread, of the various optimal control problems investigated herein, is the rich extremal solution structure. A key result is the field of extremals originating from a fixed point in state space does not, in general, provide a *simple cover* in the space of end conditions. There is an *abundance* of extremal solutions. This arises due to a fundamental *dichotomy* which exists in the mechanism for controlling roll motion. The nature of the optimal trajectory depends on whether *pitch* motion or *yaw* motion assumes the dominating role in controlling *roll* motion. In the case of *attitude* control problem, *spatial symmetries* which exist in executing a maneuver contribute to the rich extremal structure.

Usually a single sub-family of extremal solutions could not be extended for the entire range of boundary conditions. In particular, the various extremal sub-families exist in well defined regions of parameter space, i.e., they are contained in envelopes. Naturally, no single sub-family provided the *minimizing* solution over the range of boundary conditions. The "crown of royalty" associated with global minimality, passed from one sub-family of extremal solutions to another at a Darboux Point.

Numerical evidence suggests that introducing *small* amount of available roll control does not significantly alter the extremal solution structure. Thus, *zero* roll control extremal solutions are representative of features to be expected with *small* amount of roll control.

6.3: Suggestions for Future Research

The next logical step towards understanding the optimal rotational maneuvers for *super-maneuverable* aircraft is to incorporate a realistic aerodynamic model into the rigid-body dynamics. Further, it is of interest to refine the thrust-vectoring model. Study of optimal maneuvers in the presence of aerodynamics and realistic modelling of available control is anticipated to be a challenging task.

References

1. Goldstein, H., *Classical Mechanics*, Addison-Wesley, 2nd edition, 1980.

2. Meriam, J. L., *Dynamics*, John Wiley & Sons, Inc., New York, 1971.

3. Bryson, A. E., and Ho, Y. C., *Applied Optimal Control*, Hemisphere Publishing Corporation, New York, 1975.

4. Leitmann, G., *Topics in Optimization*, Academic Press, New York, 1967.

5. Leitmann, G., *The Calculus of Variations and Optimal Control*, Plenum Press, New York, 1981.

6. Lee, E.B. and Marcus, L., *Foundations of Optimal Control Theory*, John Wiley & Sons, Inc., New York, 1967.

7. Ewing, G. M., *Calculus of Variations with Applications*, Dover Publications, Inc., New York, 1985.

8. Herbst, W. B., "Design for Air Combat 1990 ", *Messerschmitt-Bölkow-Blohm GmbH, Munich, Germany.*

9. Herbst, W. B., "Dynamics of Air Combat", *Journal of Aircraft*, Vol 20, No. 7, July 1983, pp. 594-598.

10. Herbst, W. B., "Future Fighter Technologies", *Journal of Aircraft*, Vol 17, No. 8, Aug 1980, pp. 561-566.

11. Well, K. H., Faber, B., and Berger, E., "Optimization of Tactical Aircraft Maneuvers Utilizing High Angles of Attack", *Journal of Guidance and Control*, Vol 5, No. 2, March-April 1982, pp. 131-137.

12. Anon, "Yaw Vanes Improve Performance of F-14A in Initial Test Flights", *Aviation Week & Space Technology*, May 4, 1987, pp. 50.

13. Lacey, D.W., "Air Combat Advantages from Reaction Control Systems", *SAE Aerospace Congress and Exposition*, Los Angeles, CA, October 13-16, 1980, Technical Paper 801177.

14. Cord, T. J. and Suchomel, C. F., "Supermaneuverability", *AIAA/AHS/ASEE Aircraft Design Systems and Operations Meeting*, San Diego, Ca, 1984, AIAA-84-2386.

15. Athans, M. and Falb, P.L., *Optimal Control.*, McGraw-Hill, New York, 1966.

16. Debs, A.S. and Athans, M., "On the Optimal Angular Velocity Control of Asymmetric Space Vehicles", *IEEE Transactions on Automatic Control*, pp.80-83, Feb 1969.

17. Dwyer, T., "The Control of Angular Momentum for Asymmetric Rigid Bodies", *IEEE Transactions on Automatic Control,* Vol. AC-27, No. 3, pp.686-686, June 1982.

18. Golubev, Iu.V. and Demidov, V.N., "An Optimal Control Law for stopping rotation", *Akademiia Nauk SSSR, Izvestiia, Mekhanika Tverdogo Tela,* pp.18-24, Mar-Apr. 1984.

19. Junkins, J.L. and Turner, J.D., "Optimal Continuous Torque Attitude Maneuvers", *Journal of Guidance and Control,* Vol. 3, No. 3, pp.210-217, May-June, 1980.

20. Carrington, C.K. and Junkins, J.L., "Nonlinear feedback control of spacecraft slew maneuvers", *Proc AAS Rocky Mountain Guidance and Control Conference,* Keystone, CO, Feb. 5-9, 1982, paper AAS 83-002.

21. Li, F. and Bainum, P.M., "Minimum Time Attitude Slewing Maneuvers of a Rigid Spacecraft", *AIAA 26th Aerospace Sciences Meeting,* Reno, Nevada, Jan. 11-14, 1988, paper no. 88-0675.

22. Neustadt L. W., "Minimum Effort Control Systems", *SIAM Journal on Control,* Series A, Vol. 1, No. 1, 1962, pp. 16-31.

23. Mereau, P. and Powers, W. F., "The Darboux Point," *Journal of Optimization Theory and Applications,* Vol. 17, Nos. 5/6, Dec 1975, pp. 545-559.

24. Breakwell, J. V. and Ho, Y. C., "On the Conjugate Point Condition for the Control Problem," *International Journal of Engineering Science,* Vol. 2, pp.565-579, 1964.

25. Moyer, H. G., " Optimal Control Problems that Test for Envelope Contacts," *Journal of Optimization Theory and Applications,* Vol. 6, No. 4, Oct 1970, pp. 287-298.

26. Kelley, H.J. and Moyer, H. G., "Computational Jacobi-Test Procedure," *JUREMA Workshop on Current Trends in Control,* Dubrovnik, Yugoslavia, June 1984.

27. Jacobson, D. H., "Sufficient Conditions for Nonnegativity of the Second Variation in Singular and Nonsingular Control Problems," *SIAM Journal of Control,* Vol. 8, No.3, pp.403-423, Aug 1970.

28. Moyer, H. G. and Kelley, H. J., "Conjugate Points on Extremal Rocket Paths," *Proc. 19th IAF Congress,* New York 1968. Pergamon Press, Oxford (1970).

29. Cliff, E. M., Kelley, H. J. and Lefton L., "Thrust-Vectored Energy Turns," *Automatica,* 18, pp. 559-564, 1982.

30. Stoer, J. and Bulirsch, R., *Introduction to Numerical Analysis,* Springer-Verlag, New York Inc., 1980.

31. Bliss, G. A., *Calculus of Variations,* Carus Monographs, The Open Court Publishing Company, La Salle, Illinois, 1925.

32. Goh, B. S., "Necessary Conditions for Singular Extremals Involving Multiple Control Variables," *SIAM Journal of Control,* Vol. 4, No. 4, pp.716-731, 1966.

33. Krasovskii, N. N., "On the Theory of Optimal Control," *Prikl. Mat. Meh.,* Vol. 23, pp. 625-639, 1959. (English translation in *J. of Applied Mathematics and Mechanics,* Vol. 23, pp. 899-919.)

34. Artstein, Z., "The Maximum Amplitude Cost Functional in Linear Systems," *J. of Math. Analysis and Applications,* Vol. 50, No. 2, pp. 341-349, May 1975.

35. Junkins, J.L. and Turner, J.D., *Optimal Spacecraft Rotational Maneuvers,* Studies in Aeronautics, Volume 3, Elsevier Science Publishing Company Inc., New York, NY 10017, 1986.

36. Krener, A. J., "The High Order Maximal Principle and its Application to Singular Extremals", *SIAM Journal of Control and Optimization*, Vol. 15, No. 2, 1977, pp. 256-293.

37. Vadali, S. R., "On the Euler Parameter Constraint", *The Journal of the Astronautical Sciences*, Vol. 36, No. 3, July-September 1988, pp. 259-265.

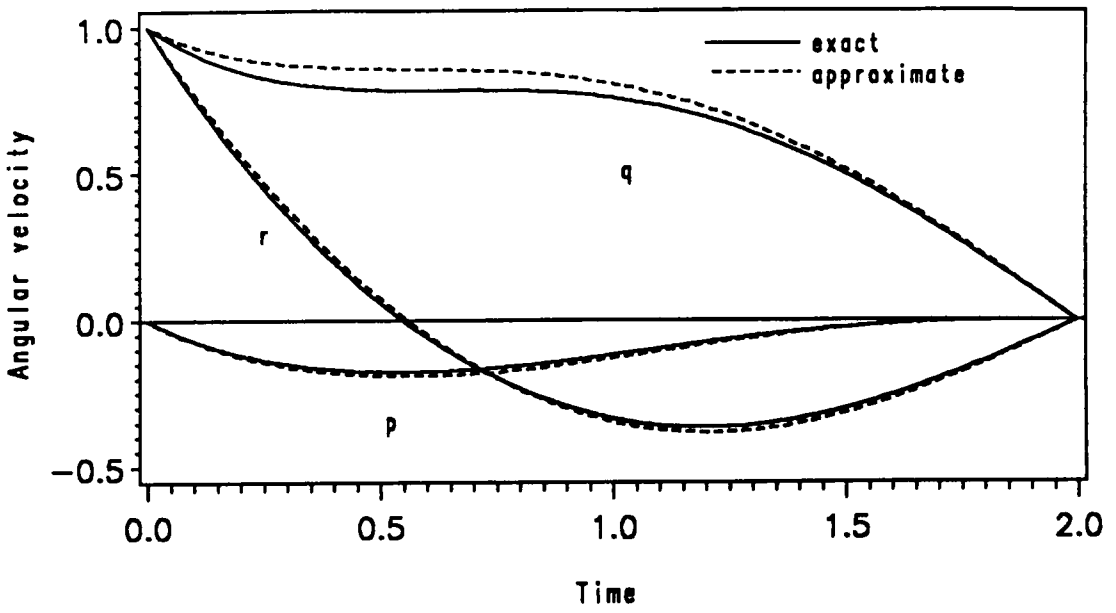

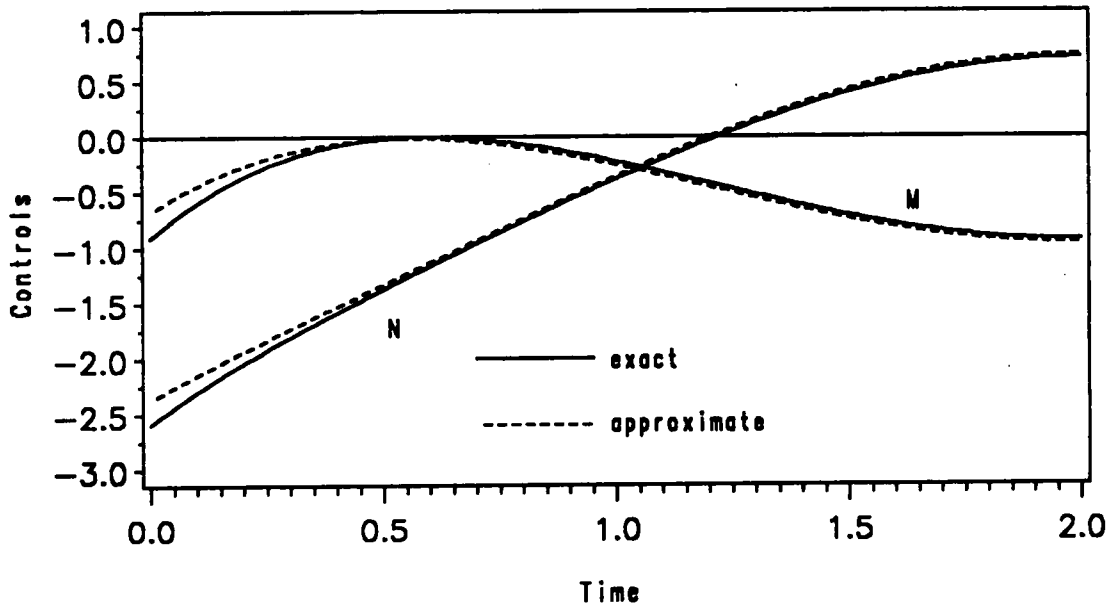

Figure [1]. Exact and Approximate problems.

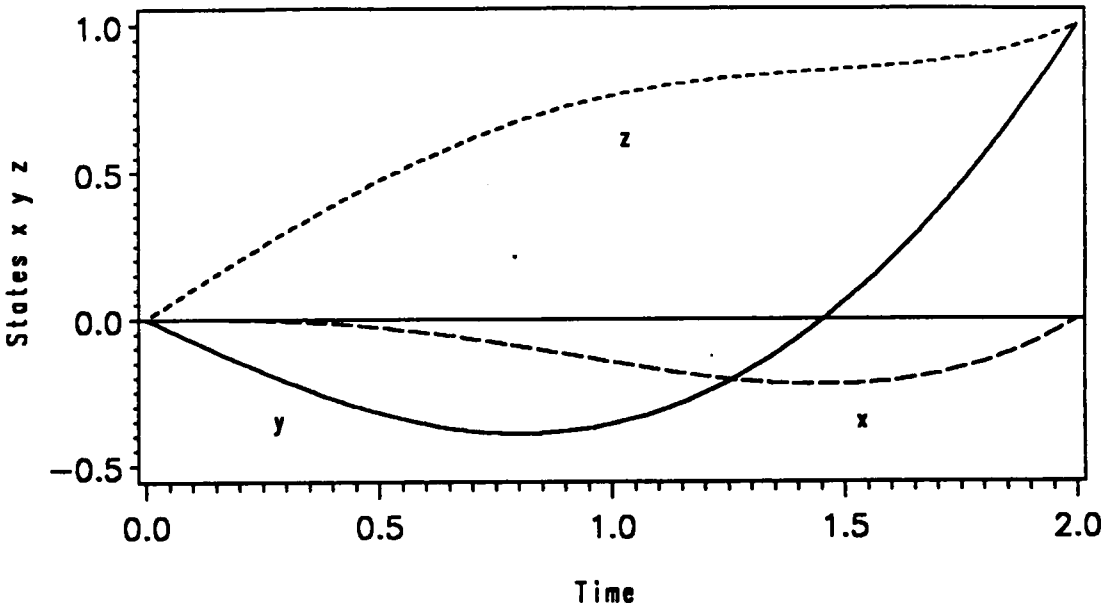

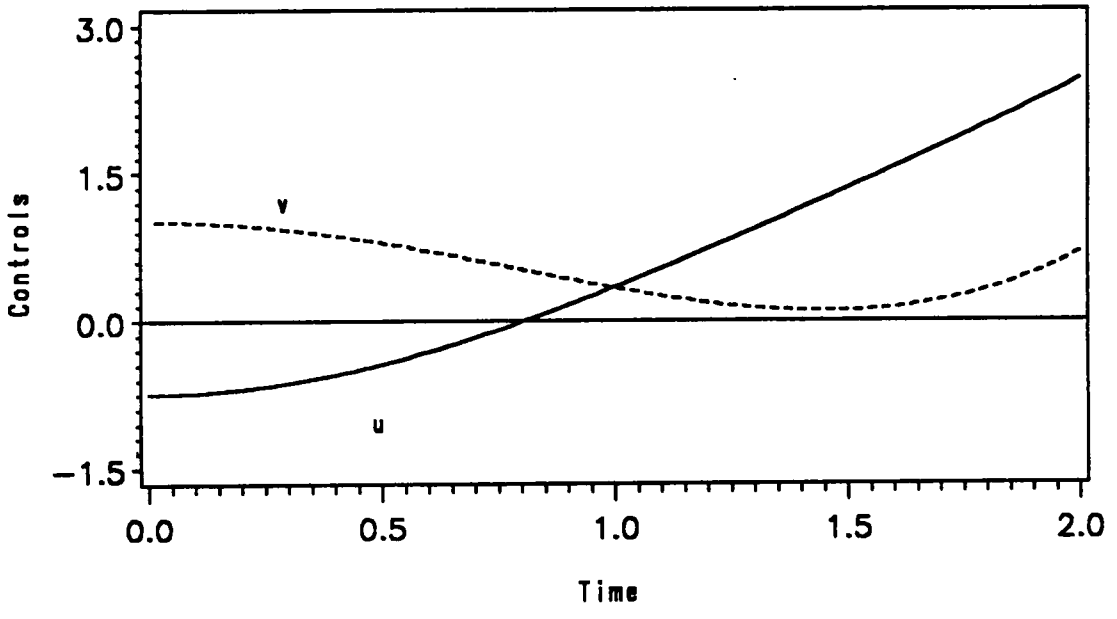

Figure [2]. States y, z and isoperimetric constraint x, and controls u and v for the y - type extremal.

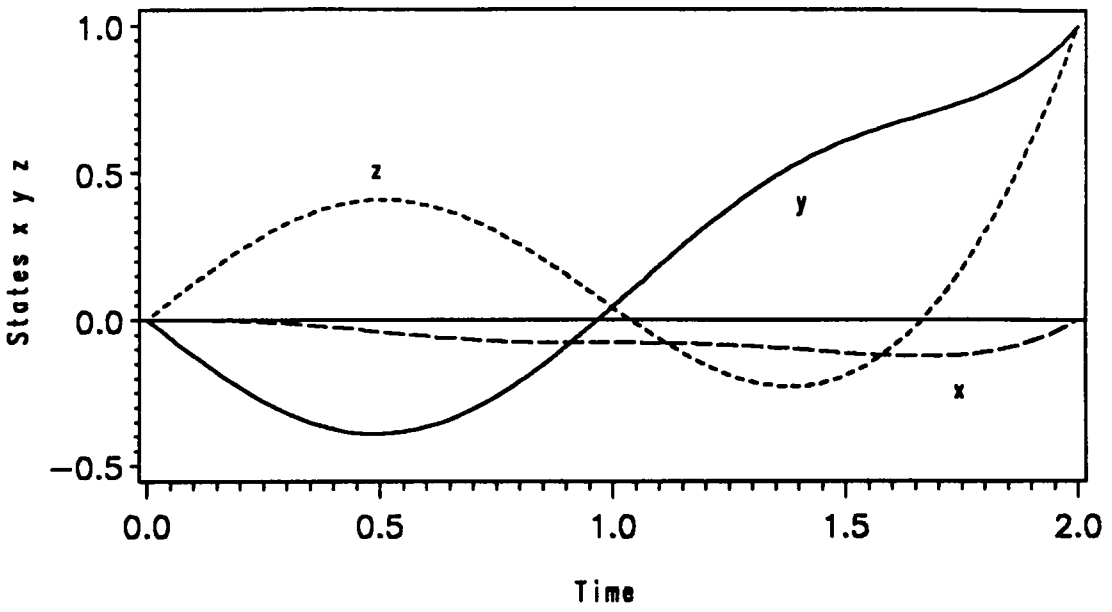

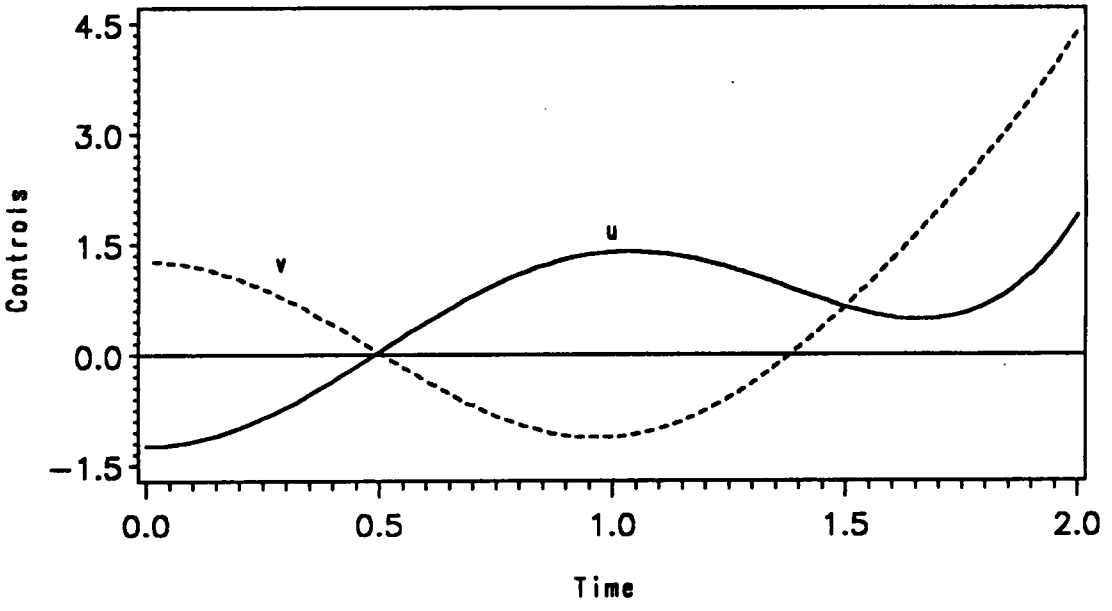

Figure [3]. States y, z and isoperimetric constraint x, and controls u and v for the $y\,z$ - type extremal.

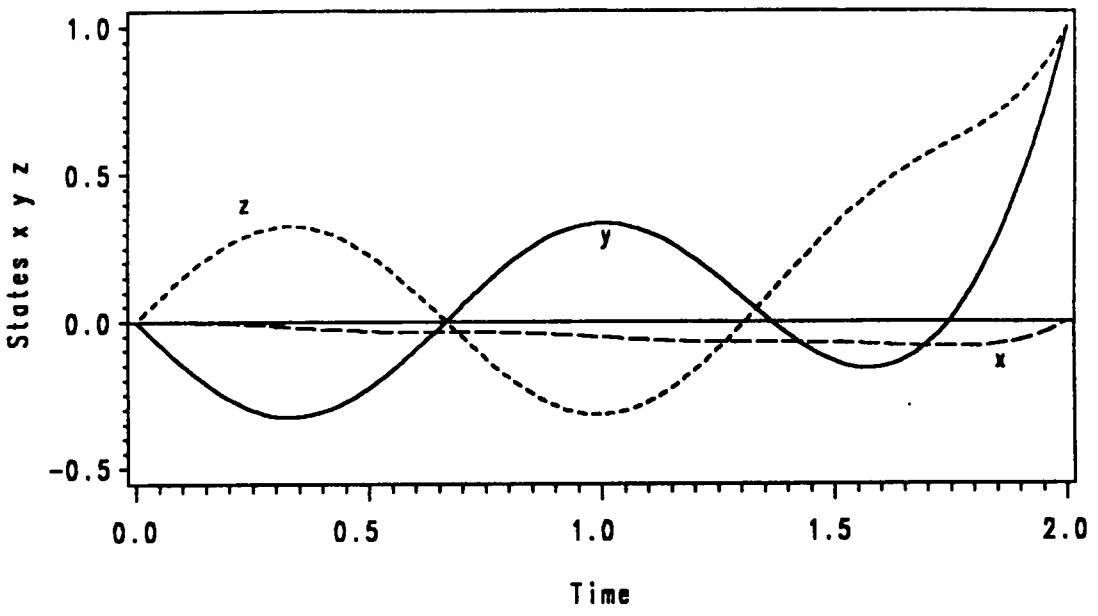

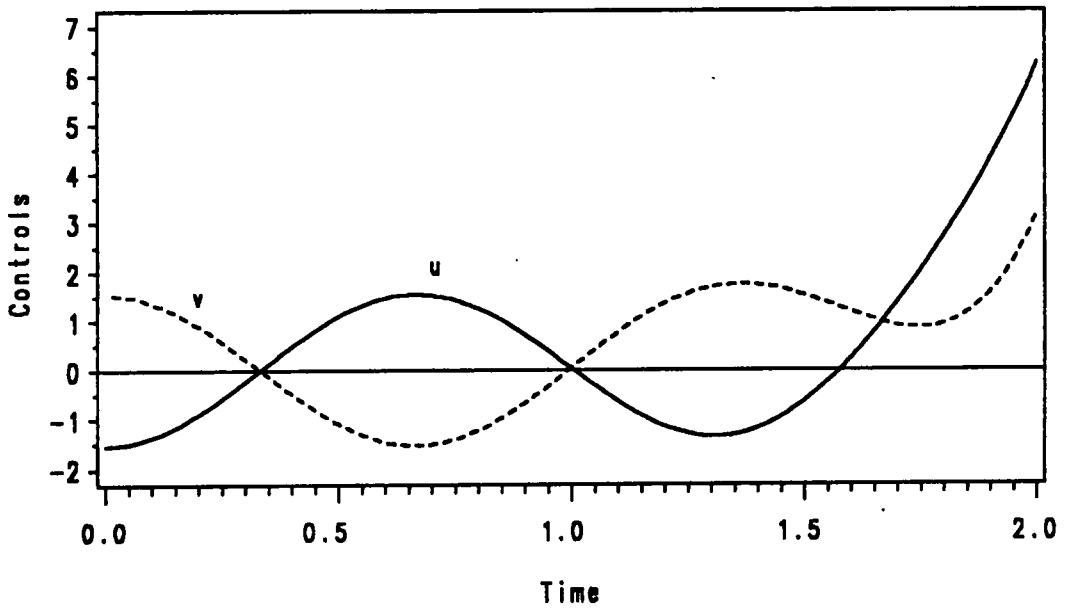

Figure [4]. States y, z and isoperimetric constraint x, and controls u and v for the $y\,z\,y$ - type extremal.

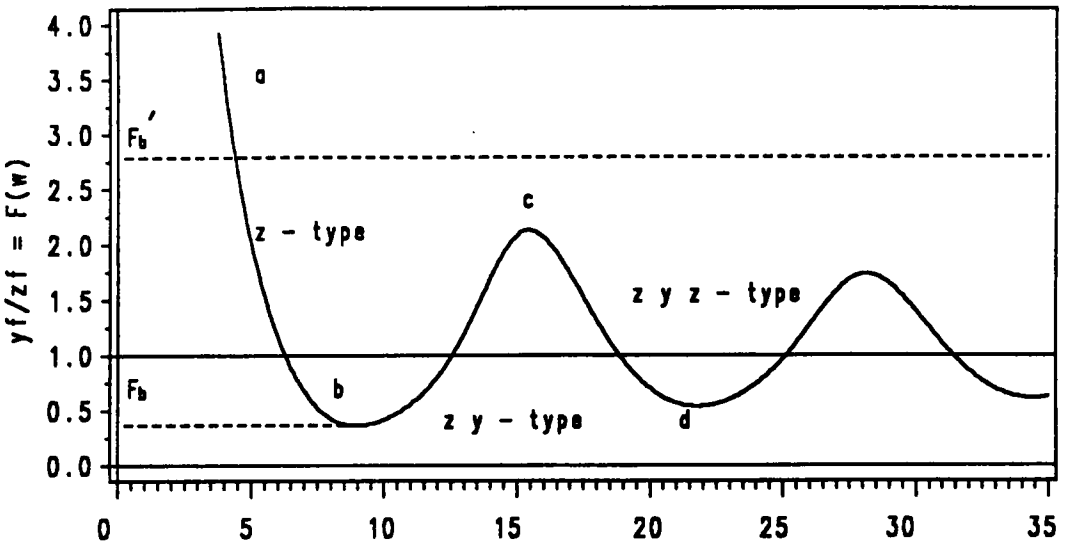

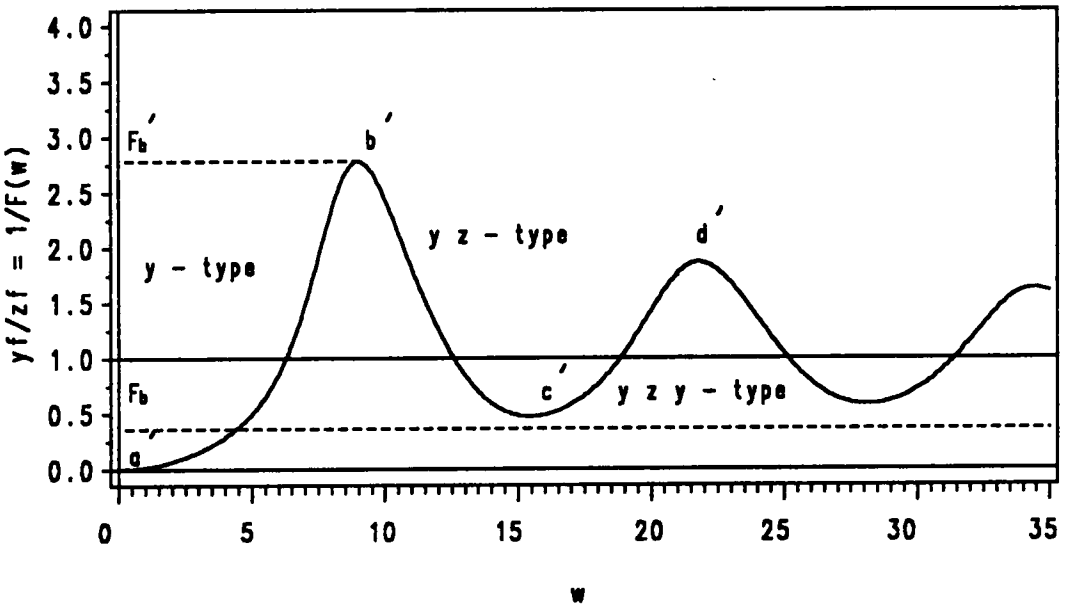

Figure [5a-b]. $F(\omega)$ vs. ω and $\dfrac{1}{F(\omega)}$ vs. ω.

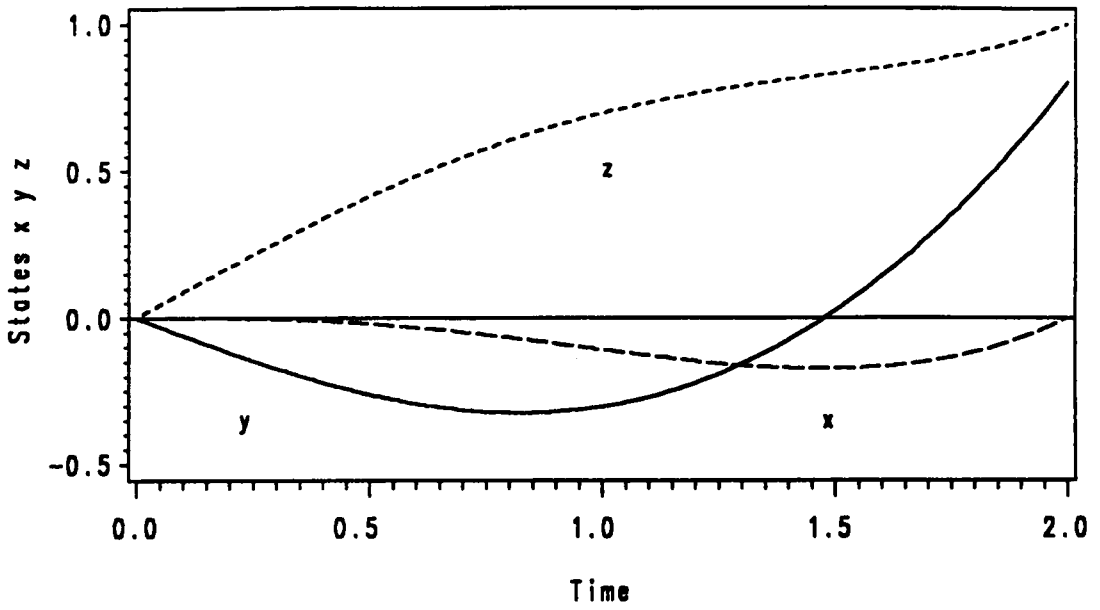

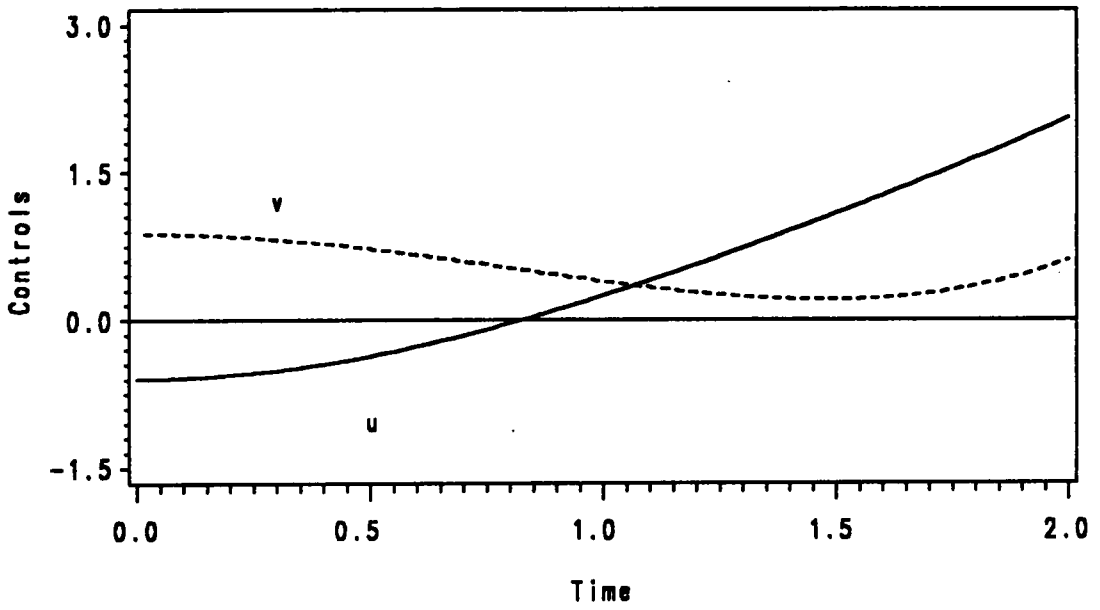

Figure [6]. States y, z and isoperimetric constraint x, and controls u and v for the y - type extremal.

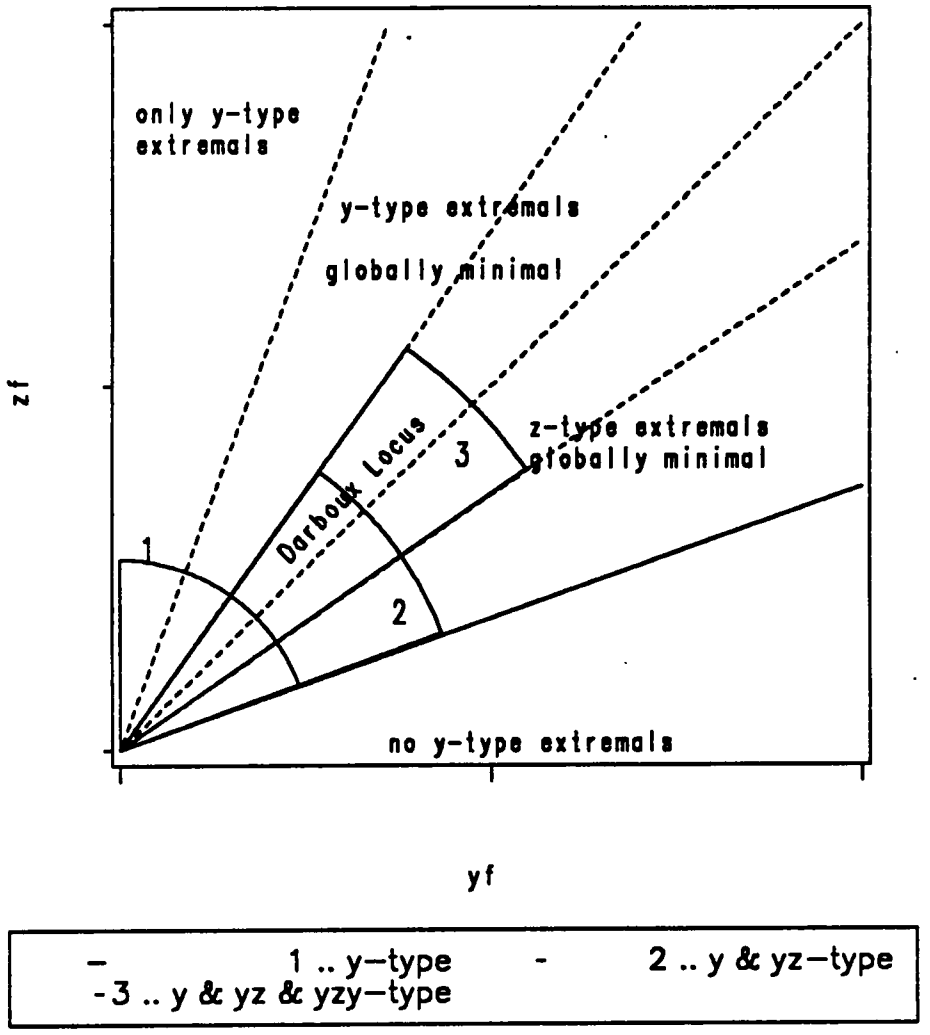

Figure [7]. Domain of $y, y\,z$ and $y\,z\,y$ - type extremal sub-families.

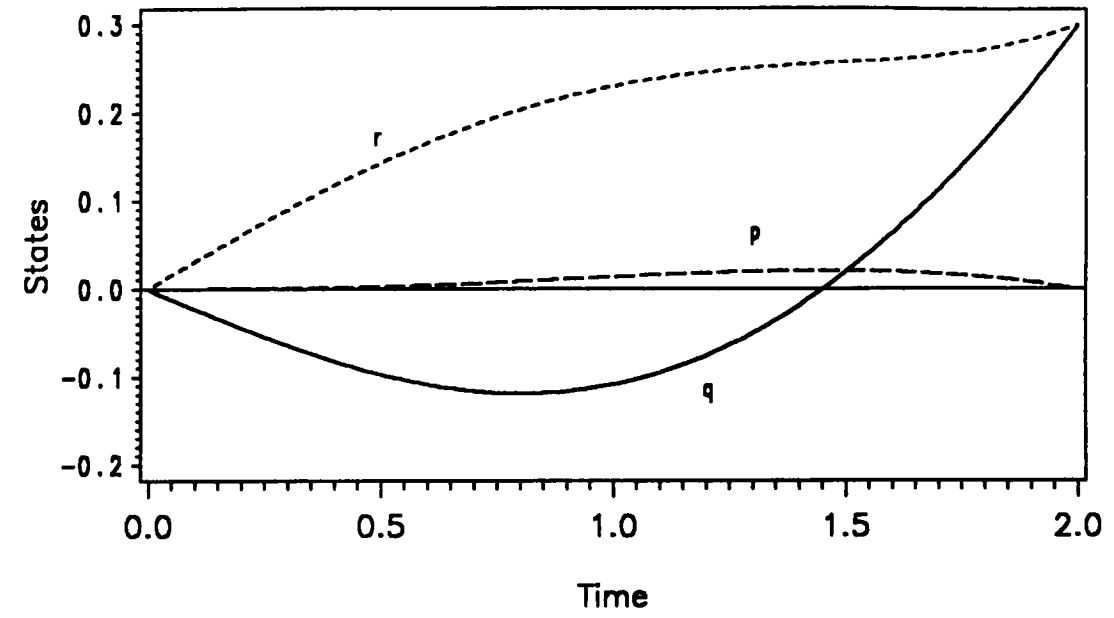

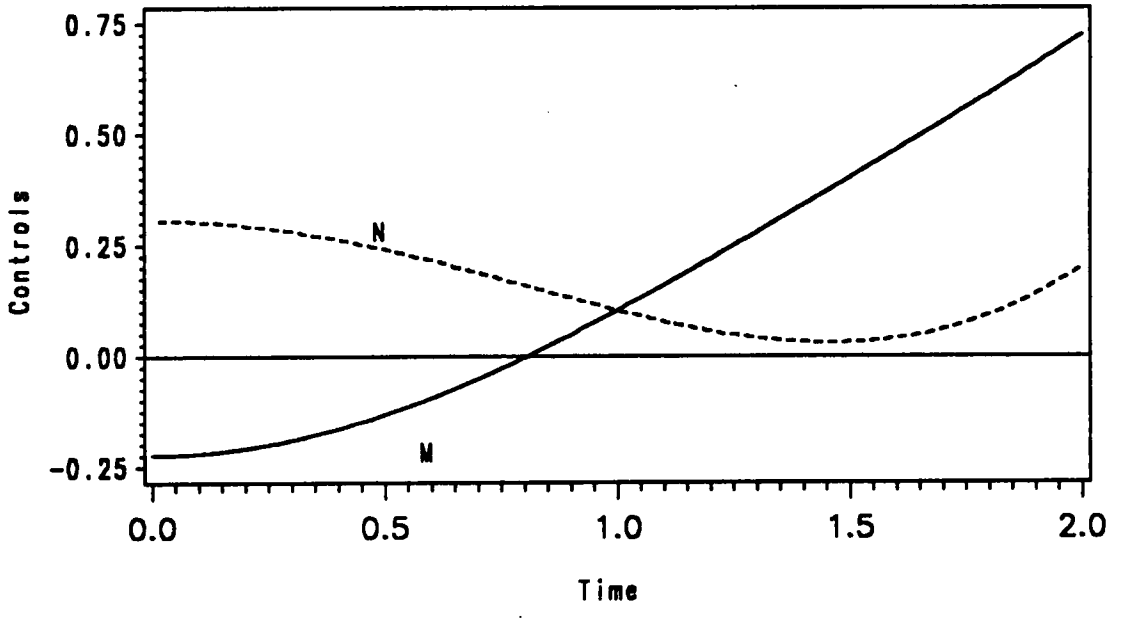

Figure [8]. States p, q and r and Controls M and N time histories, for a q - type extremal of *exact problem.*

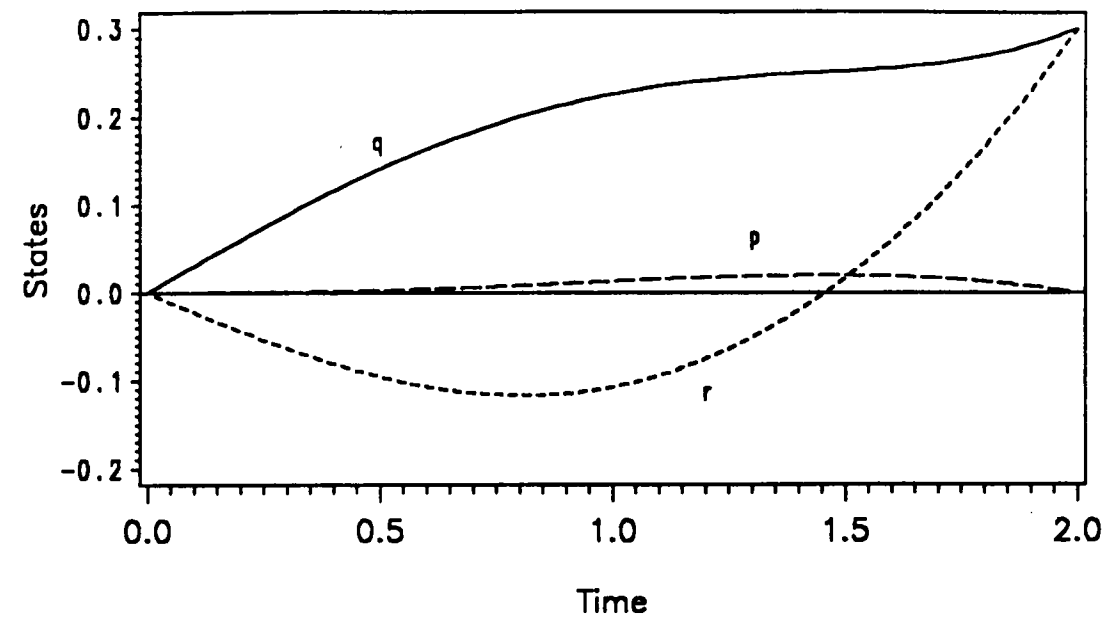

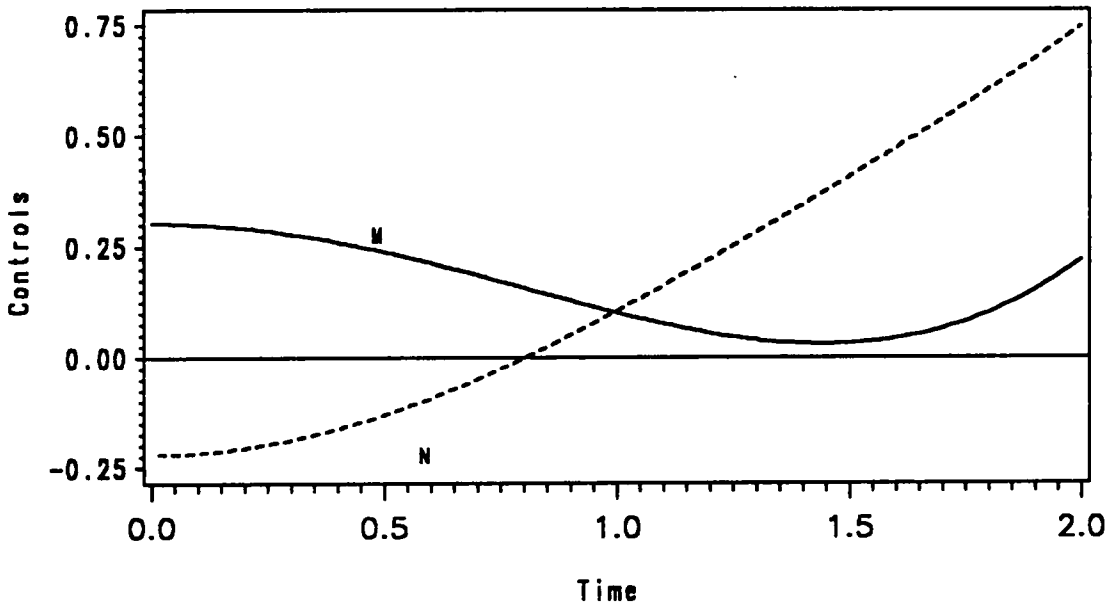

Figure [9]. States p, q and r and Controls M and N time histories, for a r - type extremal of *exact problem.*

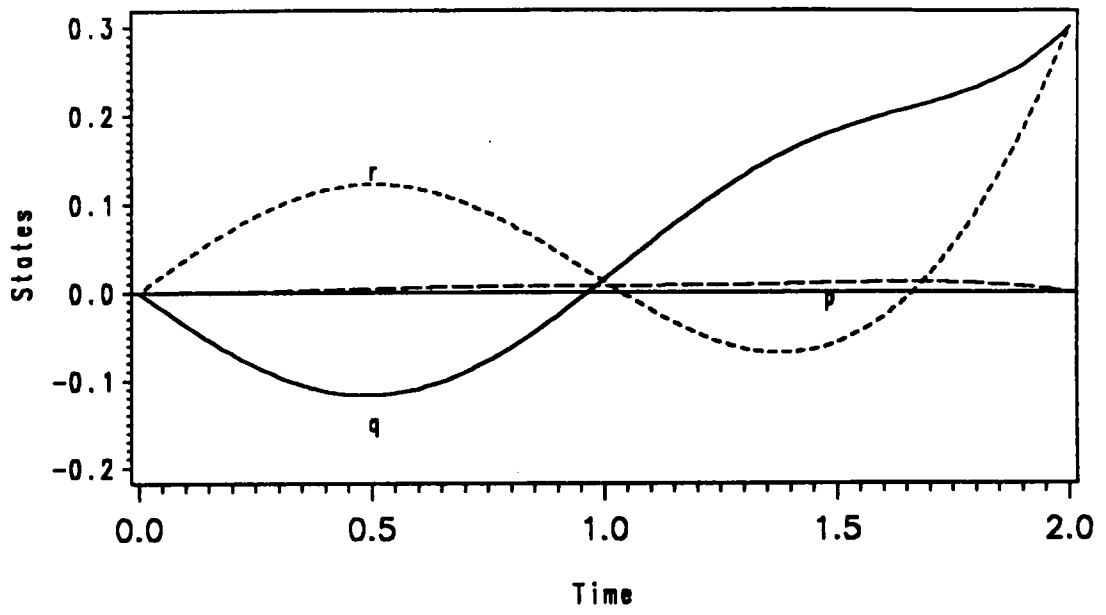

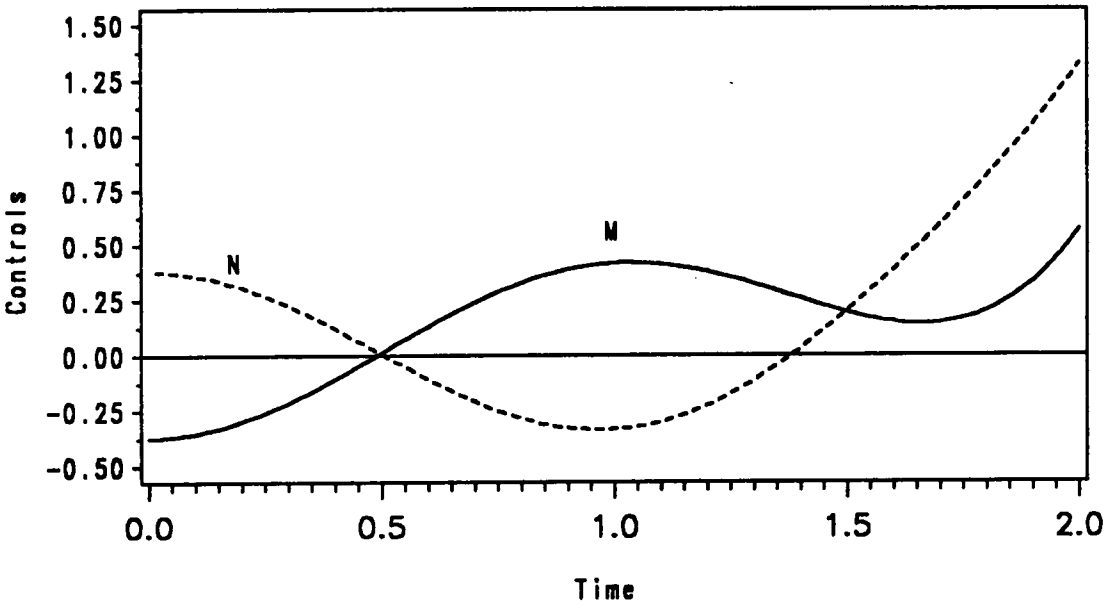

Figure [10]. States p, q and r and Controls M and N time histories, for a $q\,r$ - type extremal of *exact problem.*

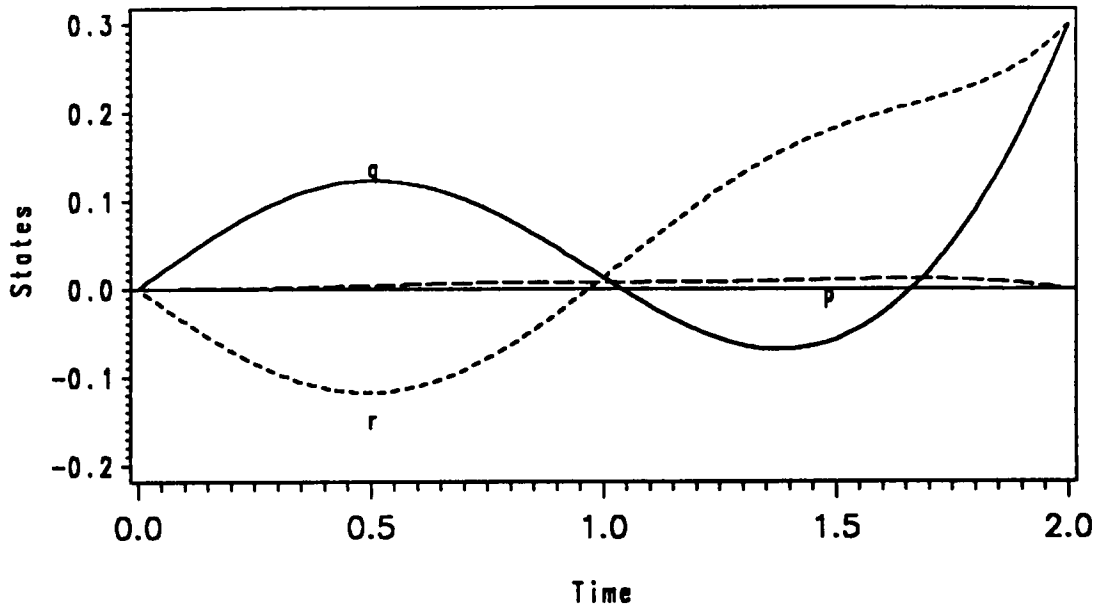

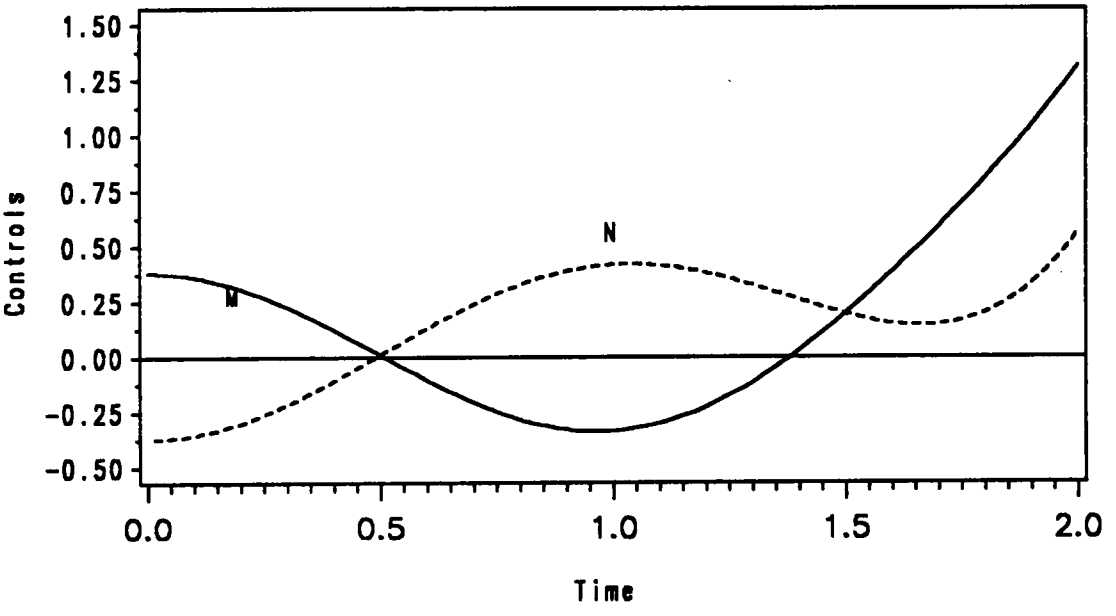

Figure [11]. States p, q and r and Controls M and N time histories, for a $r\,q$ - type extremal of *exact problem.*

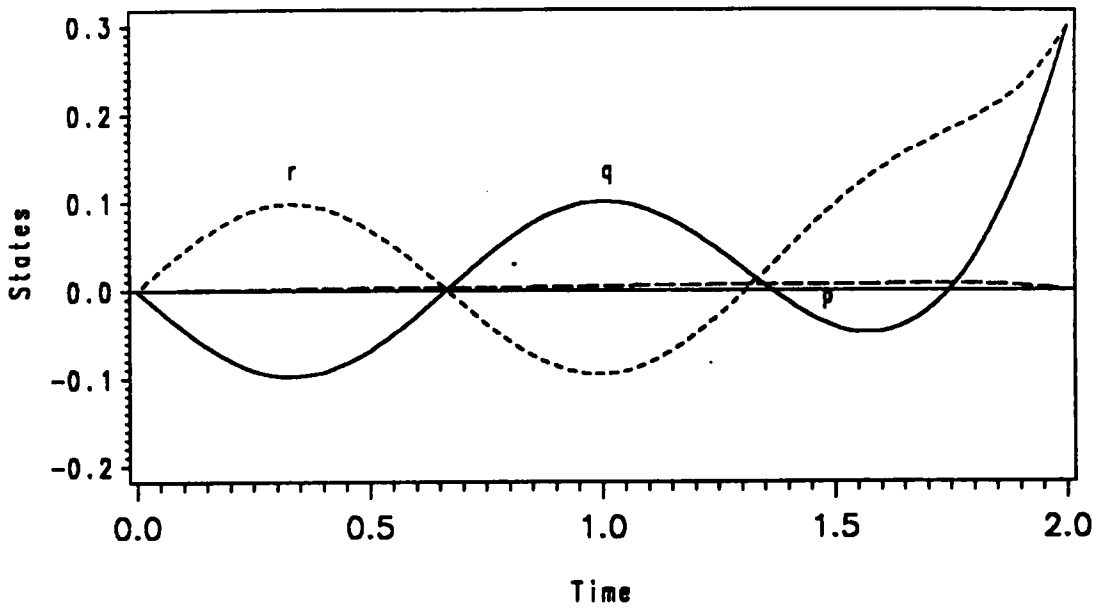

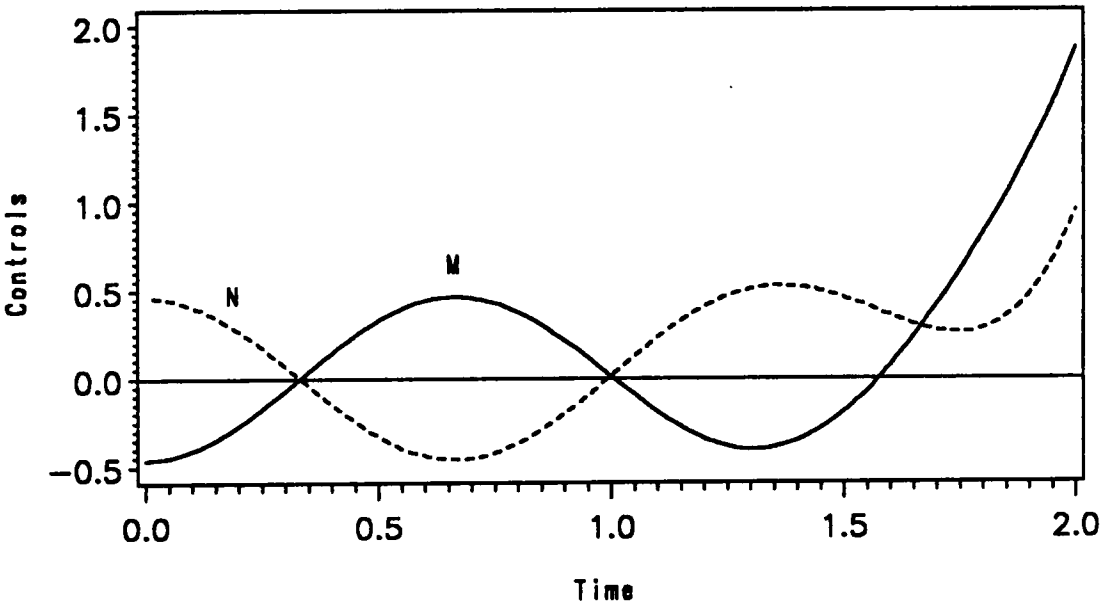

Figure [12]. States p, q and r and Controls M and N time histories, for a $q\,r\,q$ - type extremal of *exact problem.*

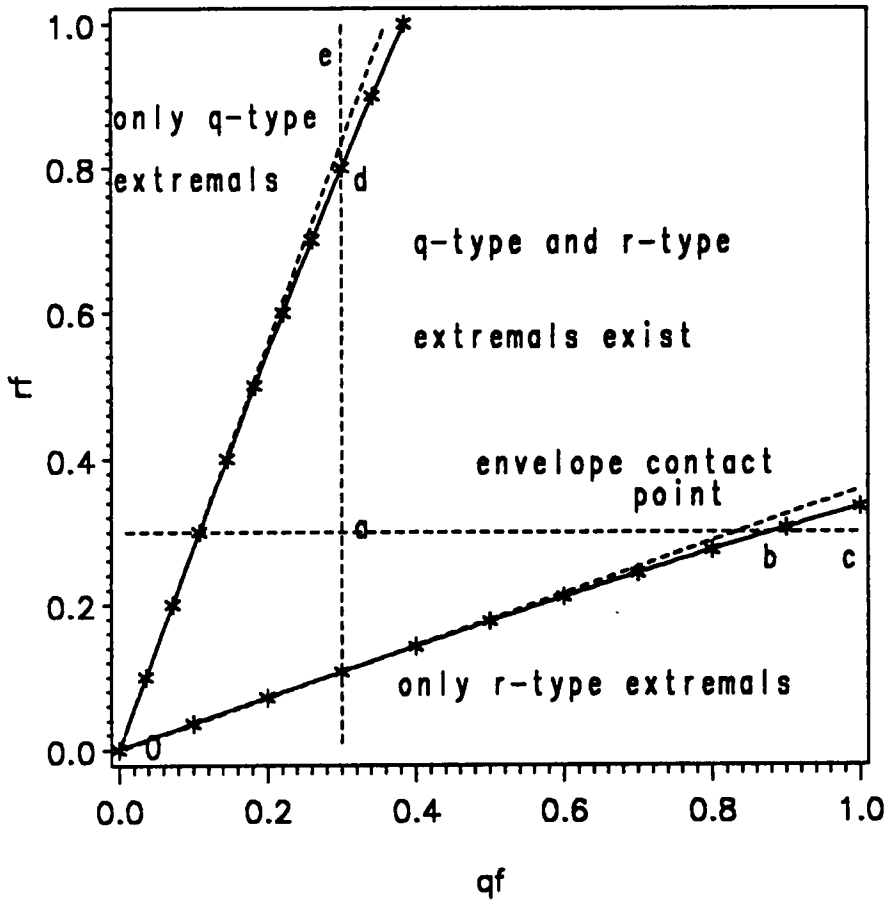

Figure [13]. Domain of Existence: q and r - type extremal sub-families.

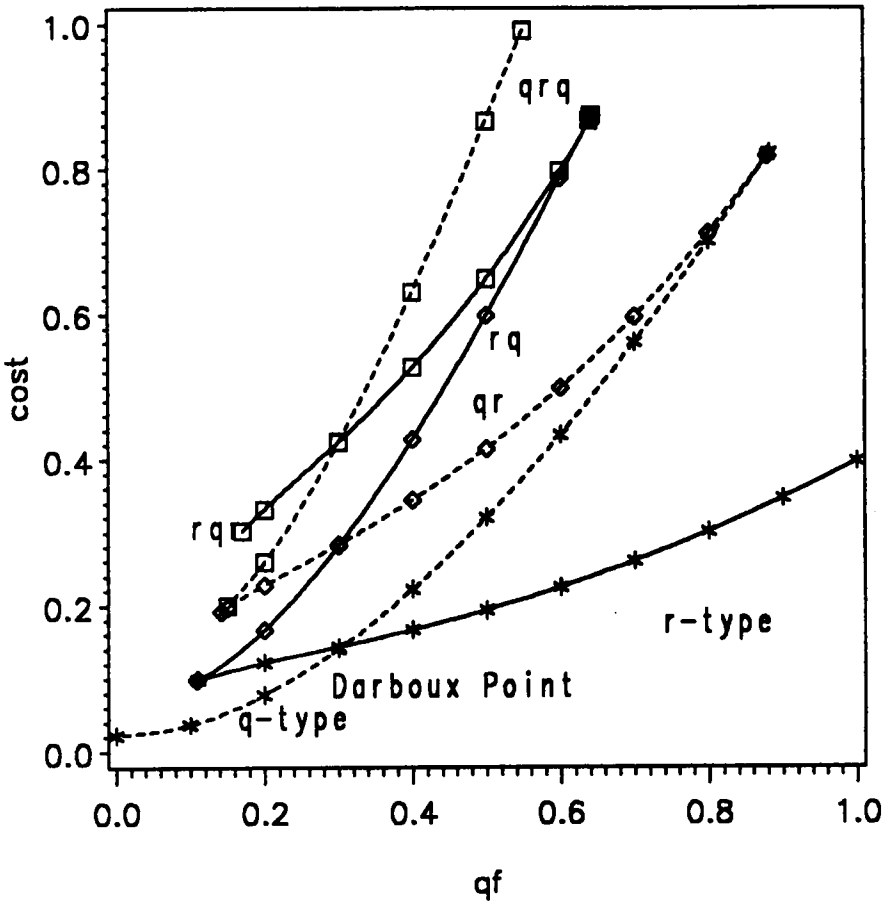

Figure [14]. Cost of different extremal sub-families: $c(t_f)$ vs. q_f, for $r_f = 0.3$.

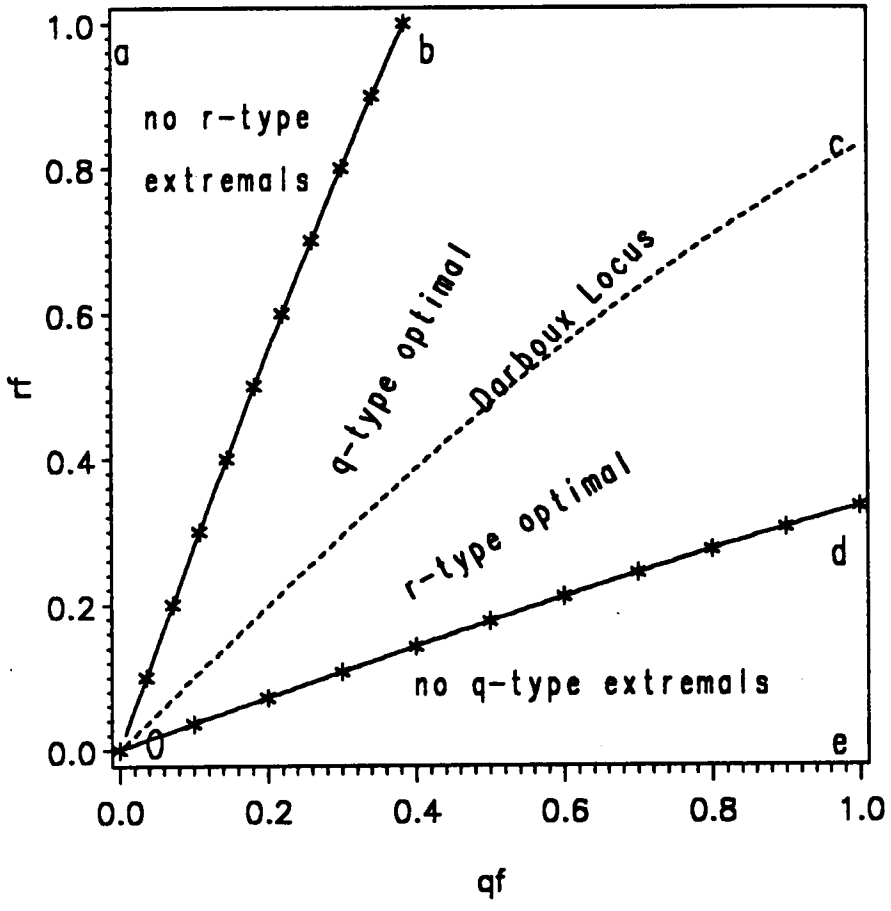

Figure [15]. Locus of Darboux points. Global optimality of q and r - type sub-families.

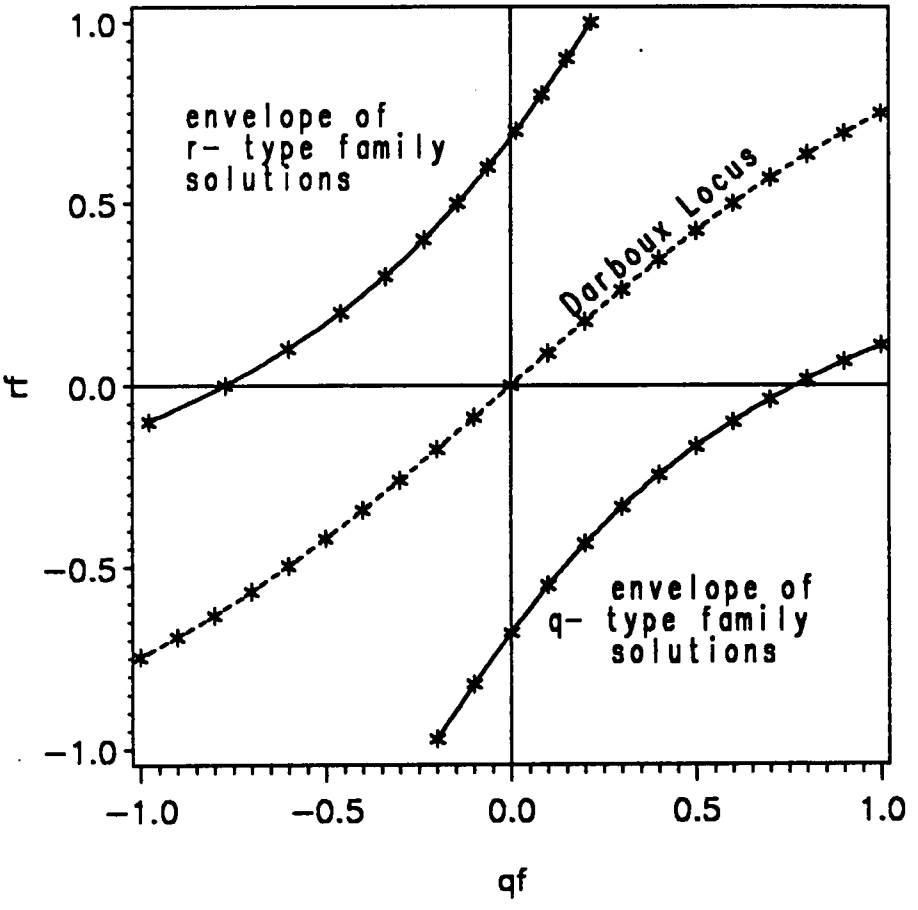

Figure [16]. Darboux Locus and Domains of : q and r - type sub-families, for $p_f = 0.1$.

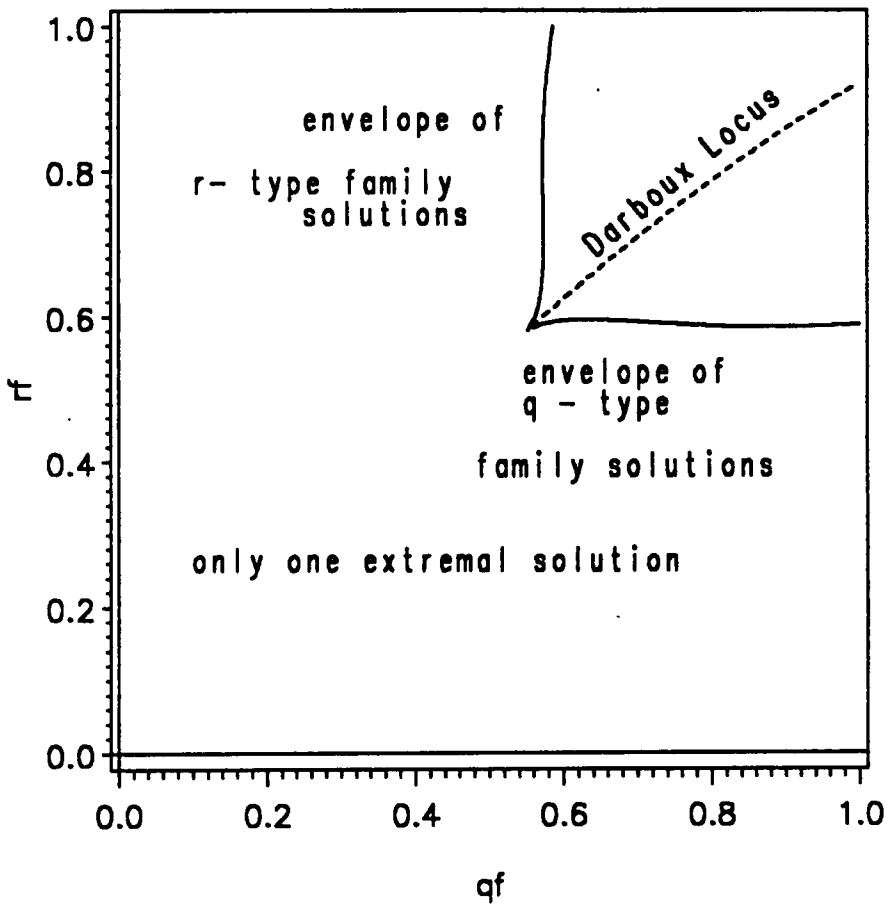

Figure [17]. Darboux Locus and Domains of : q and r - type sub-families, for $p_f = -0.1$.

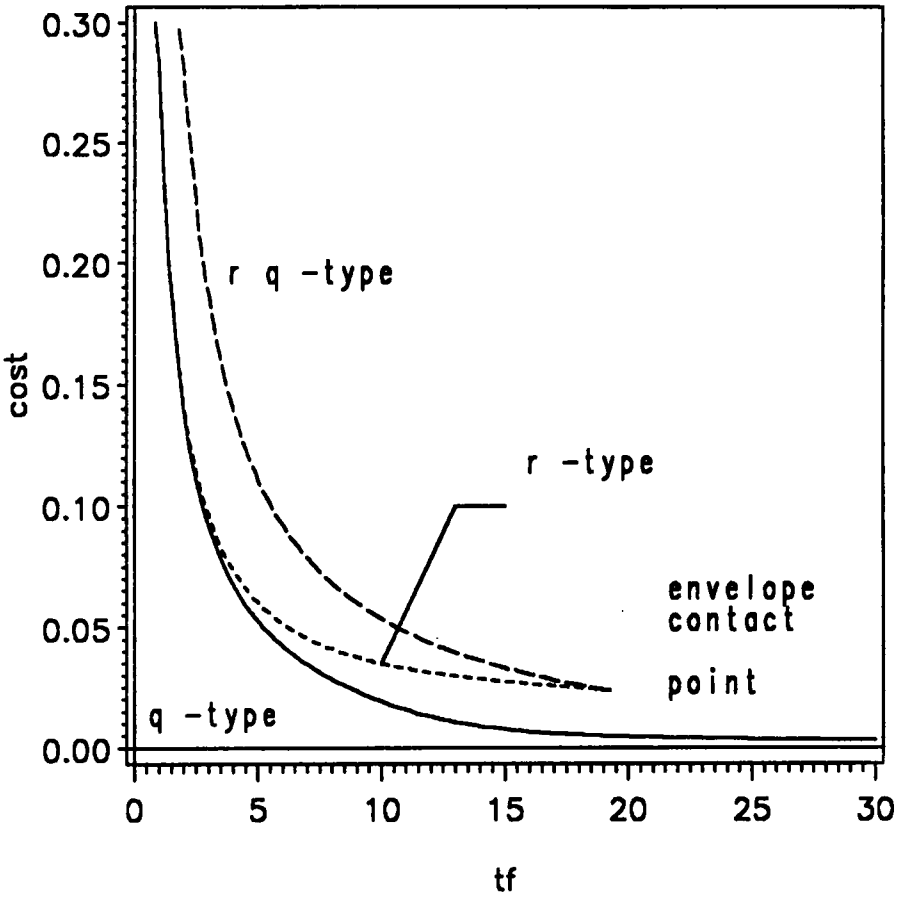

Figure [18]. Cost vs. Maneuver time trade-off.

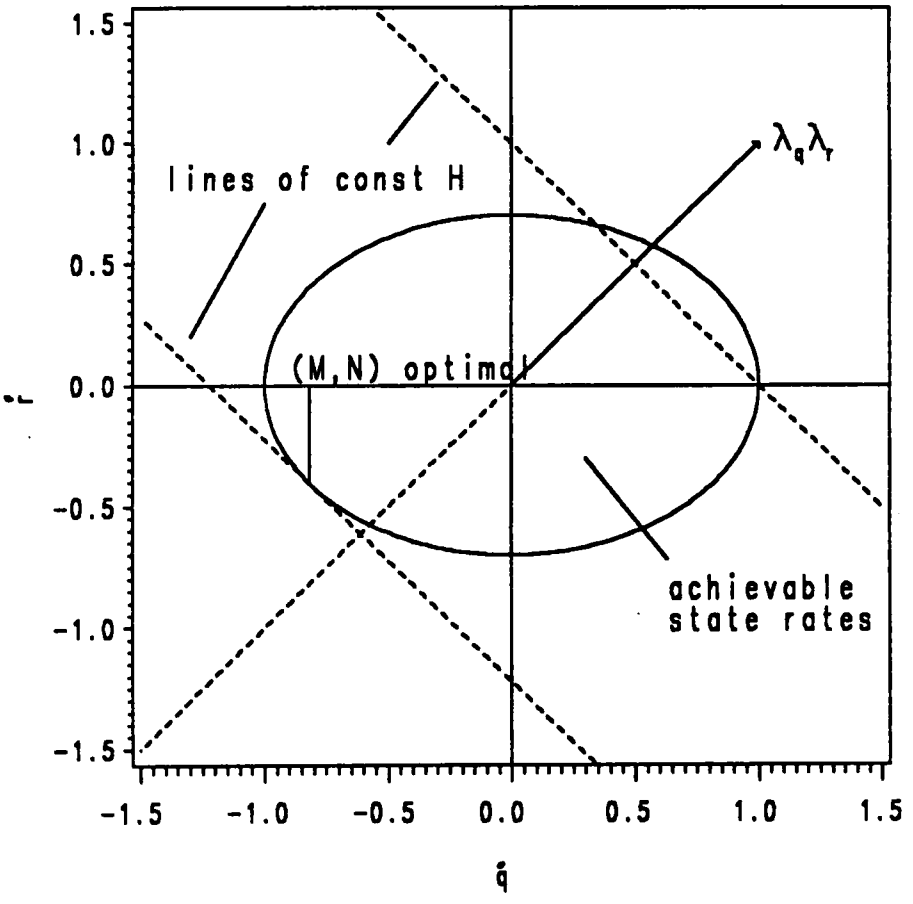

Figure [19]. The generic hodograph space - Ω_1,

$$p = q = r = 0.0.$$

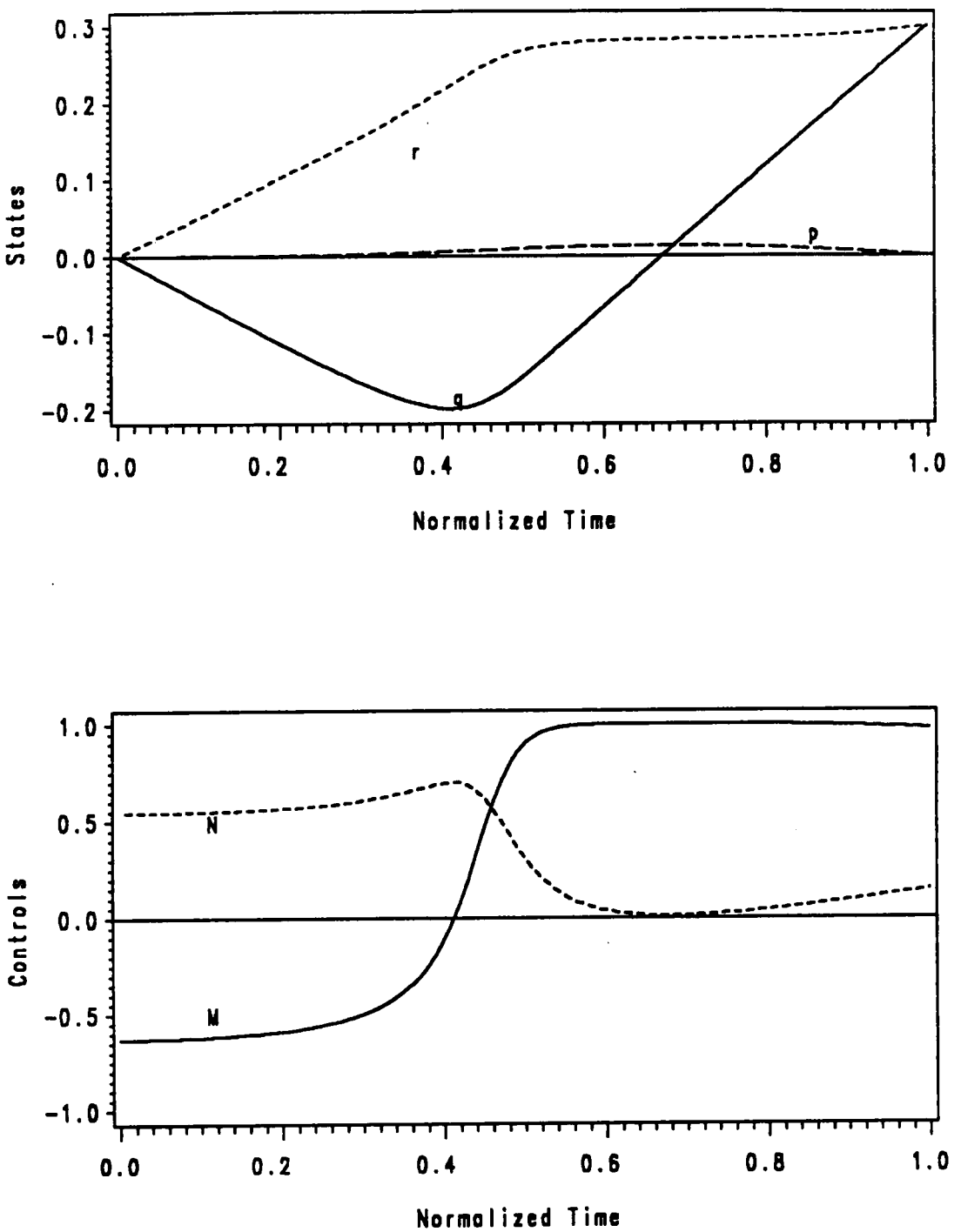

Figure [20]. States p, q and r and Controls M and N time histories, for a q - type extremal of *time-optimal* problem.

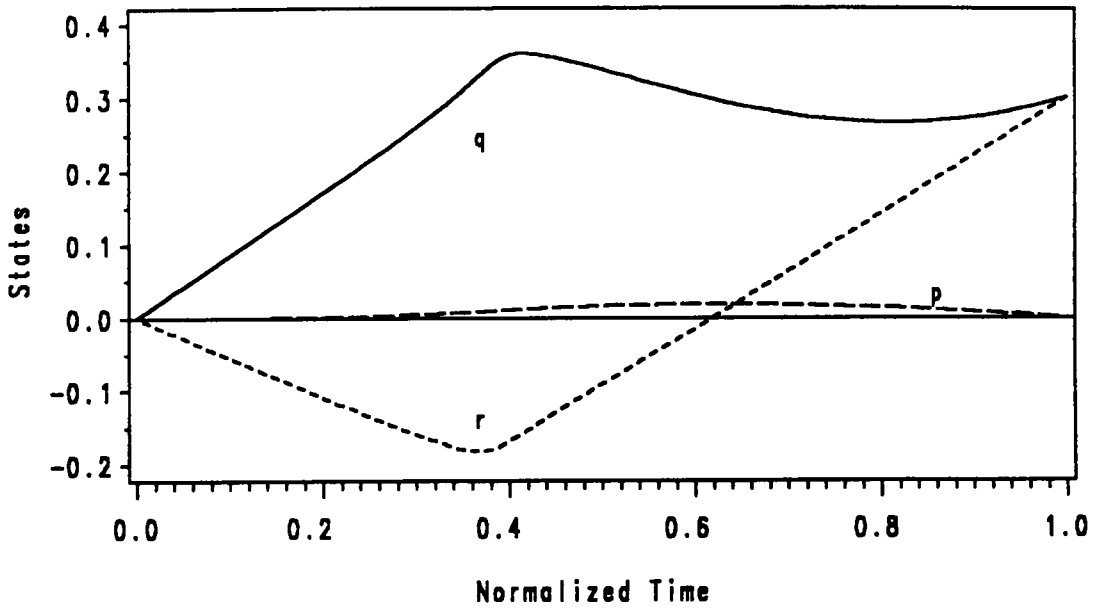

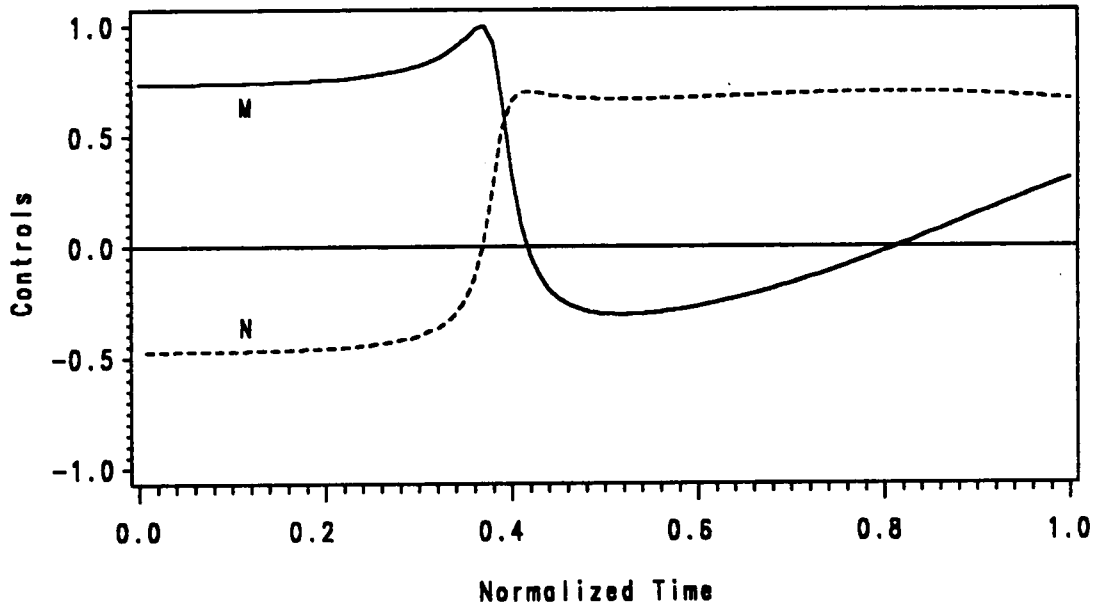

Figure [21]. States p, q and r and Controls M and N time histories, for a r - type extremal of *time-optimal* problem.

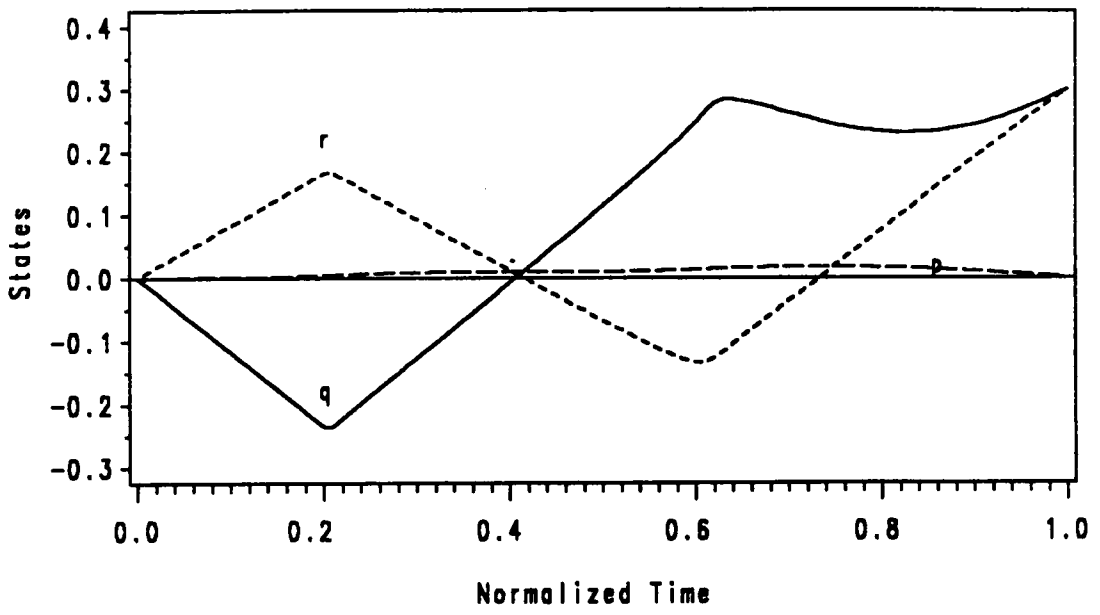

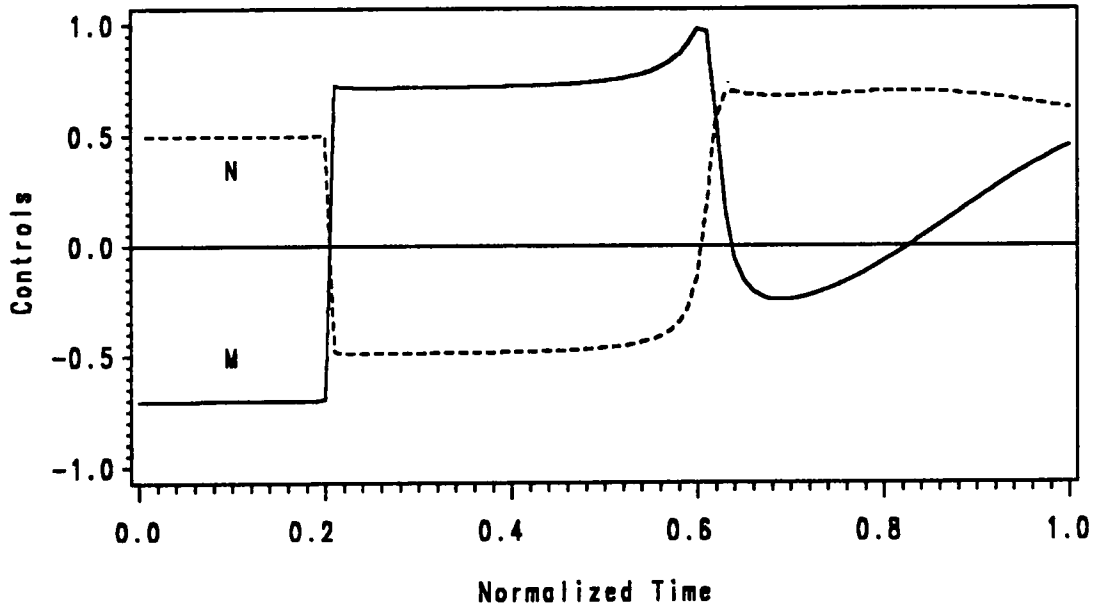

Figure [22]. States p, q and r and Controls M and N time histories, for a $q\,r$ - type extremal of *time-optimal* problem.

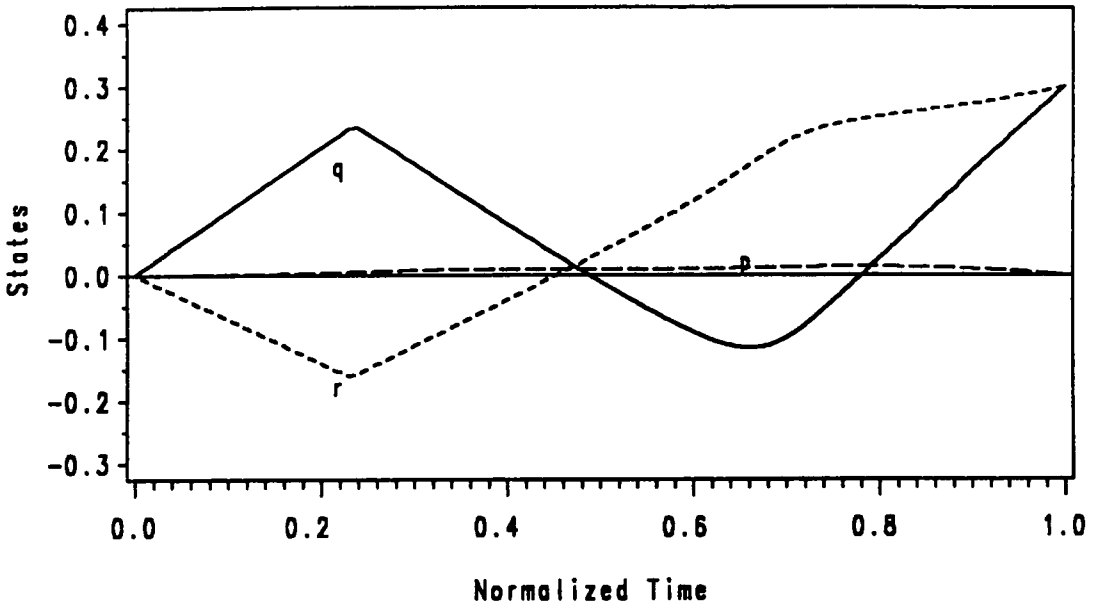

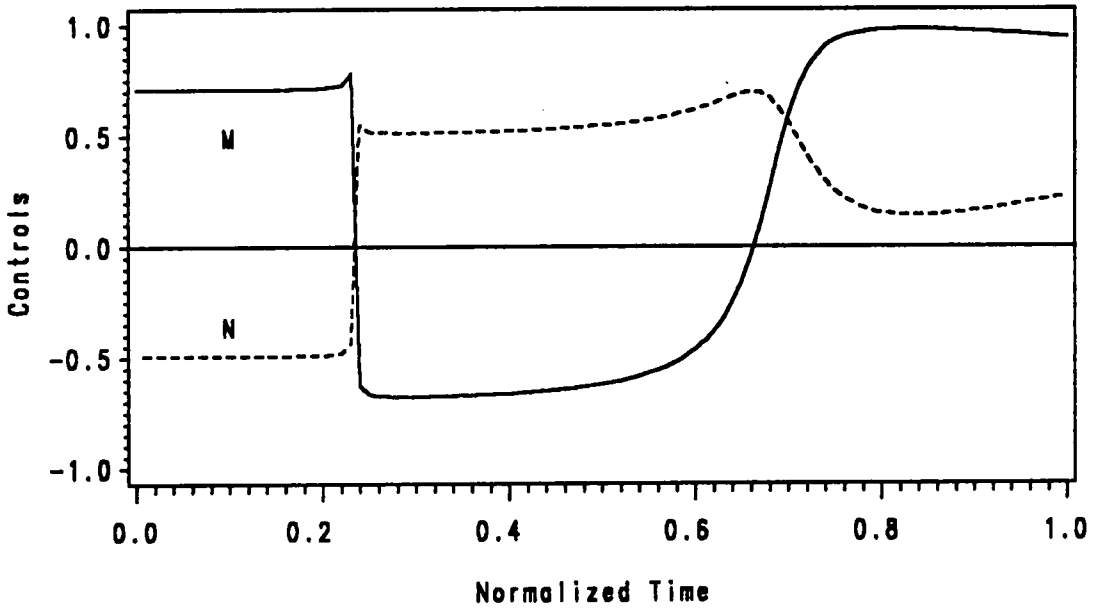

Figure [23]. States p, q and r and Controls M and N time histories, for a $r\,q$ - type extremal of *time-optimal* problem.

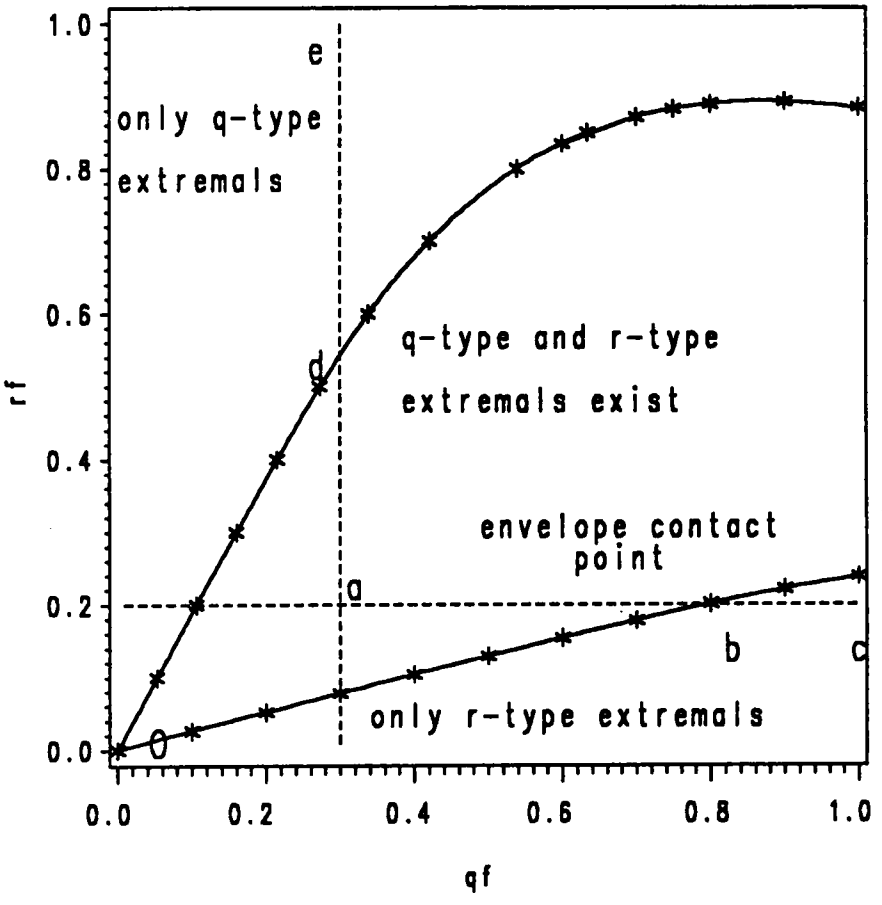

Figure [24]. Domain of q and r - type extremal sub-families of *time-optimal* problem.

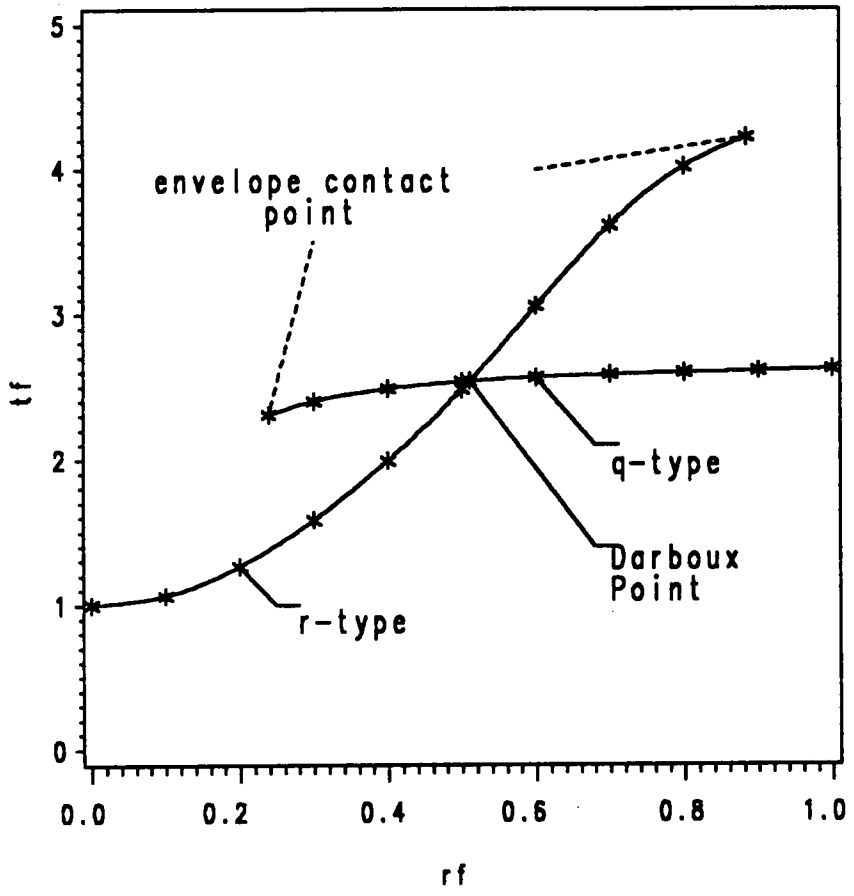

Figure [25]. Optimal Cost τ_f vs. r_f for $q_f = 1.0$,

for the *time-optimal* problem.

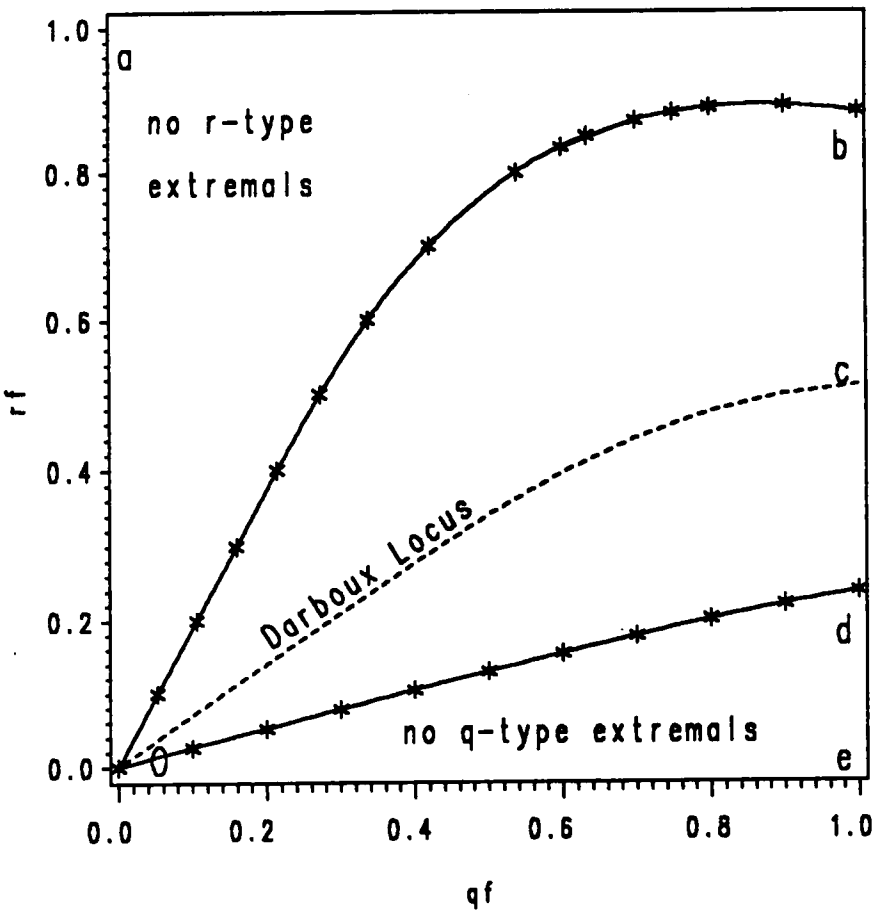

Figure [26]. Locus of Darboux points. Global optimality of q and r - type sub-families of *time-optimal* problem.

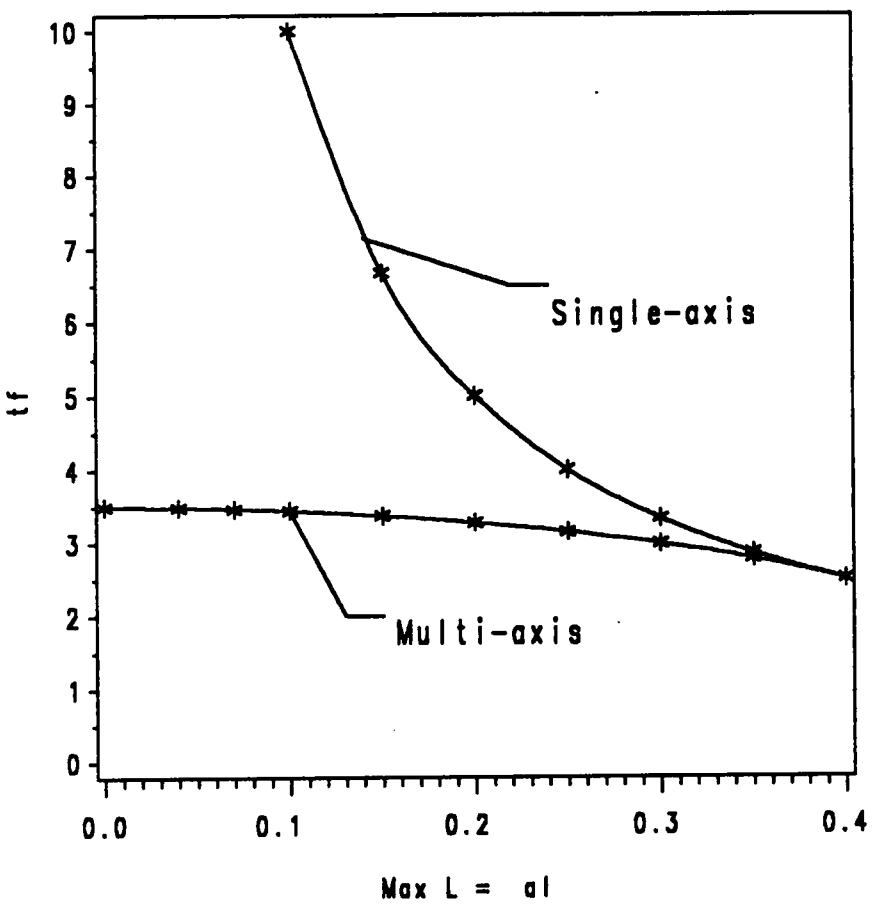

Figure [27]. Single-axis vs. Multi-axis Roll Rate Control.

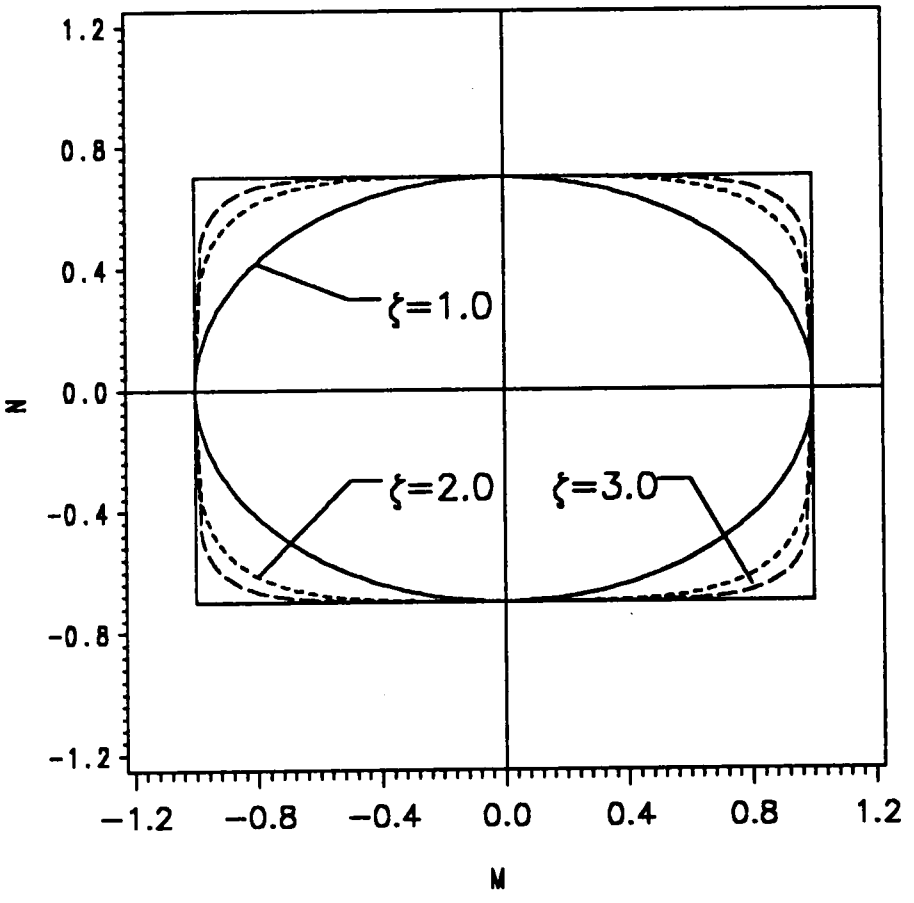

Figure [28]. Control Constraint Sets Ω_3 for $\zeta = 1.0, 2.0$ and 3.0.

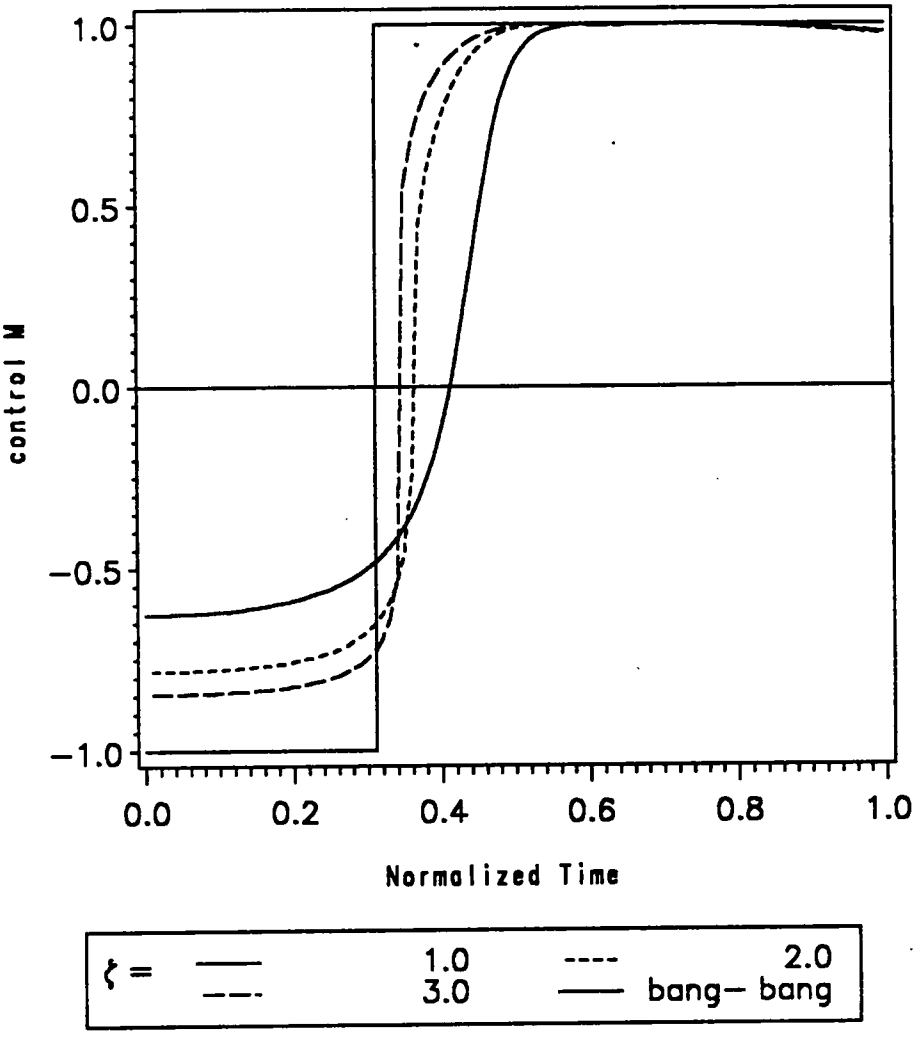

Figure [29a]. Control Moment M deformation to bang-bang solution.

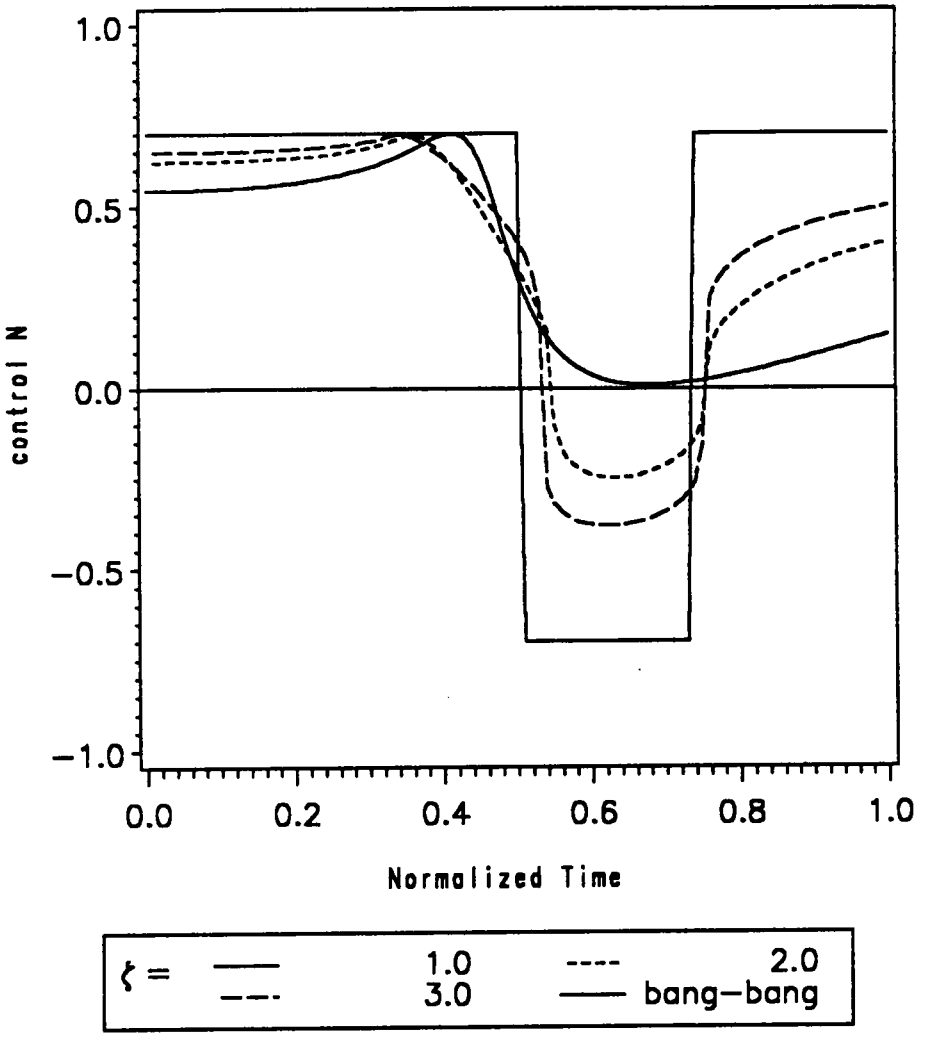

Figure [29b]. Control Moment N deformation to bang-bang solution.

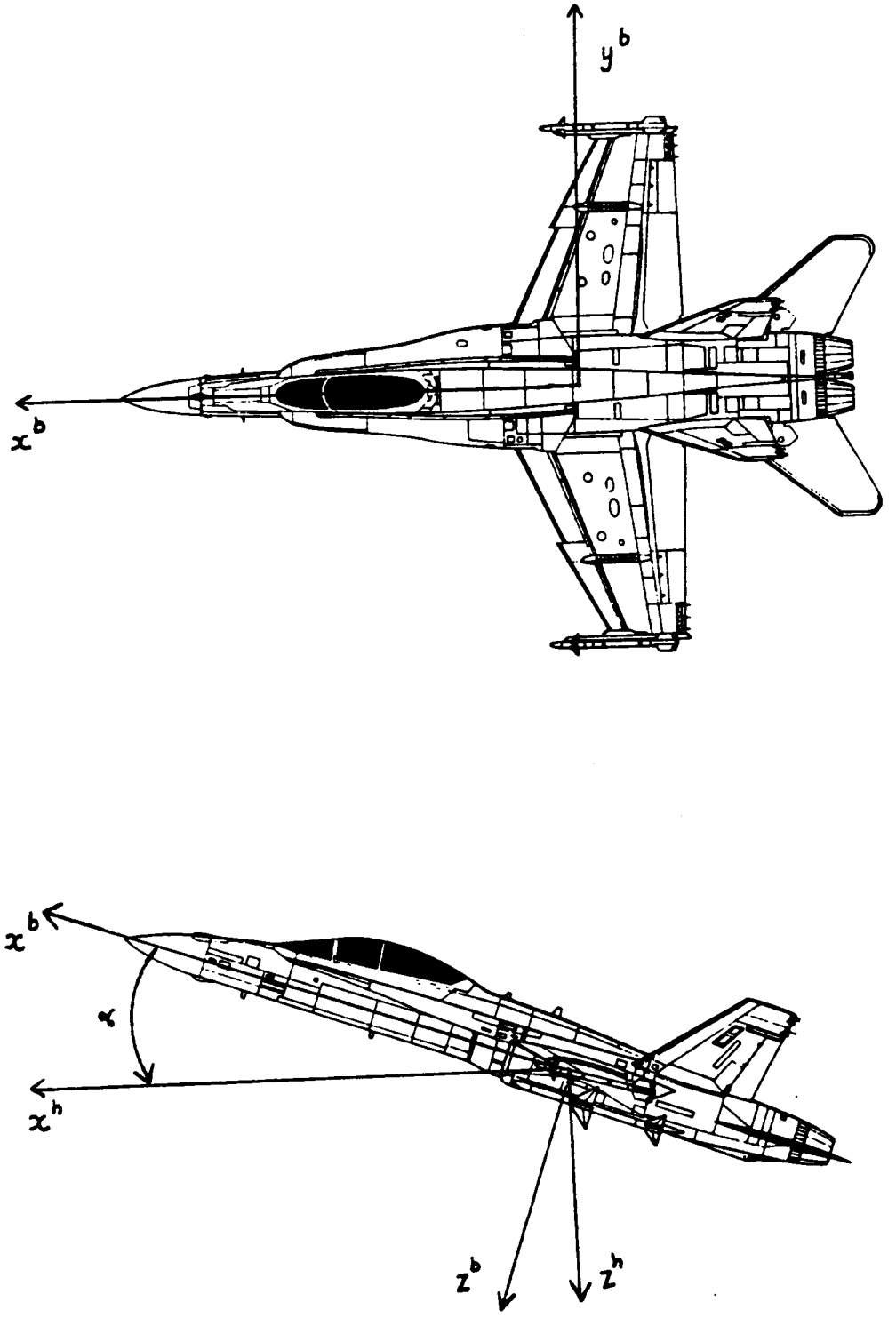

Figure [30]. The coordinate systems.

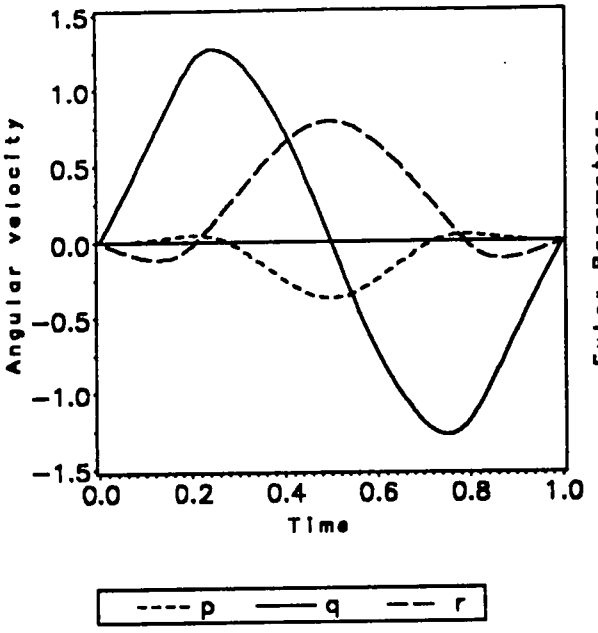

Figure [31a]. Angular Velocity p, q and r.

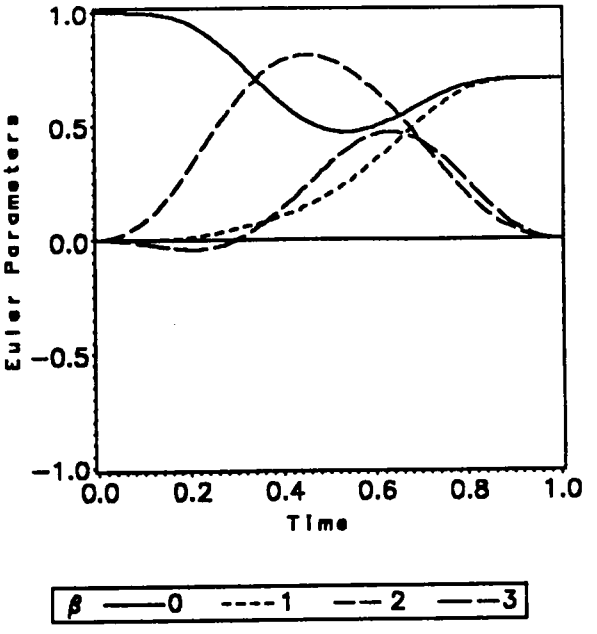

Figure [31b]. Euler Parameters β_0, β_1, β_2 and β_3.

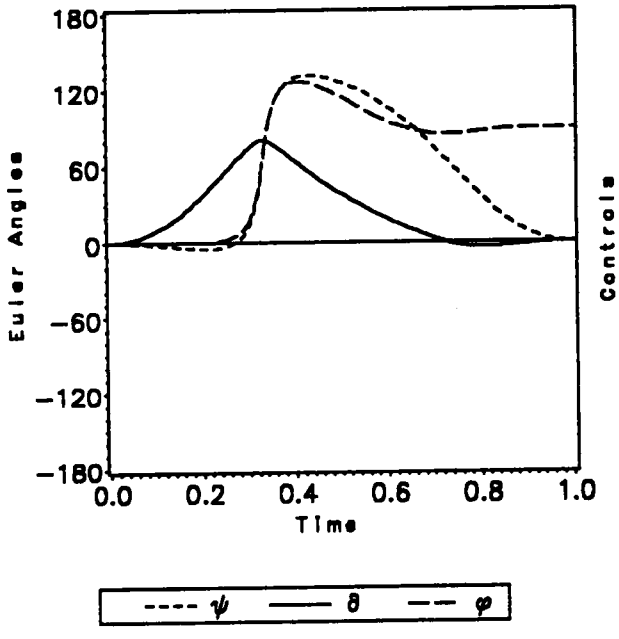

Figure [31c]. Euler Angles ψ, θ and ϕ.

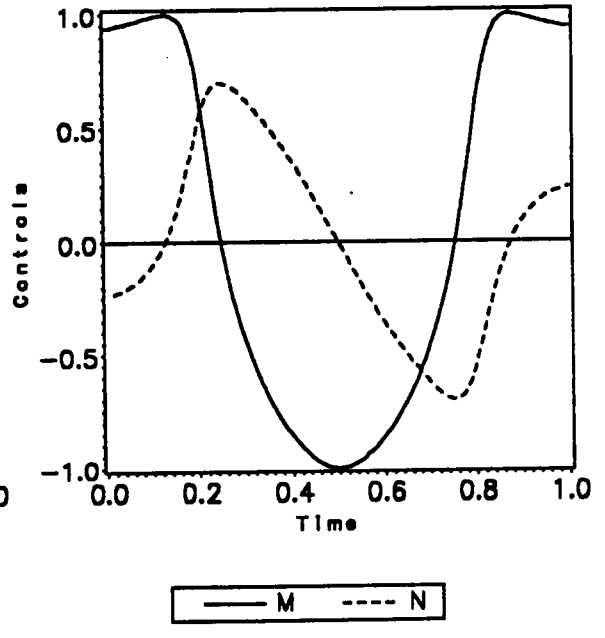

Figure [31d]. Controls M and N.

Figure [31]. A F1 extremal.

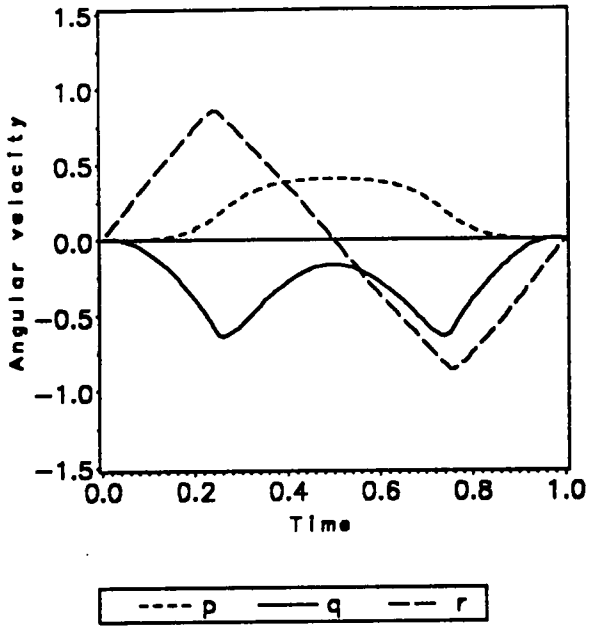

Figure [32a]. Angular Velocity p, q and r.

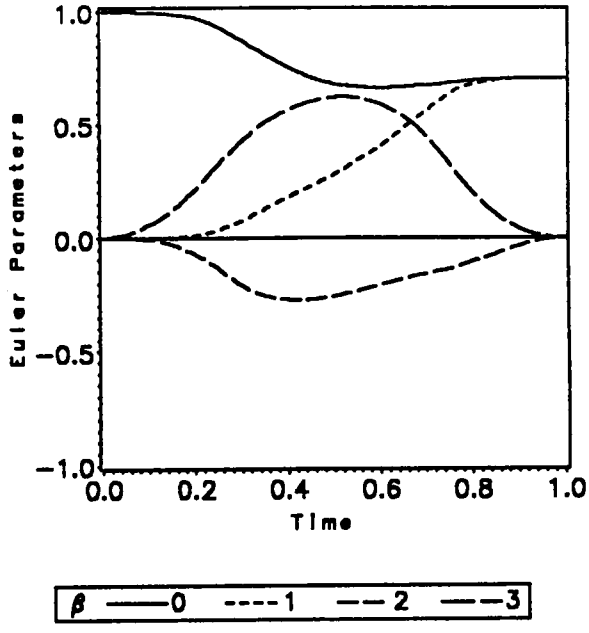

Figure [32b]. Euler Parameters β_0, β_1, β_2 and β_3.

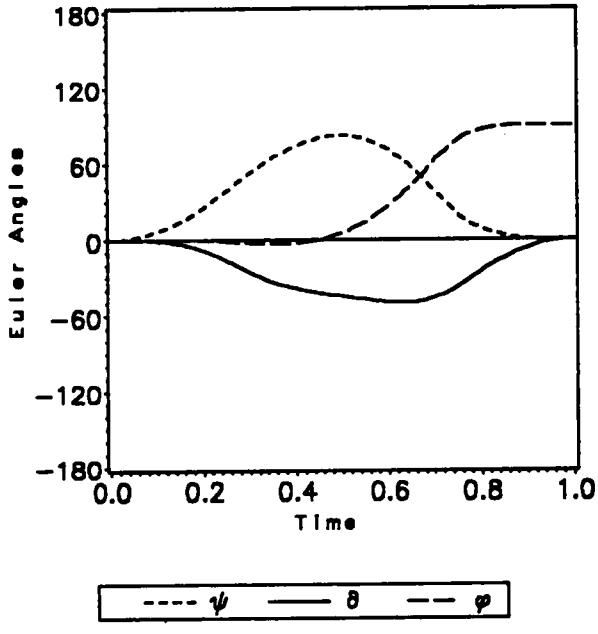

Figure [32c]. Euler Angles ψ, θ and ϕ.

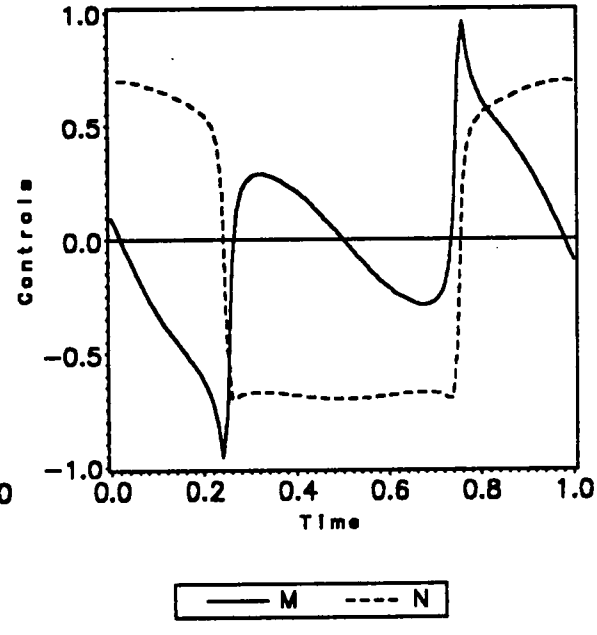

Figure [32d]. Controls M and N.

Figure [32]. A F2 extremal.

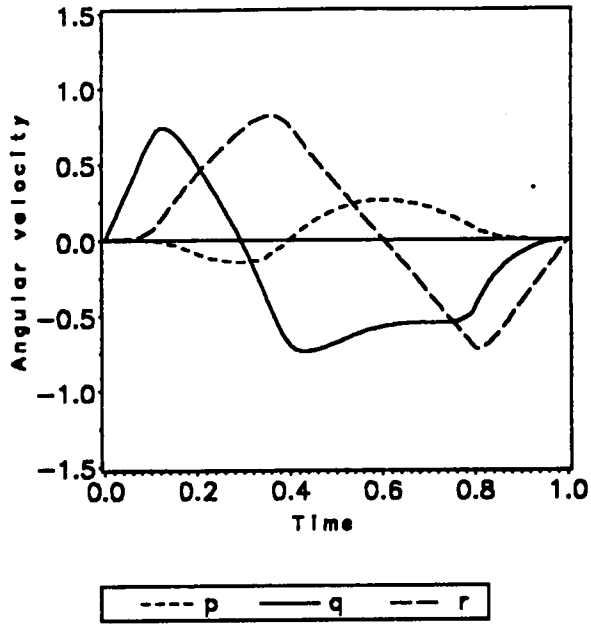

Figure [33a]. Angular Velocity p, q and r.

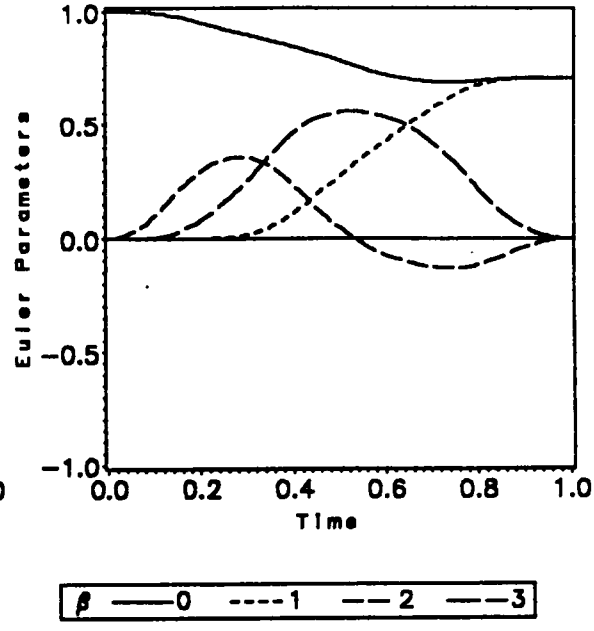

Figure [33b]. Euler Parameters β_0, β_1, β_2 and β_3.

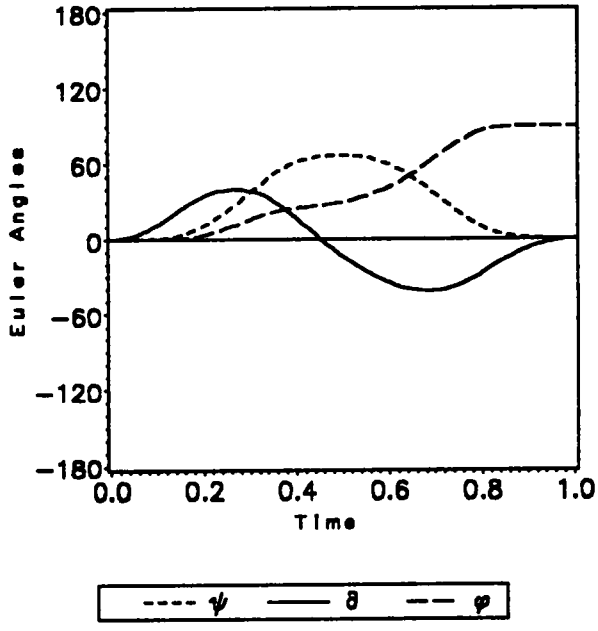

Figure [33c]. Euler Angles ψ, θ and ϕ.

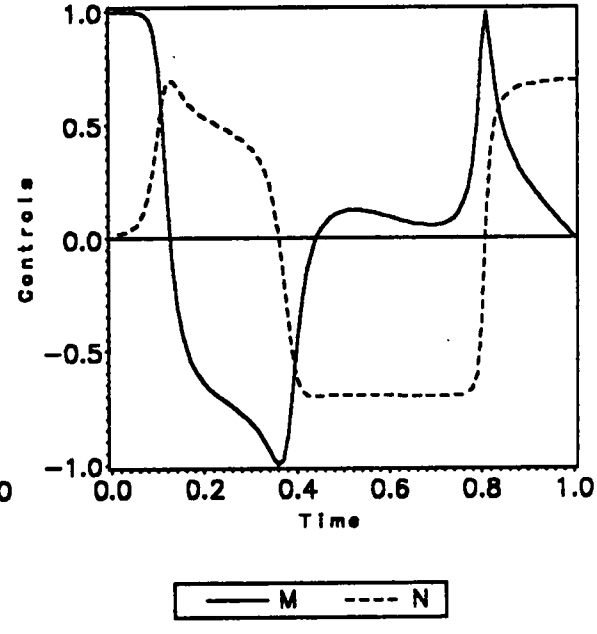

Figure [33d]. Controls M and N.

Figure [33]. A F3 extremal.

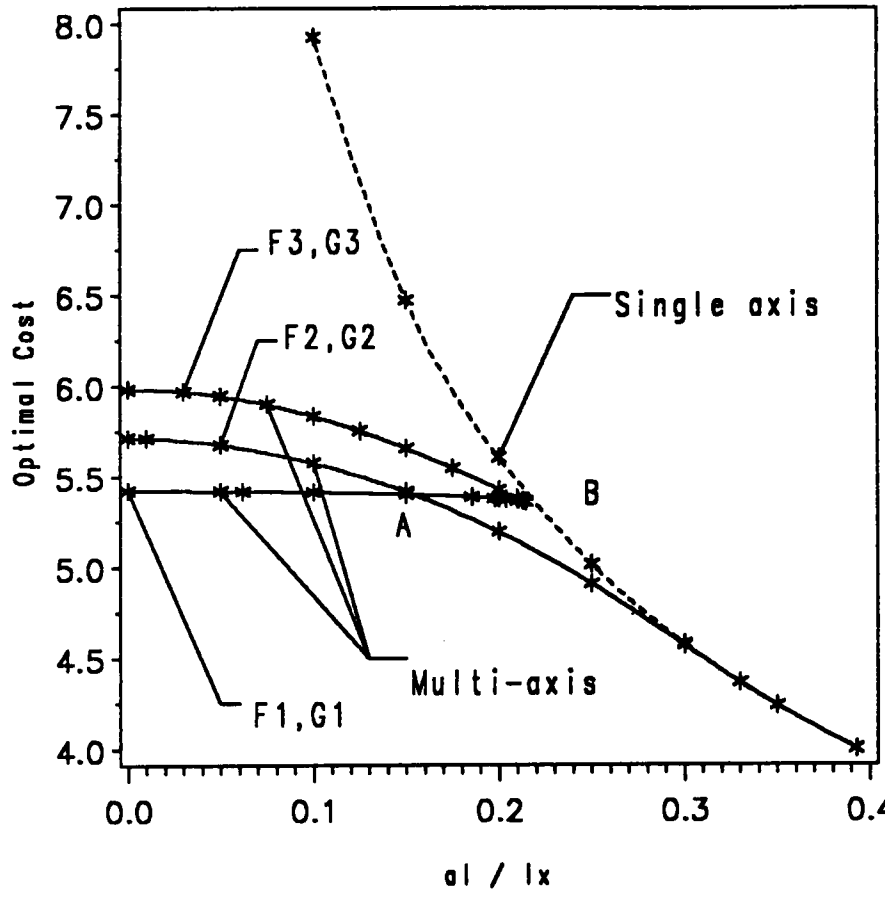

Figure [34]. Optimal cost τ_f^* as a function of roll authority.

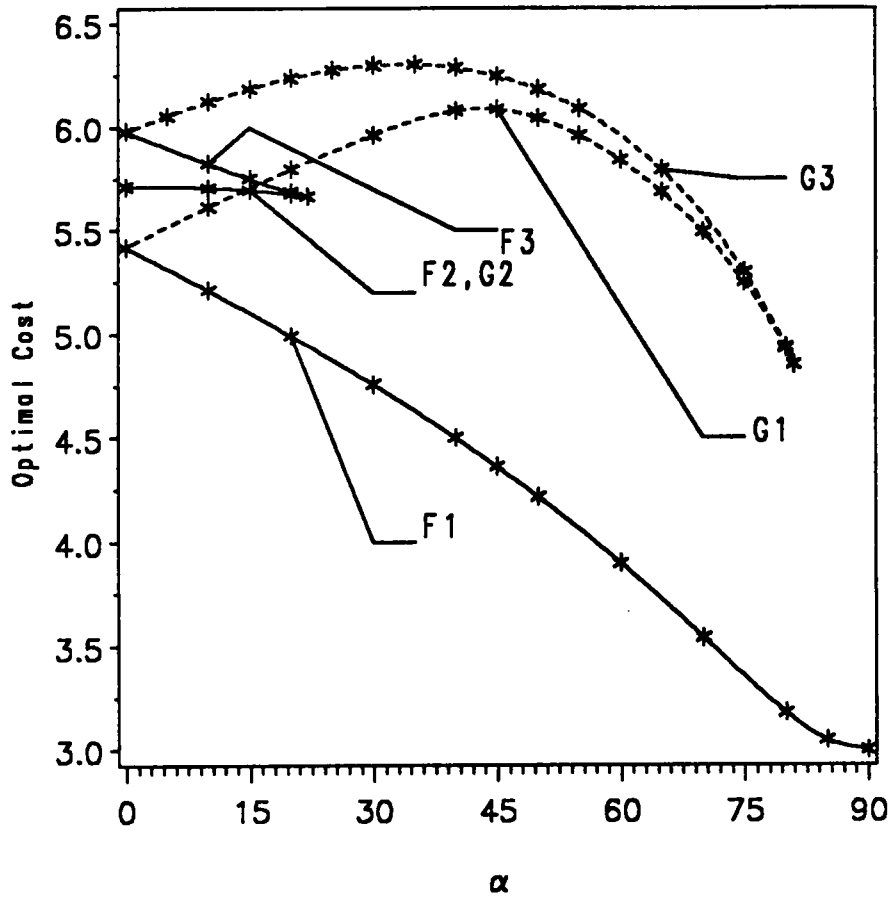

Figure [35]. Optimal cost τ_f^* as a function α.

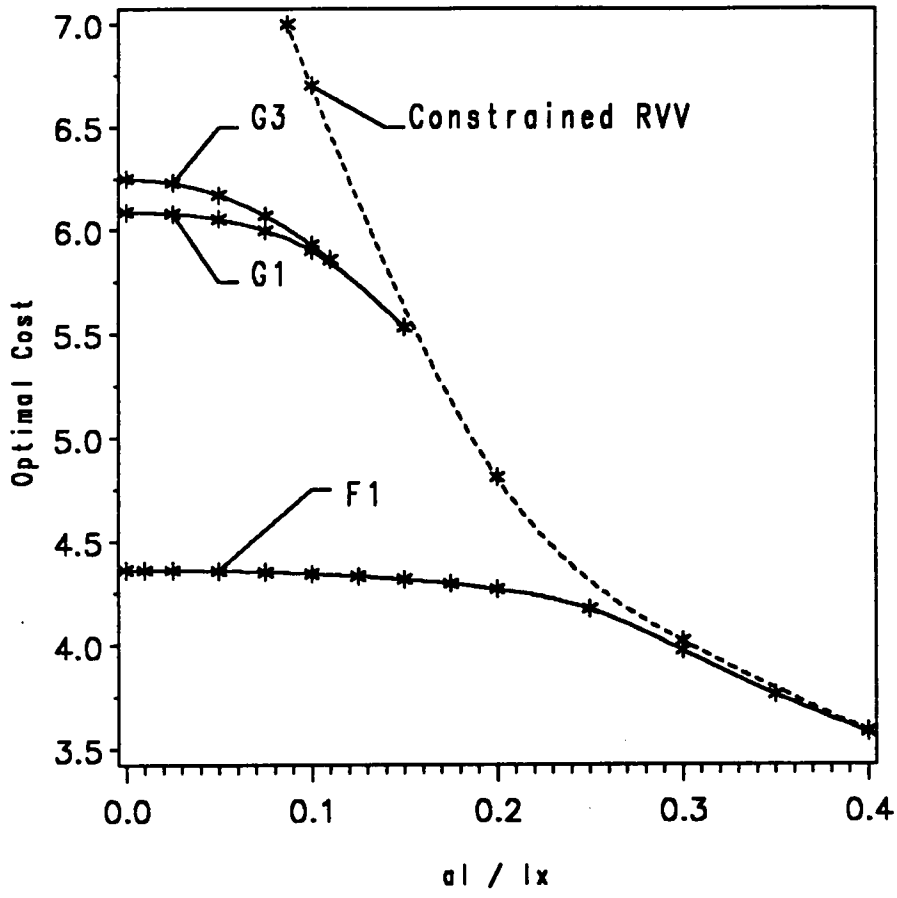

Figure [36]. Optimal cost τ_f^* vs. $\frac{a_l}{I_x}$,

for $\alpha = 45°$.

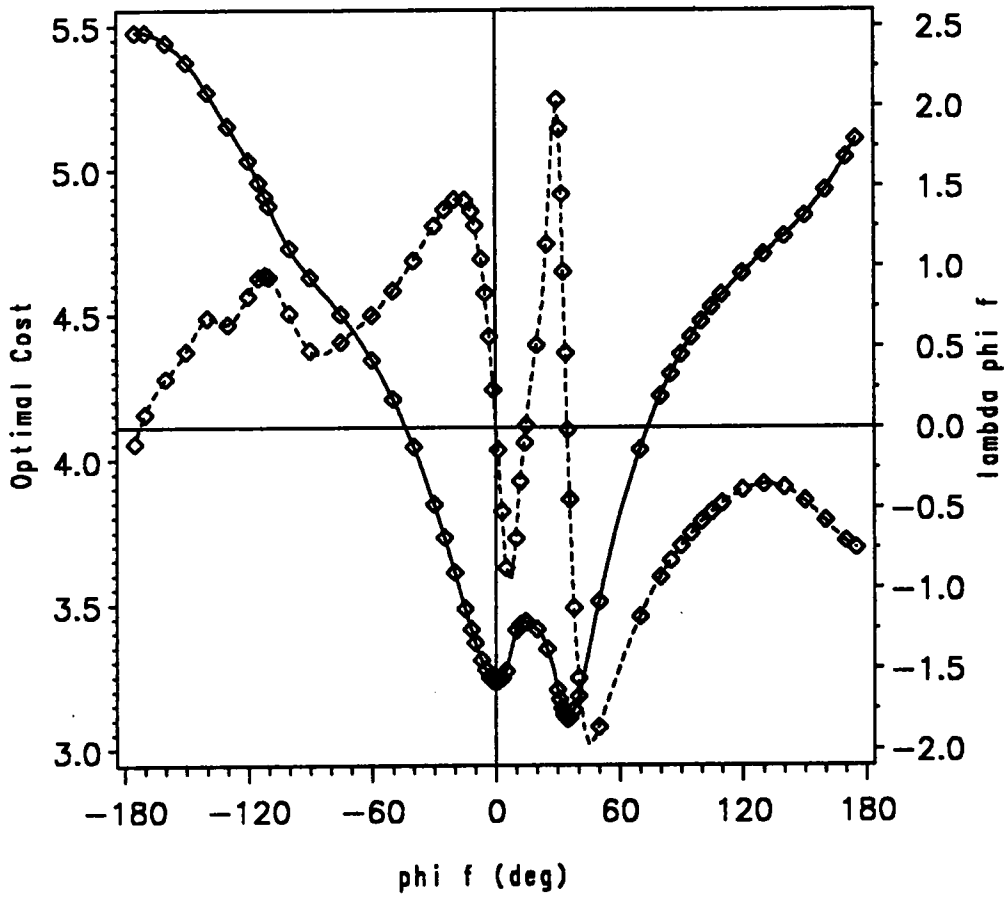

Figure [37]. Optimal cost τ_f^* vs. ϕ_f.

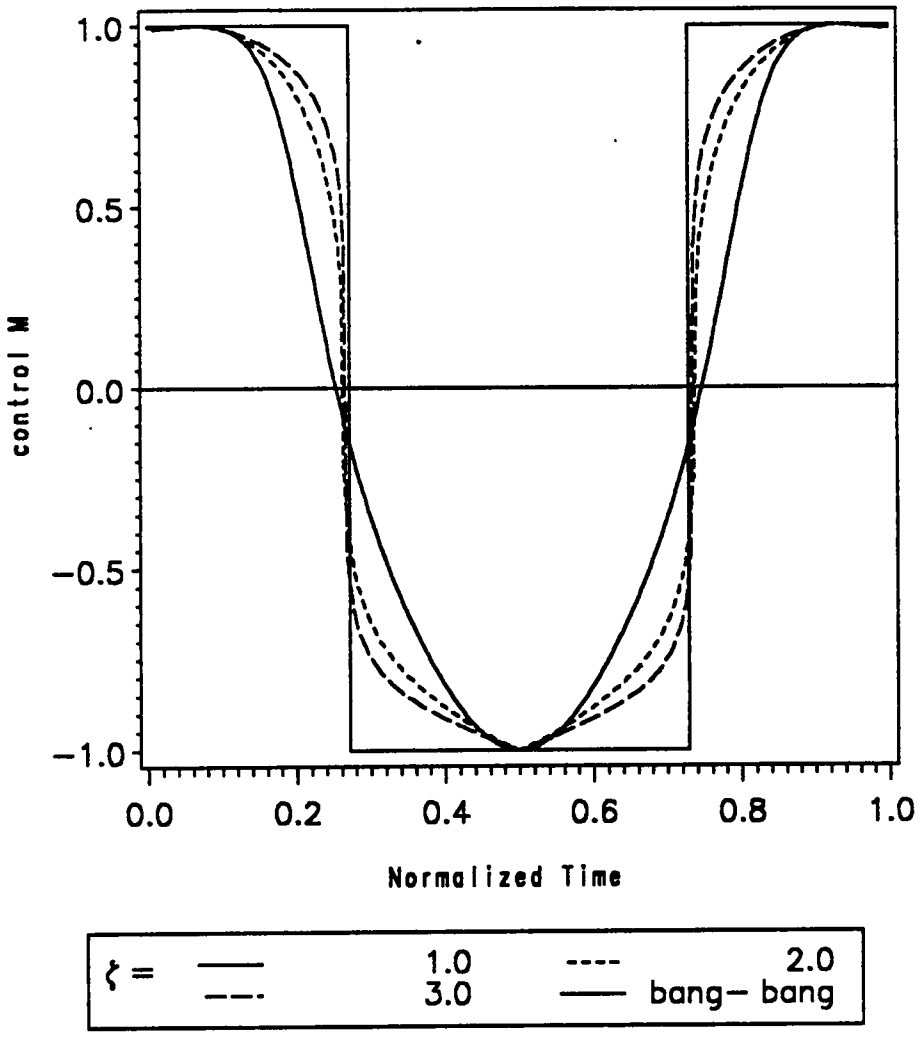

Figure [38a]. Control Moment M deformation to bang-bang solution, for *minimum-time attitude control* problem.

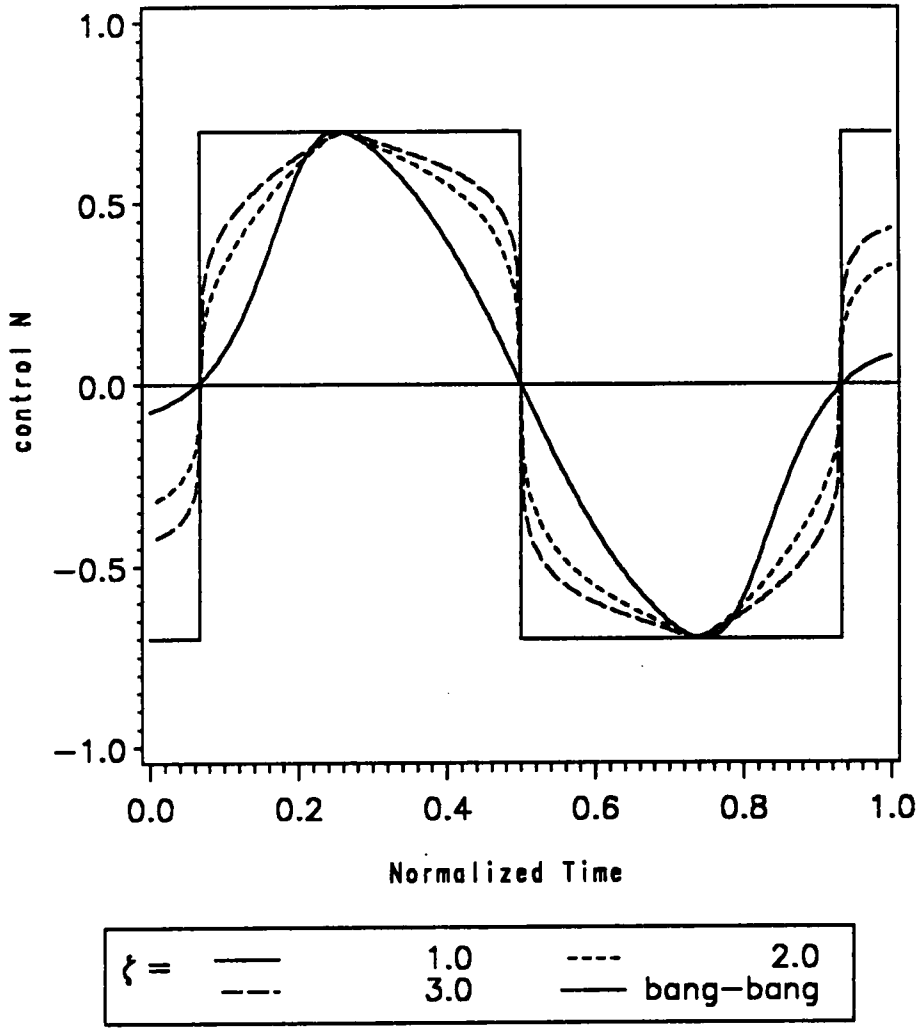

Figure [38b]. Control Moment N deformation to bang-bang solution, for *minimum-time attitude control* problem.

The vita has been removed from the scanned document